2016

Calcium Carbonate Composition And Other Measures Of Vulnerability Of The Skeletons And Shells Of Echinoderms And Gastropods Challenged By Ocean Acidification Or Climate Warming

Ashley Duquette Douglas
University of Alabama at Birmingham

CALCIUM CARBONATE COMPOSITION AND OTHER MEASURES OF VULNERABILITY OF THE SKELETONS AND SHELLS OF ECHINODERMS AND GASTROPODS CHALLENGED BY OCEAN ACIDIFICATION OR CLIMATE WARMING

by

ASHLEY DUQUETTE

JAMES B. McCLINTOCK, COMMITTEE CHAIR
CHARLES D. AMSLER
ROBERT A. ANGUS
KENNETH M. HALANYCH
ALBERTO PÉREZ-HUERTA

A DISSERTATION

Submitted to the graduate faculty of The University of Alabama at Birmingham,
in partial fulfillment of the requirements for the degree of
Doctor of Philosophy

BIRMINGHAM, ALABAMA

2016

CALCIUM CARBONATE COMPOSITION AND OTHER MEASURES OF VULNERABILITY OF THE SKELETONS AND SHELLS OF ECHINODERMS AND GASTROPODS CHALLENGED BY OCEAN ACIDIFICATION OR CLIMATE WARMING

ASHLEY DUQUETTE

BIOLOGY

ABSTRACT

Marine invertebrate calcium carbonate ($CaCO_3$) composition will likely be impacted by climate warming and ocean acidification (OA). Elevated temperature alters physiological processes that can induce stress, and OA alters the ability of calcareous marine invertebrates to maintain acid-base balances, calcify, and repair skeletal dissolution. The first of three chapters of this dissertation exploits a natural CO_2 seep to evaluate impacts of chronic exposure to OA on the shells of four gastropods: the limpets *Patella caerulea* and *P. rustica,* top-shell snail *Osilinus turbinatus,* and whelk *Hexaplex trunculus.* All four gastropods experienced shell dissolution to various degrees and reduced shell integrity as pH decreased. The limpet *P. rustica* demonstrated altered $CaCO_3$ composition of the shell with reduced pH, and there was evidence of altered shell microstructure in both limpets. The second chapter documents the variability of $CaCO_3$ composition of skeletal components of high latitude Antarctic echinoderms to further evaluate the hypothesis that skeletal magnesium content is inversely correlated with latitude in the Echinodermata. Significant inverse correlations were observed in echinoderms collected between 62° and 76°S, but not when the correlation analysis was restricted to those collected south of 70°S where seawater temperature is comparatively constant. This suggests that temperature may be an important factor driving this global relationship in echinoderms. This also suggests that climate warming may lead to

increasing levels of magnesium in skeletal components, rendering them more susceptible to dissolution under conditions of OA. The third chapter examines variability of the $CaCO_3$ composition of skeletal components of the model sea urchin *Lytechinus variegatus* exposed to ambient and near-future seawater temperature. Over the 90-day experiment, there was no increase in skeletal magnesium content in the test, spines, or Aristotle's lantern in the elevated temperature treatment. This result was likely related to thermal stress and individuals allocating their resources elsewhere. It appears that elevated temperatures may not alter $CaCO_3$ composition or impact skeletal solubility in *L. variegatus* as OA intensifies. The mineralogy of gastropods and echinoderms investigated herein exemplifies the variable nature of susceptibility to OA and the difficulty of predicting impacts of climate change without a focus at the species level.

Keywords: ocean acidification, echinoderm, gastropod, calcium carbonate, Mg/Ca ratio, Antarctica

DEDICATION

To my family. George, Kathleen, Alison, Bilal, my husband Sam, Thor, and Bailey, your unconditional love, support and faith in me made this happen. I thank God for each of you every day.

ACKNOWLEDGMENTS

I would like to thank my mentor, Dr. James McClintock, for the time, guidance, and resources he has provided for me. Drs. Charles Amsler, Robert Angus, Kenneth Halanych, and Alberto Pérez-Huerta, my graduate committee, have provided endless patience and constructive feedback over the past four years at UAB. Financial support for this research was provided by the UAB Department of Biology and an Endowed Professorship in Polar and Marine Biology provided to James McClintock. Additional support was provided by the National Science Foundation awards ANT-1041022 (James McClintock, Robert Angus, and Charles Amsler) and ANT-1043745 (Kenneth Halanych).

I would like to thank all of the labs at UAB, both in and out of the Biology Department, which provided guidance and use of their facilities to me. William Monroe in the Materials Science and Engineering Department at UAB provided invaluable assistance with the scanning electron microscope. Dr. Yogesh Vohra in the Physics Department provided the use of his lab for x-ray diffraction analyses which could not have been completed without the help and guidance of Gopi Samudrala. Dr. Stephen Watts and Jeff Barry made and provided the urchin feed used in the course of this research.

There are several labs outside of UAB which I would like to acknowledge for their support. Dr. Alberto Pérez-Huerta made the electron backscatter diffraction analyses

possible by opening his lab and equipment to me at the University of Alabama. His students Michelle Gannon and Raya Berman gave up their time to help me in the lab, often on a Saturday morning. Drs. Justin Ries and Isaac Westfield at Northeastern University graciously hosted me at their lab for two separate weeks to conduct aspects of the research presented herein. I would especially like to thank Dr. Kenneth Halanych at Auburn University. It was with his lab that I travelled to Antarctica for six weeks. His students were of great assistance in collecting and preparing samples, including Pamela Brannock, Alex Medved, and David Branson.

I could not have accomplished any of this without the friendship and support of other UAB graduate students, including Cecilia Brothers, Kenan Matterson, Ryan James, Julie Schram, Leucas Miller, and Sabrina Heiser. I cannot express my gratitude for their laughter, advice, and patience. Finally, I would like to acknowledge my wonderful family for their encouragement and never ending belief that I could achieve this goal. I could not have completed this work without their patience, love, and occasional reminders to take a deep breath and relax. Thank you Mom, Dad, Alison, and my exceptional husband, Sam.

TABLE OF CONTENTS

Page

LIST OF TABLES

Table *Page*

EFFECTS OF OCEAN ACIDIFICATION ON THE SHELLS OF FOUR MEDITERRANEAN GASTROPOD SPECIES AROUND A CO_2 SEEP

INTER- AND INTRA-SPECIFIC COMPARISONS OF THE Mg/Ca RATIO OF SKELETAL COMPONENTS IN A SUITE OF ANTARCTIC ECHINODERMS LARGELY SOUTH OF 70 DEGREES LATITUDE

NEAR-FUTURE ELEVATED TEMPERATURE IMPACTS ON THE Mg/Ca RATIOS IN THE TEST, SPINES, AND ARISTOTLE'S LANTERN OF THE SUB-TROPICAL SEA URCHIN *LYTECHINUS VARIEGATUS*

LIST OF FIGURES

Figures *Page*

EFFECTS OF OCEAN ACIDIFICATION ON THE SHELLS OF FOUR MEDITERRANEAN GASTROPOD SPECIES AROUND A CO_2 SEEP

NEAR-FUTURE ELEVATED TEMPERATURE IMPACTS ON THE Mg/Ca RATIOS IN THE TEST, SPINES, AND ARISTOTLE'S LANTERN OF THE SUB-TROPICAL SEA URCHIN *LYTECHINUS VARIEGATUS*

INTRODUCTION

Anthropogenic carbon dioxide

Marine ecosystems around the globe face several threats from rising levels of atmospheric carbon dioxide (CO_2). Atmospheric CO_2 levels are documented as having risen approximately 40% (278 to 400 ppm) since the 1800's (IPCC 2014; Gattuso et al. 2015). Fluctuations in such levels have occurred naturally in the past, but the concern today is the rate at which they are currently increasing. The current rate of increase is estimated at approximately an order of magnitude faster than has existed for millions of years (Doney and Schimel 2007).

CO_2 (as well as other air pollutants) can trap the sun's heat in the atmosphere and lead to warming temperatures. Average global sea-surface temperature has demonstrated an increase of approximately 0.4˚C since the 1950's (Levitus et al. 2009). Rising sea-temperatures contribute to factors such as increased ocean stratification, rising sea level, changes in ocean circulation, precipitation, and freshwater input (Cazenave et al. 2008; Doney et al. 2012). Those changes in physical factors can, in turn, alter oxygen and other nutrient levels and concentrations available to marine flora and fauna (Keeling et al. 2010; Doney et al. 2012).

Some species are able to circumvent the threat of warming by shifting their location until they are within a physiologically tolerable range (Mueter and Litzow 2008; Spencer 2008; Jones et al. 2009, 2010). These shifts alter species' distribution, ecosystem structure and diversity, and food web dynamics (Barry et al. 1995; Hyrenbach and Veit

2003; Hillyer and Silman 2010). Some species face geological constraints and others are sessile and not physically able to relocate. While warming temperatures are clearly a threat of their own, they are not the only threat driven by increasing levels of atmospheric CO_2.

Ocean acidification

The oceans take up approximately a third of anthropogenic CO_2 (IPCC 2014). While this uptake may temper the atmospheric effects of increasing carbon dioxide emissions, it can wreak havoc on oceans globally. CO_2 taken up from the atmosphere is converted to several forms within marine systems:

$$CO_{2(atm)} \leftrightarrow CO_{2(aq)} + H_2O \leftrightarrow H_2CO_3 \leftrightarrow H^+ + HCO_3^- \leftrightarrow 2H^+ + CO_3^{2-}$$

Carbonic acid forms when CO_2 taken up from the atmosphere combines with water, and then it dissociates into carbonate (CO_3^{2-}), bicarbonate (HCO_3^-), and hydrogen ions (H^+). This results in a drop in pH (increasing acidity). To date, the mean pH of ocean surface waters has fallen 0.1 pH units since pre-industrial times and is predicted to fall another 0.3-0.4 pH units by the end of the century (Hoegh-Guldberg et al. 2014). A predicted 0.3-0.4 pH drop by the end of the century coincides with a 150% increase in H^+ ion concentration and a 50% decrease in CO_3^{2-} ion concentration (Orr et al. 2005).

Marine invertebrates exhibit varying responses to altered sea water chemistry. Increasing acidity can directly or indirectly affect invertebrates by challenging the abilities to successfully grow, reproduce, calcify, and maintain acid-base balance (Kroeker et al. 2013a; Bray et al. 2014; Dubois 2014; Lardies et al. 2014; Gaylord et al. 2015). Responses to acidification vary among life stage, individuals, populations, and

species. Some marine invertebrates even exhibit resilience at one life stage, while they are vulnerable to ocean acidification at another. The sea urchin *Strongylocentrotus droebachiensis* exhibits a nine-fold increase in mortality in juveniles and adult females produced a fifth the number of eggs when initially cultured into acidified seawater. However, after a period of 16 months, adults began producing normal numbers of eggs while juvenile survival remained low (Dupont et al. 2013). Many marine invertebrates, including echinoderms and mollusks, have demonstrated negative effects when early life stages are exposed to CO_2 acidified seawater (Shirayama and Thornton 2005; Kurihara et al. 2007; Dupont et al. 2008; Ellis et al. 2009; Findlay et al. 2009; Albright et al. 2012; Stumpp et al. 2012, 2013; LaVigne et al. 2013). For example, the oyster *Crassostrea virginica* exhibited elevated juvenile mortality, delayed metamorphosis, and decreased soft body growth when exposed to near-future decreases in seawater pH (Talmage and Gobler 2009; Beniash et al. 2010; Dickinson et al. 2012). Similarly, abalone, mussels, and scallops demonstrated decreased growth, lower metabolism, reduced fertilization, and retarded embryonic development when exposed to decreased pH (Desrosiers et al. 1996; Michaelidis et al. 2005).

Because there are “winners” and “losers” in the face of ocean acidification, entire ecosystems are altered, often detrimentally. Observations at naturally acidified CO_2 seep sites revealed changes in community structure and reduced diversity of invertebrates under acidified conditions (Fabry et al. 2008; Hall-Spencer et al. 2008; Martin et al. 2008; Barry et al. 2010; Cigliano et al. 2010; Christen et al. 2013). There are ongoing decreases in taxa and taxonomic evenness, as well as shifts in trophic structure toward fewer trophic groups and dominance by generalists surrounding CO_2 seep systems

(Kroeker et al. 2011; Kroeker et al. 2013b; Fabricius et al. 2014; Baggini et al. 2015). Moreover, those species and individuals that survive in acidified conditions may suffer weakened shells/skeletons and are often smaller due to dissolution or physiological stress (Langer et al. 2014; Milazzo et al. 2014; Collard et al. 2015; Harvey et al. 2016).

Carbonate mineralogy

Marine calcifying invertebrates face two major challenges in response to OA: the creation or maintenance of shells/skeletons as well as increasing dissolution of shells/skeletons. As indicated above, OA is driven by increasing concentrations of hydrogen ions that, in turn, decrease concentrations of carbonate ions (CO_3^{2-}). Carbonate is a necessary component of calcium carbonate ($CaCO_3$), a primary building block of the calcified shells and skeletons of marine invertebrates. Calcium carbonate is found predominantly in two isomorphs: aragonite and calcite, with calcite being half as soluble as aragonite (Mucci 1983). Decreasing levels of carbonate result in a decline in calcium carbonate saturation state (Ω). If $\Omega > 1$ then $CaCO_3$ formation is thermodynamically favored, but when $\Omega < 1$, dissolution is more likely.

Remarkably, there is already evidence of current aragonite under-saturation in the North Pacific, Indian, Arctic, and Antarctic Oceans (Feely et al. 2002; Sabine et al. 2004; Yamamoto-Kawai et al. 2009; Schram et al. 2015). In addition, hydrogen ions building up in seawater challenge the ability of marine invertebrates to maintain their acid-base homeostasis and internal pH, implying that decreased saturation states are not the only difficulty facing marine invertebrates (Cyronak et al. 2015). Dissolution has been

suggested to be an equal, or greater, threat to calcareous marine invertebrate success as reduced calcification (Roleda et al. 2012; Eyre et al. 2014).

The solubility of calcium carbonate can be altered depending on the amount of magnesium incorporated in place of calcium. Higher levels of $MgCO_3$ are more soluble (Morse et al. 2006; Andersson et al. 2008). Bøggild (1930) identified three compositional phases of calcium carbonate in marine invertebrates: aragonite, low magnesium calcite (<4% $MgCO_3$), and high magnesium calcite (≥4% $MgCO_3$). The magnesium content of the shell/skeleton in marine calcifiers is generally linked to taxonomic history yet considered to decline as a function of increasing latitude (Chave 1954; McClintock et al. 2011). The exact driving force of this proposed latitudinal relationship with magnesium content remains unknown. Several abiotic and biotic factors are believed to affect magnesium content, some of which are Mg/Ca ratio of seawater, diet, saturation state, growth rate, and temperature (Ries 2004; Andersson et al. 2008; Hermans et al. 2010; Asnaghi et al. 2013, 2014). The question now is how changing pH levels, saturation states and carbonate availability will affect calcifying organisms.

The general expectation is that skeletal growth of marine invertebrates will decrease with declining carbonate saturation states and pH (Hofmann et al. 2010; Johnson and Carpenter 2012; Garrard et al. 2013; Kroeker et al. 2013a; Dubois 2014). Nevertheless, the variable, and often species-specific, responses to ocean acidification observed has made ecologically important marine invertebrates that build calcium carbonate shells and skeletons of increasing interest (Doney et al. 2009; Ries et al. 2009; Kroeker et al. 2013a; Parker et al. 2013). For example, if calcified marine invertebrates experience declining rates of calcification due to increased energetic costs of calcification

in increasingly corrosive waters, this will alter organic carbon and $CaCO_3$ flux to the deep sea (reviewed in Day et al. 2000; Fabry et al. 2008, 2009; Wood et al. 2008, 2010). Intolerance of acidified seawater may significantly decrease species diversity. Studies have determined that calcifiers in naturally acidified marine CO_2 vent systems are generally restricted to ambient pH regions (pH 8.1-8.2) (Hall-Spencer et al. 2008; Martin et al. 2008; Fabricius et al. 2014; Garilli et al. 2015).

Impacts of ocean acidification on molluscan shells

Given their important ecological roles and their use as environmental biomonitors, mollusks have been of great interest in the face of ocean acidification. While much of the literature predicts negative effects, the overall response to, and severity of, effects from ocean acidification vary with taxa. For example, some gastropods and bivalves have demonstrated positive (increased calcification, increased rate of calcification and/or growth) or parabolic (positive net calcification under intermediate acidification but negative under high acidification) reactions to increased acidity (Ries et al. 2009; Rodolfo-Metalpa et al. 2011). There is some evidence that certain species may be able to adapt to ocean acidification by altering the solubility of their skeleton. This is achieved by secreting one of the less soluble mineral polymorphs of calcium carbonate. For example, Ries (2011) found that the whelk *Urosalpinx cinerea* decreased the solubility of their shell by initiating the secretion of a low Mg-calcite skeleton. Additionally, the amount of tissue covering the shell/skeleton may facilitate organisms in adapting to or tolerating seawaters at lowered pH (Coleman et al. 2014). For example, the mussel *Mytilus galloprovincialis* displays no significant shell dissolution,

and continues precipitating calcium carbonate in under-saturated conditions (Thomsen et al. 2010; Rodolfo-Metalpa et al. 2011). The lack of dissolution may be related to the presence of a periostracum that covers the entire shell exterior.

Shells of a variety of other mollusk species exhibit significant negative responses to ocean acidification. Some are important ecological species including the bay scallop (Ries et al. 2009), Pacific and Eastern oysters (Gazeau et al. 2007; Ries et al. 2009), and various species of hard and soft clams (Ries et al. 2009). Responses include net shell dissolution (bivalves: Green et al. 2004; gastropods: Hall-Spencer et al. 2008), reduced shell growth or decreased calcification rates (gastropods: Shirayama and Thornton 2005; Melatunan et al. 2013; bivalves: Gazeau et al. 2007; Ries et al. 2009), and impaired shell integrity (Green et al. 2004; Beniash et al. 2010; Fitzer et al. 2014). These effects are greater in animals lacking a thick organic layer (e.g., Rodolfo-Metalpa et al. 2011; Coleman et al. 2014). The Antarctic pteropod, *Limacina helicina antarctica*, possesses an aragonite shell that exhibits severe dissolution at aragonite saturation states below 1.12 ($\Omega_A < 1.0$ = sub saturated) (Bednaršek et al. 2012). Shell dissolution not only makes them more vulnerable to predation but also to infection. As pteropods often dominate mesozooplankton biomass in polar seas, oceanic food webs can be dramatically affected by their lack of capacity to cope with acidifying and under-saturated seas (Comeau et al. 2010; Bednaršek et al. 2012; Lischka and Riebesell 2012).

Impacts of ocean acidification on echinoderm skeletal components

Echinoderms represent a significant carbonate producing phylum and, because of their high biomass, are major players in the global carbonate cycle (Lebrato et al. 2010).

They are known to have high magnesium calcite skeletons with $MgCO_3$ between 4 - 30% (Vinogradov and Odum 1953; Weber 1973). Because of this, echinoderms are of particular concern in acidifying seawaters. Negative responses to ocean acidification have been observed in all life stages of this phylum (Shirayama and Thornton 2005; Ries et al. 2009; Dupont et al. 2010; Byrne et al. 2011; Collard et al. 2014). These responses include spine degradation in sea urchins (Albright et al. 2012; Bray et al. 2014; Dubois 2014), altered gene expression and larval growth rates (Ross et al. 2011; Challener et al. 2013; Sewell et al. 2013; Chan et al. 2015), and adult echinoids build tests of reduced thickness, reduced growth, and net dissolution (Shirayama and Thornton 2005; Miles et al. 2007; Asnaghi et al. 2013). It is believed that echinoids will be especially susceptible to ocean acidification because they have a continuous, high Mg-calcite test that is covered only by a thin, permeable epithelial layer (Binyon 1976, 1980; Sewell and Hofmann 2011).

Nevertheless there is also evidence that echinoderms may be resilient in the face of acidifying seawater. The test growth rate and survival of juveniles of the sea urchin *Heliocidaris erythrogramma* exhibited resilience to both ocean acidification and seawater warming (Wolfe et al. 2013). Collard et al. (2015) found that the sea urchin *Paracentrotus lividus* did not exhibit altered mechanical properties of the test when exposed to pH levels expected by 2100. However, the ability to continue calcifying in acidified conditions often occurs at a cost to the animal. A burrowing brittle star (*Amphiura filiformis*) experienced an increased rate of calcification, but fitness was reduced due to a loss of muscle (Wood et al. 2008). The sea star *Pisaster ochraceus* exemplifies the complicated nature of echinoderm responses to ocean acidification. Growth rates for this sea star increased with end-of-century levels of CO_2; however, the

relative calcified mass of the organism declined in the same environment (Gooding et al. 2009). Clearly, a general statement about or expectation for echinoderm responses to ocean acidification cannot be made. More research is necessary to explore skeletal properties and susceptibility of these and other calcareous marine invertebrates.

Objectives

The purpose of the present dissertation was to elucidate the effects of and potential susceptibility to ocean acidification and/or warming on the major calcium carbonate structures of key carbonate-producing benthic marine invertebrates. My studies focus on the magnesium to calcium ratio in the skeletons and shells of gastropods and echinoderms from a variety of ecosystems. Each ecosystem provides an opportunity to appropriately evaluate a different aspect of how biomineralization may or may not be altered with future climate warming and ocean acidification.

I hypothesized that a suite of echinoderm species collected from varying latitudes in Antarctica would demonstrate an inverse relationship between skeletal magnesium content and latitude previously observed in temperate and tropical species (the latitudinal hypothesis). I expected that individuals from lower latitudes would have higher levels of magnesium than conspecifics collected from higher latitudes. Assuming that this relationship was driven, at least in part, by temperature and applying this construct to a temperate echinoderm, I hypothesized that the model sea urchin *Lytechinus variegatus* would construct skeletal components with higher levels of magnesium when chronically exposed to an elevated near-future temperature. Because seawater surface temperatures are rising concurrent with ocean acidification, it is important to consider if higher

temperature induces increasing levels of skeletal magnesium as this would increase the solubility of the calcium carbonate skeleton with ocean acidification. Increase in solubility would render calcified marine invertebrates to greater risk of dissolution and weakening of shells and skeletons elevating risks of predation by crushing or drilling predators. Along with controlled laboratory experiments to evaluate the role of temperature mineralogy and skeletal susceptibility to ocean acidification, I exploited a natural CO_2 seep as an *in vivo* model to study impacts of acidification on shell mineralogy, dissolution, and structural integrity. I hypothesized that four species of shelled gastropods living across a range of seep-induced pH levels would demonstrate increasingly negative impacts as elevated acidification increasingly challenged shell composition and structure.

In summary, to discern possible impacts of ocean acidification or ocean warming on the elemental composition of the skeletal components and shells of marine invertebrates, I utilized invertebrates collected from three distinct and relevant ecosystems: a CO_2 seep system, Antarctica, and a Florida coastal bay. This involved examinations, at both the micro- and macroscopic level, of gastropod shells from individuals exposed to chronic acidification at a CO_2 seep system; the determination of baseline magnesium content of echinoderms from a particularly threatened and climate-susceptible marine environment, Antarctica; and an experiment focusing on the effect of warming on calcium carbonate composition in skeletal components (test, spines, and Aristotle's lantern) of the sea urchin *Lytechinus variegatus* currently living at the northern extent of its thermal tolerance.

EFFECTS OF OCEAN ACIDIFICATION ON THE SHELLS OF FOUR MEDITERRANEAN GASTROPOD SPECIES AROUND A CO_2 SEEP

by

ASHLEY DUQUETTE, JAMES B. MCCLINTOCK, CHARLES D. AMSLER, ALBERTO PÉREZ-HUERTA, MARCO MILAZZO, JASON M. HALL-SPENCER

In preparation for *Marine Biology*

Format adapted for dissertation

Abstract

Marine CO_2 seeps allow the study of the long-term effects of ocean acidification on marine organisms. Four common species of benthic gastropod (the limpets *Patella caerulea* and *P. rustica*, the top-shell snail *Osilinus turbinatus*, and the whelk *Hexaplex trunculus*) were sampled across a CO_2 gradient created by volcanic seeps off Vulcano Island in Italy. Specimens were collected from three stations with ambient (pH 8.15), moderate (pH 8.03) and low (pH 7.73) seawater mean pH. Shell mineralogy, microstructure and microtexture, and mechanical strength were examined using X-ray diffraction, scanning electron microscopy, electron backscatter diffraction, and point compression analysis. The shells of both species of limpets were composed of calcite and aragonite, while the top-shell and whelk shells were entirely aragonite. Shell mineralogy was affected by acidification in the limpet *P. rustica* where the calcite/aragonite ratio increased with reduced pH. Each of the four gastropod species displayed reductions in either toughness or elasticity of the inner shell surface at the Low pH site as well as altered shell microstructure. This indicates that near-future ocean acidification will cause altered shell biomineralization in all four gastropods tested. The severity of the mechanical effects of acidification varied between species, but each had the potential to render individuals more susceptible to infection or predation.

Introduction

Ocean acidification is a process characterized by a decrease in seawater pH and an increase in pCO_2 that results from the absorption of anthropogenic carbon dioxide from the atmosphere into the ocean (Caldeira and Wickett 2003). Since the onset of the Industrial Revolution, levels of atmospheric CO_2 have increased from approximately 280

to 400 ppm and the oceans have absorbed about one third of anthropogenic CO_2 emissions (IPCC 2014). Present day oceans have higher concentrations of dissolved CO_2, bicarbonate, and hydrogen ions, with the latter resulting in acidified surface waters. Mean surface seawater pH levels have fallen 0.1 pH units (corresponding to about a thirty percent increase in $[H^+]$) since the onset of the Industrial Revolution and are predicted to fall, on average, another 0.3-0.4 pH units by the end of the century (Orr et al. 2005).

Decreases in seawater pH have been accompanied by reductions in the availability of carbonate (CO_3^{2-}) ions, which are a crucial component of calcium carbonate ($CaCO_3$). Calcite and aragonite, the most common $CaCO_3$ polymorphs, are the primary building blocks of calcified shells and skeletons in marine invertebrates (Lowenstam 1954). Declining levels of CO_3^{2-} result in a decline in the $CaCO_3$ saturation state (Ω) of seawater. If $\Omega > 1$ then shell/skeletal formation is facilitated, but when $\Omega < 1$, dissolution of shells or seawater-exposed skeletal elements becomes likely, and the cost of mineralization increases (Rodolfo-Metalpa et al. 2011; 2015). The taxon-specific polymorph of $CaCO_3$ used in the production of shells or skeletons also affects the potential for dissolution, since calcite is about half as soluble as aragonite (Mucci 1983). It is now well established that anticipated changes in pH and carbonate chemistry will have significant cellular, physiological, and ecological consequences for many calcifying marine invertebrates (Ries et al. 2009; Hahn et al. 2012; Chen et al. 2014; Swiney et al. 2016).

The majority of ocean acidification research to date has been laboratory-based and suggests that the impacts are likely to be species-specific with a few species benefitting, but many others being negatively impacted either through direct or indirect

effects of rising CO_2 levels (Gaylord et al. 2015). Most laboratory-based studies have been carried out over relatively short time scales, and whilst this offers valuable information about species-specific physiological responses to hypercapnia, it is difficult to scale-up from this body of research to assess the likely effect of ocean acidification on coastal ecosystems. When exposed to acidification in natural environments, organisms that thrive in the laboratory may become poor competitors against similar species in the wild (Gaylord et al. 2015; Harvey et al. 2016), and species that demonstrate negative responses in the laboratory may acclimatize in the field to acidified conditions and resume normal functionality after chronic exposure (Calosi et al. 2013).

Certain shallow submarine seeps provide opportunities for the study of the long-term ecological effects of increasing pCO_2 levels (Hall-Spencer et al. 2008). These seeps naturally acidify surrounding waters such that marine organisms living at increasing distances from areas with CO_2 bubbling up through the seafloor are exposed to a gradient of acidification. Importantly, exposure to acidified conditions occurs across different life history stages and over extended periods of time. Studies at CO_2 seeps in the Mediterranean and Papua New Guinea have revealed significant reductions in the biodiversity of marine invertebrates under acidified conditions, as well as shifts in trophic structure and simplified food webs (Cigliano et al. 2010; Kroeker et al. 2013b; Fabricius et al. 2014; Baggini et al. 2015). Much of this decline in biodiversity is due to reductions in the presence of calcifying marine organisms including scleractinian corals, mollusks and echinoderms (Inoue et al. 2013; Fabricius et al. 2014; Garilli et al. 2015). Those calcified species that do survive near CO_2 seeps may suffer from weakened shells or

skeletons (Rodolfo-Metalpa et al. 2011; Langer et al. 2014; Collard et al. 2015; Newcomb et al. 2015).

The aim of the present study was to determine how chronic exposure to elevated CO_2 influences the shells of four common species of sympatric gastropods (two limpets, a top-shell, and a whelk). All four gastropod species we studied are conspicuous inhabitants of rocky intertidal and upper sublittoral habitats of the Mediterranean Sea. The two limpet species display vertical zonation patterns with *Patella caerulea* (Linnaeus, 1758) occupying the upper sublittoral and *P. rustica* (Linnaeus, 1758) occupying the intertidal (Mauro et al. 2003). Limpets generally have a small home range and some even employ 'home' behavior, returning to the same spot after daily foraging (Keasar and Safriel 1994). The top-shell *Osilinus turbinatus* (Von Born, 1778) and the whelk *Hexaplex trunculus* (Linnaeus, 1758) occur primarily in the upper sublittoral zone (Crothers 2001; Rilov et al. 2004). The two limpets and the top-shell are herbivores that feed on microbial biofilms or microalgae (Crothers 2001; Jenkins et al. 2005; Coleman et al. 2006). In contrast, the whelk is carnivorous and a voracious predator on other species of gastropods (Sawyer et al. 2009). All four species are subject to harvest for human consumption or use as fish bait (Peharda and Morton 2006; Katsanevakis et al. 2008).

Our study site was a CO_2 seep system located in the shallow, nearshore waters of Vulcano Island approximately 25 km north of Sicily, Italy (Boatta et al. 2013). We measured shell size and microstructure at sites with increasing levels of pCO_2, based on scanning electron microscopy (SEM) and electron backscatter diffraction (EBSD). We also assessed shell mineralogy (percent calcite and percent aragonite) based on X-ray

diffraction (XRD) analysis, and mechanical strength (based on point compression to determine the force to fracture the shell, along with shell toughness, and elasticity).

Methods

Collection Sites

Gastropods were collected from three field stations (designated from this point forward as Ambient, Moderate, and Low pH sites) off the northeastern coast of Levante Bay, northeastern Vulcano Island (Fig. 1). Levante Bay is a shallow (2-3 m depth), micro-tidal region that contains active CO_2 seeps which creates a pH gradient (~6.8 – 8.2) along the northeastern shoreline (Boatta et al. 2013). The seawater carbonate chemistry gradient at our three stations was defined by Milazzo et al. (2014), and based on data collected during 2011-2012. The Ambient site served as a reference site with a mean pH of 8.15±0.01 (n=95) and was located approximately 850 m from the main CO_2 seep; the Moderate site was approximately 390 m distant from the seep with a mean pH of 8.03±0.01 (n=95) which is a predicted near-future level of pH (Nakicenovic and Swart 2000); the Low site was approximately 300 m distant from the seep with a mean pH of 7.73±0.02 (n=95), predicted to occur by the end-of-century (IPCC 2014; Milazzo et al. 2014).

All gastropods were collected haphazardly by hand (every individual encountered was collected) while snorkeling or wading in the intertidal in May 2013 from the three sites described above. Site-specific sample sizes of gastropods at the time of collection were: *P. caerulea* (Ambient: n=20; Moderate: n=31; Low: n=47), *P. rustica* (Ambient: n=81; Moderate: n=32; Low: n=35), *O. turbinatus* (Ambient: n=50; Moderate: n=31;

Low: n=28), *H. trunculus* (Ambient: n=24; Moderate: n=34; Low: n=25). Intact individuals of each species were placed into zip-lock bags, sealed, then placed inside tightly capped 2-liter plastic bottles, and transported to the University of Alabama at Birmingham, USA. Immediately upon arrival, the gastropods were removed from their shells and their respective soft tissues placed into labeled, 250 mL plastic jars with a solution of 4% formalin. All shells were rinsed repeatedly under flowing, distilled water and gently scrubbed clean by hand, labeled, and then air dried and digitally photographed using a Nikon D5100 digital camera. For each shell, length, width, height, and shell aperture width and height were measured to the nearest tenth of a millimeter using a digital caliper (iGaging 6" External Caliper). Shell length data were used for intraspecific comparisons of the mean sizes of individuals of each gastropod species at each of the three seep sites.

The numbers of shells examined varied with the type of analysis. A quantitative approach was taken for determinations of shell mineralogy and shell strength (point compression). Numbers of shells examined for mineralogy using XRD ranged from 11 to 25 for a given site, while sample sizes of shells used for shell strength analysis (Ambient and Low sites only) ranged from 7 to 23 for a given site (Table 1). Shells for these analyses were randomly selected from the pool of available shells by numbering all of them and using a random number generator in Microsoft Excel to choose those for analysis. A qualitative approach was taken for digital photographs of shells (a representative shell of each species from each site). Similarly, micro-imaging (SEM, EBSD) of shells of each species was carried out on a representative shell from each of the three sites. The representative shells (one shell per species per site) depict the general

condition of all shells collected from each site for each species. Individuals on the extreme ends of shell condition were not used as representatives.

X-ray diffraction analysis (XRD)

Shells of each gastropod species were examined for their mineralogy (aragonite and calcite in both limpets; only aragonite in the top-shell snail and whelk) by XRD (Ries 2011). Shells were prepared by repeatedly submerging each shell in a 10% NaClO solution to digest away all residual organic tissue (McClintock et al. 2011). Clean shells were rinsed under distilled water, and then air-dried for a period of 12 hrs. Shells were wrapped in sterile gauze and broken into fragments with a hammer. Fragments were subsequently placed into an agate mortar along with one to two mL of 95% ethanol and then ground to a slurry with an agate pestle. The resultant slurry was placed onto a 25mm x 75mm x 1mm glass microscope slide and air dried for 12 hrs to a powder.

Powdered shell was analyzed using a Philips X'Pert Analytical X-ray diffraction system (PANalytical B.V., Almelo, Netherlands). XRD data were collected at 45kV and 40 mA, and the 2Θ scan range was from 25˚ to 50˚, with a step size of 0.06 and scan speed of 2 $s \cdot step^{-1}$ to obtain precise measurements of calcite and aragonite peaks. The resulting XRD pattern for each shell was used to determine the levels (percent) of calcite and/or aragonite using equations given in (Ries 2011). The primary calcite peak (d(104)) corresponded to 2Θ = 29.5-30.2˚ on the XRD pattern generated. The two primary aragonite peaks (d(111) and d(021)) corresponded to 2Θ = 26.3˚ and 27.2˚, respectively (Milliman 1974).

Scanning electron microscopy (SEM) and *electron backscatter diffraction (EBSD) analyses*

Whole shells of representative individuals from each gastropod species from the Ambient and Low sites were examined using SEM and EBSD by first immersing each shell in epoxy resin (EpoThin Epoxy System) followed by a curing period of at least 24hr. Epoxy-embedded shells were then cut in half longitudinally using a diamond tipped saw. The exposed surface of the embedded shell was then ground and polished for analysis following the protocol described in Pérez-Huerta and Cusack (2009) excluding the use of colloidal silica. One-half of a shell from each species from the Ambient and Low sampling sites was examined using SEM. The other half of the same shell from each individual was examined using EBSD.

Resin-embedded shell halves for SEM analysis were etched with 2% HCl, generously coated with gold, and imaged using a Quanta FEG 650 Scanning Electron Microscope (FEI) set on high-vacuum mode at 20kV with a spot of four. SEM images were collected from the apex region of the limpet shell halves. The apex of the shell is the oldest portion of the shell and erosion becomes evident at this location first. Images for the shell halves of top-shell snails and whelks were collected for a single uniform ventral location on the first shell whorl above the aperture.

Shell halves for EBSD analysis were coated with a 2.5 nm layer of carbon and the epoxy resin surrounding each shell hand-painted with silver paint to decrease electron charging (see Pérez-Huerta and Cusack 2009). EBSD was carried out with a Hikari EDAX camera mounted on a Field Emission Scanning Electron Microscope (Tescan Lyra XMU). OIM 7.0 software was employed to collect data at 30kV, under a high vacuum mode, large beam intensity (20), and at a step size resolution of 1 μm or less.

EBSD images were collected from the apex of the representative limpet shells. EBSD data were analyzed using OIM 5.3 from EDAX-TSL and presented in diffraction maps and crystallographic maps, with different colors representing different crystal orientations within a given region of shell (further details in Pérez-Huerta et al. 2011).

Shell strength analysis

Replicate shells of individuals of each gastropod species collected from the Ambient and Low sample sites were used for mechanical strength analysis. Shells were cut with a diamond saw such that portions of both the external and internal surfaces of the shell were isolated for analysis. Shells of the two species of limpets were cut horizontally, two-thirds of the way down each shell's length as measured from the anterior tip. The apex of limpet shells was selected as the site for measures of external shell surface strength, and a site approximately 1-3mm (adjusted proportionately to the total length of the shell) from the posterior tip of the shell was chosen for measures of internal shell surface strength. Shells of top-shell snails were cut at a horizontal diagonal to expose the inner surface of the shell just within the aperture. The shell apex was selected for measurements of external shell strength, and a point located approximately 4 mm within the aperture at its halfway mark was selected for measurements of inner shell surface strength. Whelk shells were cut horizontally just above the aperture opening, to expose the external shell surface above the aperture for strength measurements. The region of the internal shell surface used for strength measures was located on the ventral shell face approximately 4mm from the outer edge of the aperture, half way down the shell's aperture length.

Prior to shell strength measurements, each shell sample was embedded in resin such that only the outer and inner shell surfaces described above were left exposed. Two different types of epoxy resin were used, JB Weld epoxy for limpet shells and EpoThin Epoxy Resin for shells of the top-shell snail and whelk.

Shell mechanical strength analyses were conducted using a point compression measure of the force necessary to crack a given shell. This technique also allowed for indirect calculations of shell toughness and shell elasticity. For each point compression analysis, a shell sample was placed onto the flat stage of a force stand (LRX *Plus*, Lloyd Instruments) and the compression measure performed using a metal point affixed to the stand. A 5-kN load cell was used with the metal point lowered at $0.03 mm \cdot min^{-1}$ for shells of both limpets and at a speed of $0.06 mm \cdot min^{-1}$ for shells of the top-shell snail and whelk. During each run, the point was lowered until shell fracture occurred. The force exerted on the shell during the run and the machine extension (distance the machine arm moved between readings) was continuously recorded using NEXYGENPlus software. Data derived from force and machine extension measures were used to determine Young's Modulus (elasticity) via stress-strain curves employing the following equations:

$$\text{Stress} = \sigma = \frac{F}{A},$$

$$\text{Strain} = \varepsilon = \frac{\Delta L}{L_e}.$$

Where F is force (N) at a given time point; A is the area (m^2) of the metal point used for the compression test; ΔL is the machine extension (m), and L_e is the effective length (m). The amount of energy per unit volume the shell withstands before breaking (toughness; $J \cdot m^{-3}$) was calculated as the area under the stress-strain curve.

Statistical Analyses

Mean shell lengths of all individuals collected from the Ambient, Moderate, and Low sites were compared within each of the four gastropod species. Shell length data that were normally distributed were compared using an ANOVA followed by a post-hoc Tukey test. For shell length data that were not normally distributed, log transformed data were subjected to a nonparametric Kruskal-Wallace rank sum test followed by a Dunn's test.

For data generated from XRD analysis, covariance of mean percent (± SE) of calcite and aragonite with both site (Ambient, Moderate, and Low) and size (shell length) was tested using a linear regression model. The mean percent (± SE) of calcite and aragonite were compared across the three sites (pH) for both of the limpet species. These data were not normally distributed and were therefore subjected to a Kruskal-Wallis test followed by a Dunn's test. As the top-shell snail and the whelk were composed entirely of aragonite, no site comparisons were necessary.

Shell mechanical strength data were compared separately for internal and external shell surfaces for each of the four gastropod species. For each shell surface type, data were compared between the Low and the Ambient sites for three shell structure measures (force, toughness, and elasticity). Covariance of these variables with both site (pH) and size (shell length) was determined using a linear regression model. There were several cases in which the data were adjusted for shell size (length) because a covariance between site (pH) and size (shell length) was detected. These included both the toughness and elasticity of the external shell surface in the limpet *P. rustica*, the force required to break the internal shell surface in the top-shell snail *O. turbinatus*, and the toughness of

and force required to break the internal shell surface in the whelk *H. trunculus*. Normally distributed data were compared between the Ambient and Low sites using a Student's t-test. Data that were not normally distributed were compared using a Mann-Whitney U test. R Statistical Software (R Development Core Team 2010) was used to conduct all statistical analyses and a $p<0.05$ was considered significant.

Results

Mean (± SE) sizes (shell length) of the four species of gastropod collected from each of the three pH sites are presented in Fig. 2. Intraspecific mean shell length did not differ significantly among the three pH sites in the limpet, *P. caerulea*, (ANOVA, $F_{(2,95)} = 2.717$, $p = 0.071$) and the whelk *H. trunculus* (Kruskal-Wallis test, $H_2=2.95$, $p =0.229$). However, mean shell length differed significantly between sites for the limpet, *P. rustica*, (ANOVA, $F_{(2,126)} = 4.05$, $p = 0.02$) and the top-shell snail *O. turbinatus* (Kruskal-Wallis test, $H_2=9.07$, $p = 0.011$). Specifically, shells of the limpet *P. rustica* were longer at the Low site than those at the Ambient site (Tukey HSD test, $p =0.015$). In contrast, shells of top-shell snail collected from the Low site were shorter than those at the Ambient site (Dunn's test, $p = 0.0013$), and similar in length to those collected at the Moderate site (Dunn's test, $p = 0.031$).

X-ray Diffraction

XRD analysis confirmed that the shells of both limpets, *P. caerulea* and *P. rustica* were composed of aragonite and calcite. Mean (± SE) percentages of aragonite and calcite in shells did not differ significantly for *P. caerulea* (Kruskal-Wallis test,

H_2=1.143, p = 0.5647), but differed significantly for *P. rustica* (Kruskal-Wallis test, H_2=13.569, p = 0.0011) (Fig. 3). Significant differences in ratios of aragonite to calcite were found in the shells of *P. rustica* collected at the Low and Moderate sites (Dunn's test, p = 0.0004) with levels of aragonite in shells of limpets from the Low site about a third (5.4% versus 15.6%) of those in shells of individuals from the Moderate site (Fig. 3). XRD also reported that shells of the top-shell snail *O. turbinatus* and the whelk *H. trunculus* are composed entirely of aragonite.

Shell Imaging

Digital photographs of representative shells collected from each of the three pH sites revealed varying levels of dissolution among the four species of gastropods (Fig. 4). Shells of the whelk *H. trunculus* collected at the Low site showed the most dramatic shell dissolution with considerable pitting and erosion of the outermost layer (Fig. 4a-c). In some instances, whelk shells from this site displayed holes that measured up to 5mm diameter, the apparent result of dissolution through all shell layers. The top-shell snail and the sublittoral limpet *P. caerulea* showed a similar, but more modest level of shell dissolution that increased with proximity to the Low site. Shells of both species from the Moderate site had reduced luster and faded pigmentation, while shells at the Low site displayed mild dissolution of the outermost layer (Fig. 4: d-f; j-l respectively). The gastropod shells least affected by increased proximity to the seep were of the intertidal limpet *P. rustica,* a species submerged only at high tide (Fig. 4g-i). Here, slight shell dissolution was evident at the shell apex (oldest region) at the Low site, but not evident at the other two sites.

The shell of the representative limpet *P. caerulea* from the Low site had an outer prismatic calcite layer above a thicker, inner crossed-lamellar aragonite layer (Fig. 5b), while the representative shell from the Ambient site revealed only the crossed-lamellar aragonite layer clearly. The outer prismatic calcite layer was obscured by epibionts or microbial infestation (Fig 5a). The thickness of the apex region of the Low site shell of *P. caerulea* was 8.9% greater than that for the representative individual from the Ambient site. In contrast, the shell of the representative individual of *P. rustica* from the Low site was 16.0% thinner than that of the representative individual from the Ambient site (Fig. 5c-d). A crossed-lamellar aragonite layer is visible in the representative shell of *P. rustica* from both the Ambient and Low sites, but the distinct external prismatic calcite layer is only visible in the representative individual from the Low site (Fig. 5c-d).

SEM imagery indicated that the representative aragonite shells of both the top-shell snail and whelk are constructed of multiple layers (Fig. 6). The outermost layer for the snail appeared eroded for the representative individual's shell from the Ambient site, while the outer shell layer of the individual from the Low site appeared to contain microbes (Fig. 6c-d). The next shell layer of the top-shell snail was a layer of prismatic microstructure followed by several additional layers with crossed-lamellar microstructure. There was no obvious degradation of microstructural organization among these layers in shells of representative snails collected from the Ambient and the Low sites. In contrast, SEM imagery indicated that representative shells of the whelk from the Low site had a shell microstructure characterized by degradation and less structural diversity as well as a smooth, eroded external surface (Fig. 6a-b).

EBSD images of representative shells of the limpet *P. caerulea* collected from the Low site demonstrated increased disorganization of the crystallography of the calcite layer (Fig. 7). The outermost edge of the representative shell collected from the Ambient site displays a thin layer (< 20 μm) of small, irregularly shaped calcite crystals (Fig. 7a-b). These crystals show a preferred (most common) crystallographic orientation with the *c*-axis parallel to the outermost edge of the shell. This outermost shell layer of the individual from the Ambient site was separated from an inner calcite layer by a distinct organic layer (Fig. 7a). The inner sublayer of the calcite layer was composed of larger, prismatic crystals oriented with the *c*-axis perpendicular to the outermost shell layer (Fig. 7b). A transition from the outer calcite layer to the inner aragonite layer is denoted by progression to a region of discontinuous diffraction. The representative shell of an individual from the Low site had a single thinner, more disorganized calcite layer (Fig. 7d-e), without the prismatic layer and the outermost thinner layer. The preferred crystallographic orientation is with the *c*-axis parallel to the horizontal plane of the shell.

EBSD images of representative shells of the limpet *P. rustica* collected from the Ambient and Low sites revealed relatively similar shell crystallography at both sites (Fig. 8). While the shell from the Ambient site had overall lower electron diffraction (Fig. 8a), it is evident that two discrete portions make up the calcite layer: an outer sublayer with smaller crystals oriented with the *c*-axis parallel to the outermost edge of the shell, and an inner sublayer composed of larger crystals with a preferred orientation with the *c*-axis perpendicular to the outermost edge of the shell (Fig. 8b). The same two sublayers within the calcite layer are even more obvious within the shell of a representative individual collected from the Low site (Fig. 8c-d). The outer sublayer of the calcite layer is

composed of small, irregularly shaped crystals, which demonstrate a preferred orientation with the *c*-axis parallel to the outermost edge of the shell. The inner sublayer of the calcite layer is less well defined, but is composed of larger crystals oriented with the *c*-axis perpendicular to the outermost edge of the shell. There is no obvious simplification of the crystallographic structure of the calcite layer within the shell of *P. rustica* at the Low site (Fig. 8d). There does appear, however, to be some loss of organization of the inner (and newer) portion of the calcite layer in the shell from the representative individuals from the Low site (Fig. 8d). As with the shell of *P. caerulea*, the calcite layer at the Low site is thinner than that of the shell of the representative individual from the Ambient site.

Shell Strength Characteristics

The mean force required to fracture the shell did not differ significantly between the Ambient and Low sites for any of the four gastropod species for either the external (*P. caerulea: p* =0.5242; *P. rustica: p* =0.6349; *O. turbinatus: p* =0.8506; *H. trunculus: p*=0.2905) or internal surfaces (*P. caerulea*: *p*=0.355; *P. rustica*: *p* =0.650; *O. turbinatus*: *p*=0.118; *H. trunculus*: *p*=0.574). The mean shell toughness ($J \cdot m^{-3}$) of external shell surfaces also did not differ significantly between shells of individuals from the Ambient and Low sites for any of the gastropod species (*P. caerulea: p* =0.6207; *P. rustica: p* =0.9362; *O. turbinatus: p* =0.8586; *H. trunculus: p* =0.8672). In contrast, the mean shell toughness of internal shell surfaces differed significantly between the two sites for two of the four gastropod species, the limpet *P. rustica* (T-test, t_{35}=2.776, *p* =0.009) and the whelk *H. trunculus* (T-test, t_{14}=2.565, *p* = 0.022). Inner surfaces of shells of the limpet

P. rustica collected from the Low site had significantly higher toughness values than those of individuals collected at the Ambient site. In contrast, inner surfaces of the whelk shells collected from the Low site had significantly lower toughness values than those of individuals collected at the Ambient site.

A significant difference in the mean elasticity (ability to deform and rebound) of the external shell surface was detected in the top-shell snail (T-test, t_{18}=2.423, p =0.026), but not among any of the three other species (*P. caerulea:* p =0.639; *P. rustica:* p =0.629; *H. trunculus:* p =0.431). The external surface elasticity was significantly reduced in top-shell snail shells from individuals at the Low site (0.25 ± 0.02 GPa; n = 8) when compared to those from the Ambient site (0.34 ± 0.02 GPa; n = 12). Both limpets had inner shell surfaces with significantly lower elasticity at the Low site (*P. caerulea*: T-test, t_{21}=2.736, p = 0.012; *P. rustica*: T-test, $t_{32.63}$=4.45, p < 0.0001). Mean elasticity of the inner shell surface did not differ significantly among shells of individuals of the top-shell snail (T-test, t_{15}=0.639, p = 0.533) or whelk (T-test, t_{14}=1.127, p = 0.279) collected from the Ambient and Low sites.

Discussion

A wide variety of mollusks are highly susceptible to the effects of ocean acidification, including those of high commercial importance (Cooley et al. 2012; 2015). Studies carried out at Mediterranean CO_2 seeps have shown that gastropod species diversity declines as seawater pH levels fall and that pH-tolerant species are often smaller than conspecifics living under ambient pH conditions due to increased physiological stress and shell dissolution (Cigliano et al. 2010; Milazzo et al. 2014; Garilli et al. 2015; Harvey et al. 2016). Laboratory studies on a variety of mollusks have also shown that

metabolic costs increase, growth decreases, and overall body size decreases in individuals exposed to acidified conditions (reviewed by Kroeker et al. 2013a). The two species of limpets examined in the present study, *P. caerulea* and *P. rustica*, are clearly exceptions to this general trend, as shell length did not decrease with increasing proximity to the CO_2 seeps. Rodolfo-Metalpa et al. (2011) found that *P. caerulea* living at high CO_2 levels were able to upregulate calcification rates to counteract dissolution, and that this adaptation to hypercapnia was retained even when individuals were transplanted to ambient pH conditions. Here, we found that *P. caerulea* demonstrated a statistically non-significant trend towards increased size with decreasing pH, while *P. rustica* significantly increased in shell size with decreasing pH. Ransome (2007) found that although the abundances of *P. caerulea* decreased with declining pH at a CO_2 seep off the island of Ischia, Italy, mean shell length increased significantly. The larger size of *P. caerulea* at low-pH sites at multiple CO_2 seep systems suggests that this species may be reaping the benefits of increased productivity of the microphytobenthos (Johnson et al. 2015) and decreased competition from less resilient grazers.

A number of investigators have noted that marine invertebrates able to persist in acidified conditions are likely to benefit from decreased competition for the abundant algal food resources known to characterize sites close to seeps (Porzio et al. 2011; Baggini et al. 2015). The larger sizes of *P. caerulea* collected from the site nearest the CO_2 seep may also be the result of individuals allocating greater amounts of energy to shell growth. As shells of juvenile or early adult mollusks are at greater risk of dissolution (Bamber 1990; Green et al. 2004), limpets may necessarily be compensating

by depositing addition shell material that ultimately generates larger shell size in a more acidic environment.

In contrast to the limpets, the top-shell O. *turbinatus* exhibited a significant decrease in shell length with decreasing pH. Similarly, the whelk *Hexaplex trunculus* displayed a trend towards smaller shell size with increasing hypercapnia, which has since been verified statistically by Harvey et al. (2016). Both gastropods have shells composed entirely of aragonite, a mineral known to be twice as soluble as calcite (Mucci 1983), while containing crystals that are smaller and more densely packed than calcite (Weiner and Addadi 1997). This difference in crystalline microstructure makes it more energetically demanding to build or replace shell material that is composed of aragonite (Allemand et al. 2011). Combined, these factors increase the challenges for calcified marine invertebrates with aragonite shells to grow to adult size and maintain their shells under low pH stress. Accordingly, the aragonitic shell of new recruits of the reef-building vermetid gastropod *Dendropoma petraeum* transplanted along the CO_2 gradient off Vulcano Island, dissolved at low pH levels (Milazzo et al. 2014). Moreover, the Mg/Ca content of their shells significantly increased in seawater with lowered carbonate ion concentrations, reflecting an impaired ability of the vermetids to remove Mg from haemolymph and extrapallial fluids

Because there are differences in the vulnerability of shells to reduced pH based on their ratio of calcite to aragonite, it is important to evaluate the lability of the ratio of these $CaCO_3$ polymorphs at the three pH sites sampled in the present study. Our XRD analyses indicated that there was no change in the ratio of calcite to aragonite in the shells of the limpet *P. caerulea.* This observation was contrary to our expectations, as two

previous studies of *P. caerulea* found that individuals counteract dissolution of their shells in reduced pH seawater by up-regulating calcification, resulting in a thickening of the shell's aragonite layer (Rodolfo-Metalpa et al. 2011; Langer et al. 2014). Accordingly, we expected to find that the ratio of calcite to aragonite in the shells of individuals would decrease as pH decreased. One possibility for this discrepancy is that both studies cited above were conducted at much lower levels of pH than those at the established field sites in the present study. The low pH in both previous studies was between 6.4 and 6.8, levels well below the 7.73 pH that characterized our Low site. It is possible that a pH threshold exists, below which limpets will begin up-regulating calcification. If collection of *P. caerulea* had occurred closer to the CO_2 seep, we may have detected a thickening of the aragonitic layer, and the expected decline in the ratio of calcite to aragonite.

In contrast to the limpet *P. caerulea*, the shells of its congener *P. rustica* displayed a significant increase in the calcite to aragonite ratio for shells of individuals collected at the Low site. Since this species also had a longer shell at the Low site, it may be that the observed increase in calcite stems from the allocation of calcite along the shell margins during shell lengthening. If this increase in shell length occurred without a corresponding increase in shell thickness, this could explain the higher calcite to aragonite ratio detected. Lastly, because the shell of *P. rustica* is known to have an outer periostracum (not all limpets possess a periostracum), this proteinaceous outer layer may provide additional protection from dissolution and, therefore, the loss of calcitic shell material (Prusina et al. 2015).

Recent studies have suggested that dissolution of shells may be an equal, if not greater, threat than the altered calcification rates known to occur under conditions of ocean acidification (Roleda et al. 2012; Eyre et al. 2014). If true, our ability to predict the prospective impacts of ocean acidification will require considerable knowledge of shell mineralogy, microstructure, and microtexture. In the present study, scanning electron microscopy (SEM) confirmed the presence of both aragonitic and calcitic layers in the shells of both limpet species (MacClintock 1967; Langer et al. 2014). Interestingly, while our XRD data did not reveal an increase in the amount of aragonite in shells of individuals collected from the Low site, a representative shell from the same site examined with SEM was 8.9% thicker than a representative shell from an individual from the Ambient site. This thickening of the shell supports previous studies with *P. caerulea* which indicate that individuals compensate for dissolution under ocean acidification conditions by thickening of the aragonite layer coincident with the apex of the shell (Rodolfo-Metalpa et al. 2011). In contrast to the shell of *P. caerulea*, the representative shell of *P. rustica* collected at the Low site showed no evident increase in thickness at the apex of the Low site shells. In fact, the Low site shell is thinner than the Ambient site shell. The thinning of the shell could be a result of dissolution or decreased energy allocation to thickening of the shell. Given that *P. rustica* had significantly larger shells at the Low site, it is possible that the growth in length was achieved at the expense of increasing shell thickness.

The top-shell snail, which possesses a periostracum, exhibited greater microbial bioerosion at the Low site as compared to the Ambient site. This could be explained by damage to, or erosion of, the periostracum, a likely result of chronic exposure to

hypercapnia. The representative top-shell snail collected at the Low site showed no reduction in layering when compared to that collected at the Ambient site. Contrary to the top-shell snail, a difference was clearly evident in the layering in shells of representative whelks collected at the Ambient and the Low sites. The representative shell collected at the Low site exhibited reduced microstructural layering visible in the shell's cross-section. This reduction in complexity may contribute to structural weaknesses detected in shell compression analyses (see below). As seen in the sublittoral limpet *P. caerulea*, shell cross-section analysis also indicated evidence of greater microbial bioerosion in the outer shell of the representative whelk collected at the Ambient site. Both the limpet *P. caerulea* and the whelk lack a periostracum, so their external shell is likely to be more vulnerable to biotic and abiotic erosion.

In the present study, electron backscatter diffraction (EBSD) facilitated the identification of differences in crystallography within the calcite regions of the shells of the two limpet species collected from the Ambient and Low sites. Although EBSD analysis of aragonitic shell microstructures is possible, including those of limpets (e.g., Suzuki et al. 2010), the absence of sufficient diffraction and continuous data prevented the use of this technique to examine the aragonitic shells of the whelk and top-shell snail and the aragonite portions of the limpet shells. EBSD revealed that the shell of a representative individual of *P. caerulea* collected at the Ambient site exhibited two well-defined sublayers of organized calcite crystals. The two sublayers, in combination, are 42.8% thicker in the shell of the individual collected at the Ambient site when compared to that of the individual from the Low site. This reduction in thickness was the result of simplification of the calcite layer (reduction in sublayers) at decreased pH. Interestingly,

the orientation of the crystals in this single layer more closely resembles that seen in the outer calcite layer of the shell collected at the Ambient site. This suggests that simple dissolution of the outer layer is not the case, but may rather reflect a reduction in the capacity to produce new shell material. The shell of *P. caerulea* collected at the Low site also had less organized crystallography within its single layer of calcite, indicating less control over the biological processes regulating biomineralization. For example, several studies have shown that shell ultrastructure can be altered and the level of disorganization of calcite or aragonite crystals increased under conditions of ocean acidification (Welladsen et al. 2010; Hahn et al. 2012; Fitzer et al. 2014; Li et al. 2014).

In contrast to its congener, there was no difference in the crystallography of the shells of *P. rustica* at the Ambient and the Low sites. Other than the entire calcite layer being 47.5% thinner in the shell of the individual from the Low site, the two calcite sublayers in the shell at the Low site were similar to those at the Ambient site. This lack of difference may reflect the presence of the outer protective periostracum. Fortuitously, our use of two closely related limpet species that differ in the presence or absence of a periostracum, a difference that might be attributed to occupying strikingly different habitats (intertidal versus subtidal) provides a mechanism to evaluate the role of the periostracum in resisting ocean acidification.

Finally, various measures of shell material properties in the gastropod species were employed to determine quantitatively if shell integrity had been compromised with chronic exposure to reduced pH. Each of the four species experienced a significant decrease in either toughness or elasticity of the shell with reduced pH. Despite visible evidence of dissolution of shells from the Low site, no significant effect on the force

required to crack the shell was observed in any species. Welladsen et al. (2010) reported that while exposure to near-future levels of ocean acidification decreased the force required to crush the shell of the oyster *Pinctada fucata*, there was no change in the force needed to initially crack the shell. While no significant change in force to crack shells was seen between gastropods collected from the Low and Ambient sites, it is possible that additional shell strength analyses, such as measures of crushing compression, could reveal a decrease in required force to crush shells of individuals living at low pH. However, even compromising a single material property can result in a decrease in shell integrity that increases the vulnerability under conditions of ocean acidification.

Patella rustica sampled from the Low site experienced a significant increase in shell toughness but decrease in shell elasticity of the internal shell surface. Therefore, the surface of the internal shell was less brittle and stiffer. The lack of similar changes (toughness and elasticity) in the external surface of the shell could be due to the protective nature of the periostracum. This outer shell layer slows the rate of dissolution, prevents entry of bioeroding organisms, and ultimately reduces physiological stress by lowering the investment of energy to shell maintenance (Neves et al. 2007; Coleman et al. 2014). Another factor that can influence shell elasticity is shell mineralogy. In a study of calcareous tubes produced by the serpulid tubeworm *Hydroides elegans*, Chan et al. (2012) postulated that shells composed of both aragonite and calcite have lower elasticity when their aragonite content declines. Indeed, invertebrate calcareous structures that are composed predominantly of aragonite have greater elasticity than those that are largely calcite (Pérez-Huerta et al. 2008; Weiner 2008). In the present study, the percent aragonite decreased in shells of *P. rustica* at the Low site and shell elasticity was also

significantly reduced. This reduction was detected on the interior surface near the edge of the shell, the site of most predator attacks on limpets (Lowell 1986). Both crabs and sea birds have been observed to pry or chip at the edges of limpet shells to gain access to the soft body tissues (Coleman et al. 1999). Reduced shell elasticity may compromise the ability to withstand such predator attacks.

Similar to its intertidal congener, the subtidal limpet *P. caerulea* exhibited a decrease in shell elasticity of the inner shell surface at the Low site. However, there was no corresponding reduction in percent aragonite. As a subtidal species, the prolonged exposure to acidified water could result in the change in shell elasticity. Chronic exposure to reduced pH may also affect the organization of shell minerals. Welladsen et al. (2010) reported that the aragonitic inner shell layer of the pearl oyster *Pinctada fucata* became disorganized, with crystal structures developing as misshapen and irregular when chronically exposed to reduced pH. In the present study, crystallographic analysis revealed a decrease in crystal organization and a simplification in the calcite layering in a representative shell of *P. caerulea* collected from the Low site. While not investigated in the present study, if layers of aragonite crystals are similarly reduced, the hardness of the shell will be reduced (He et al. 1991; Yang et al. 2011). These differences in the material properties of shells of two closely related limpets, *P. rustica* and *P. caerulea*, exposed chronically to low pH highlight the complicated nature of predicting the impacts of ocean acidification on a given species (Kroeker et al. 2013b).

The top-shell snail *Osilinus turbinatus* was the only species among the four gastropods examined in the present study to exhibit a significant decrease in elasticity of the external surface of the shell with exposure to chronic low pH. The obvious loss of the

outer protective periostracum along with a decrease in shell elasticity is likely to make shells more susceptible to bioeroding organisms and boring and crushing predators. Coleman et al. (2014) reported the impacts of laboratory-simulated ocean acidification on the shells of two common intertidal gastropods that are in the same superfamily (*Trochoidea*) as *O. turbinatus*. One of the species, *Austrocochlea procata*, demonstrated a decrease in shell strength (force required to crack the shell) in response to reduced pH. However, the second gastropod, *Subninella undulata*, which in contrast to *A. procata* possessed a periostracum, showed no reduction in shell strength at low pH. The top-shell snail investigated in the present study demonstrated decreased shell integrity in terms of elasticity but no overall decrease in force required to crack the shell as seen with *S. undulata*. It is possible that in the top-shell snail a reduction in shell elasticity, but not the force required to break the shell, is partially due to the periostracum and its added resilience to dissolution in acidic environments.

Shells of the whelk *H. trunculus* at the Low site revealed a significantly reduced measure of toughness of the internal shell surface when compared to those from the Ambient site. While not significant, there were also strong trends towards a decrease in the force necessary to crack the shell and the elasticity of the external shell surface of individuals collected at the Low site. The reduced toughness of the internal shell surface suggests either dissolution is occurring or calcification is impaired due to physiological stress associated with a low pH environment or the undersaturation of aragonite that characterizes the Low site (Milazzo et al. 2014). As *H. trunculus* has a shell comprised entirely of aragonite, a mineral that requires a greater energetic investment to produce than calcite (Allemand et al. 2011), pH stress may reduce the capacity to maintain or

produce the inner shell surface. Costs of shell maintenance and production are not trivial. For example, the cost of producing the organic matrix within calcium carbonate can cost an organism 10-60% of the energy invested in somatic growth, and the polymorph aragonite has a higher level of organic material within its matrix than does calcite (Palmer 1992). *H. trunculus* is unique among the four gastropods examined as it not only depends on its shell as refuge from predators, but uses the toothed lip of the shell aperture to chip off the shells margins of prospective prey including gastropods and bivalves (Peharda and Morton 2006; Morton et al. 2007). With high levels of dissolution and pitting observed in the external shell and the decreased toughness of the internal shell detected, it is likely that a shell chipping mode of predation will be compromised.

The present study is consistent with the general consensus that there is a wide degree of species-specific variation in responses of marine mollusks to ocean acidification (Parker et al. 2013). For example, significant differences were found even among gastropods (limpets) of the same genus in the present study. While various properties of the $CaCO_3$ shells appear to be resilient to chronic pH levels as low as 7.7, evidence of dissolution, disorganized and simplified crystallographic arrangement of minerals, and impaired shell integrity suggest challenges to survival in a near future pH environment. Whether these compromised shell features hinder populations remains to be determined. However, it is noteworthy that Hall-Spencer et al. (2008) found that both the whelk and top-shell snail in the present study were reduced or absent at a separate seep site (Ischia, Italy) at pH levels similar to our Low site. The results presented here depict a situation in which gastropods experience alterations in biomineralization and mechanical

properties of their shells. These alterations have the potential to render individuals more susceptible to infection or predation.

Acknowledgements

The authors thank Gopi Samudrala and Yogesh Vohra for their assistance with X-ray diffraction measurements performed in the UAB Department of Physics, as well as William Monroe in the UAB SEM Facility of the Department of Materials Science and Engineering. We also extend our gratitude to Margaret Amsler for assistance with sample preparations. We thank Raya Berman and Michelle Gannon in the Department of Geology at the University of Alabama for their aid with electron backscatter diffraction analyses. Finally, we thank Justin Ries and Isaac Westfield for assistance with material strength analyses carried out in the Department of Marine and Environmental Sciences at Northeastern University. The present study was supported in part by National Science Foundation grant ANT-1041022 awarded to JBM, CDA, and Robert A. Angus. JBM acknowledges support provided by the UAB Endowed Professorship in Polar and Marine Biology.

References

Allemand D, Tambutté É, Zoccola D, Tambutté S (2011) Coral Calcification, Cells to Reefs. In: Dubinsky Z, Stambler N (eds) Coral Reefs: An Ecosystem in Transition. Springer Netherlands, Dordrecht, pp 119-150

Baggini C, Issaris Y, Salomidi M, Hall-Spencer J (2015) Herbivore diversity improves benthic community resilience to ocean acidification. J Exp Mar Biol Ecol 469: 98-104 doi 10.1016/j.jembe.2015.04.019

Bamber R (1990) The effects of acidic seawater on three species of lamellibranch mollusc. J Exp Mar Biol Ecol 143: 181-191 doi 10.1016/0022-0981(90)90069-O

Boatta F, D'Alessandro W, Gagliano A, Liotta M, Milazzo M, Rodolfo-Metalpa R, Hall-Spencer J, Parello F (2013) Geochemical survey of Levante Bay, Vulcano Island (Italy), a natural laboratory for the study of ocean acidification. Mar Pollut Bull 73: 485-494 doi 10.1016/j.marpolbul.2013.01.029

Caldeira K, Wickett ME (2003) Oceanography: anthropogenic carbon and ocean pH. Nature 425: 365-365 doi 10.1038/425365a

Calosi P, Rastrick SP, Lombardi C, de Guzman HJ, Davidson L, Jahnke M, Giangrande A, Hardege JD, Schulze A, Spicer JI (2013) Adaptation and acclimatization to ocean acidification in marine ectotherms: an *in situ* transplant experiment with polychaetes at a shallow CO_2 vent system. Phil Trans R Soc Lond B 368: 20120444 doi 10.1098/rstb.2012.0444

Chan VBS, Li C, Lane AC, Wang Y, Lu X, Shih K, Zhang T, Thiyagarajan V (2012) CO_2-driven ocean acidification alters and weakens integrity of the calcareous tubes produced by the serpulid tubeworm, *Hydroides elegans*. PLoS ONE 7: e42718 doi 10.1371/journal.pone.0042718

Chen Y, Wu J, Chen C, Liu L (2014) Effects of low pH stress on shell traits and proteomes of the dove snail, *Anachis misera*, inhabiting shallow vent environments off Kueishan Islet, Taiwan. Biogeosci Discuss 11: 17207-17226 doi 10.5194/bgd-11-17207-2014

Cigliano M, Gambi M, Rodolfo-Metalpa R, Patti F, Hall-Spencer J (2010) Effects of ocean acidification on invertebrate settlement at volcanic CO_2 vents. Mar Biol 157: 2489-2502 doi 10.1007/s00227-010-1513-6

Coleman DW, Byrne M, Davis AR (2014) Molluscs on acid: gastropod shell repair and strength in acidifying oceans. Mar Ecol Prog Ser 509: 203-211 doi 10.3354/meps10887

Coleman RA, Goss-Custard JD, dit Durell SELV, Hawkins SJ (1999) Limpet *Patella* spp. consumption by oystercatchers *Haematopus ostralegus*: a preference for solitary prey items. Mar Ecol Prog Ser 183: 253-261

Coleman RA, Underwood AJ, Benedetti-Cecchi L, Åberg P, Arenas F, Arrontes J, Castro J, Hartnoll RG, Jenkins SR, Paula J (2006) A continental scale evaluation of the role of limpet grazing on rocky shores. Oecologia 147: 556-564 doi 10.1007/s00442-005-0296-9

Collard M, De Ridder C, David B, Dehairs F, Dubois P (2015) Could the acid–base status of Antarctic sea urchins indicate a better-than-expected resilience to near-future ocean acidification? Global Chan Biol 21: 605-617

Cooley SR, Lucey N, Kite-Powell H, Doney SC (2012) Nutrition and income from molluscs today imply vulnerability to ocean acidification tomorrow. Fish and Fisheries 13: 182-215 doi 10.1111/j.1467-2979.2011.00424.x

Crothers J (2001) Common topshells: an introduction to the biology of *Osilinus lineatus* with notes on other species in the genus. Field Studies 10: 115-160

Eyre BD, Andersson AJ, Cyronak T (2014) Benthic coral reef calcium carbonate dissolution in an acidifying ocean. Nat Clim Change 4: 969-976 doi 10.1038/nclimate2380

Fabricius K, De'ath G, Noonan S, Uthicke S (2014) Ecological effects of ocean acidification and habitat complexity on reef-associated macroinvertebrate communities. Proc R Soc Lond B 281: 20132479 doi 10.1098/rspb.2013.2479

Fitzer SC, Phoenix VR, Cusack M, Kamenos NA (2014) Ocean acidification impacts mussel control on biomineralisation. Sci Rep 4 doi 10.1038/srep06218

Garilli V, Rodolfo-Metalpa R, Scuderi D, Brusca L, Parrinello D, Rastrick SP, Foggo A, Twitchett RJ, Hall-Spencer JM, Milazzo M (2015) Physiological advantages of dwarfing in surviving extinctions in high-CO_2 oceans. Nat Clim Change 5: 678-682 doi 10.1038/nclimate2616

Gaylord B, Kroeker KJ, Sunday JM, Anderson KM, Barry JP, Brown NE, Connell SD, Dupont S, Fabricius KE, Hall-Spencer JM (2015) Ocean acidification through the lens of ecological theory. Ecology 96: 3-15 doi 10.1890/14-0802.1

Green MA, Jones ME, Boudreau CL, Moore RL, Westman BA (2004) Dissolution mortality of juvenile bivalves in coastal marine deposits. Limnol Oceanogr 49: 727-734

Hahn S, Rodolfo-Metalpa R, Griesshaber E, Schmahl WW, Buhl D, Hall-Spencer J, Baggini C, Fehr K, Immenhauser A (2012) Marine bivalve shell geochemistry and ultrastructure from modern low pH environments: environmental effect versus experimental bias. Biogeosci 9: 1897-1914 doi 10.5194/bg-9-1897-2012

Hall-Spencer JM, Rodolfo-Metalpa R, Martin S, Ransome E, Fine M, Turner SM, Rowley SJ, Tedesco D, Buia M-C (2008) Volcanic carbon dioxide vents show

ecosystem effects of ocean acidification. Nature 454: 96-99 doi 10.1038/nature07051

Harvey BP, McKeown NJ, Rastrick SP, Bertolini C, Foggo A, Graham H, Hall-Spencer JM, Milazzo M, Shaw PW, Small DP (2016) Individual and population-level responses to ocean acidification. Sci Rep 6: 20194 doi 10.1038/srep20194

He MY, Bartlett A, Evans AG, Hutchinson JW (1991) Kinking of a Crack out of an Interface: Role of In-Plane Stress. J Am Ceram Soc 74: 767-771 doi 10.1111/j.1151-2916.1991.tb06922.x

Inoue S, Kayanne H, Yamamoto S, Kurihara H (2013) Spatial community shift from hard to soft corals in acidified water. Nat Clim Change 3: 683-687 doi 10.1038/nclimate1855

IPCC (2014) Climate Change 2014: Synthesis Report. Contribution of Working Groups, I, II, and III to the Fifth Assessment Report of the Intergovernmental Panel on Climate Change, Geneva, Switzerland

Jenkins S, Coleman R, Della Santina P, Hawkins S, Burrows M, Hartnoll R (2005) Regional scale differences in the determinism of grazing effects in the rocky intertidal. Mar Ecol Prog Ser 287: 77-86

Johnson VR, Brownlee C, Milazzo M, Hall-Spencer JM (2015) Marine Microphytobenthic Assemblage Shift along a Natural Shallow-Water CO_2 Gradient Subjected to Multiple Environmental Stressors. J Mar Sci Eng 3: 1425-1447 doi 10.3390/jmse3041425

Katsanevakis S, Lefkaditou E, Galinou-Mitsoudi S, Koutsoubas D, Zenetos A (2008) Molluscan species of minor commercial interest in Hellenic seas: distribution, exploitation and conservation status. Mediterr Mar Sci 9: 77-118 doi 10.12681/mms.145

Keasar T, Safriel U (1994) The establishment of a territory: effects of food and competitors on movement patterns in *Patella caerulea* limpets. Ethol Ecol Evol 6: 103-115 doi 10.1080/08927014.1994.9523012

Kroeker KJ, Kordas RL, Crim R, Hendriks IE, Ramajo L, Singh GS, Duarte CM, Gattuso JP (2013a) Impacts of ocean acidification on marine organisms: quantifying sensitivities and interaction with warming. Global Chan Biol 19: 1884-1896 doi 10.1111/gcb.12179

Kroeker KJ, Micheli F, Gambi MC (2013b) Ocean acidification causes ecosystem shifts via altered competitive interactions. Nat Clim Change 3: 156-159 doi 10.1038/nclimate1680

Langer G, Nehrke G, Baggini C, Rodolfo-Metalpa R, Hall-Spencer J, Bijma J (2014) Limpets counteract ocean acidification induced shell corrosion by thickening of aragonitic shell layers. Biogeosci 11: 7363-7368 doi 10.5194/bg-11-7363-2014

Li C, Chan V, He C, Meng Y, Yao H, Shih K, Thiyagarajan V (2014) Weakening Mechanisms of the Serpulid Tube in a High-CO_2 World. Environ Sci Tech 48: 14158-14167 doi 10.1021/es501638h

Lowell RB (1986) Crab predation on limpets: predator behavior and defensive features of the shell morphology of the prey. The Biological Bulletin 171: 577-596

MacClintock C (1967) Shell structures of patelloid and bellerophontoid gastropods (Mollusca). Peabody Museam of Natural History Bulletin

Mauro A, Arculeo M, Parrinello N (2003) Morphological and molecular tools in identifying the Mediterranean limpets *Patella caerulea*, *Patella aspera* and *Patella rustica*. J Exp Mar Biol Ecol 295: 131-143 doi 10.1016/S0022-0981(03)00291-0

McClintock JB, Amsler MO, Angus RA, Challener RC, Schram JB, Amsler CD, Mah CL, Cuce J, Baker BJ (2011) The Mg-calcite composition of Antarctic echinoderms: important implications for predicting the impacts of ocean acidification. The Journal of Geology 119: 457-466 doi 10.1086/660890

Milazzo M, Rodolfo-Metalpa R, San Chan VB, Fine M, Alessi C, Thiyagarajan V, Hall-Spencer JM, Chemello R (2014) Ocean acidification impairs vermetid reef recruitment. Sci Rep 4: 4189 doi 10.1038/srep04189

Milliman J (1974) Marine Carbonates, Part I. Springer-Verlag, New York

Morton B, Peharda M, Harper E (2007) Drilling and chipping patterns of bivalve prey predation by *Hexaplex trunculus* (Mollusca: Gastropoda: Muricidae). J Mar Biol Ass UK 87: 933-940 doi 10.1017/S0025315407056184

Mucci A (1983) The solubility of calcite and aragonite in seawater at various salinities, temperatures, and one atmosphere total pressure. Am J Sci 283: 780-799 doi 10.2475/ajs.283.7.780

Nakicenovic N, Swart R (2000) Emissions Scenarios: A Special Report of Working Group III of the Intergovernmental Panel on Climate Change, New York

Neves JP, Rodrigues SC, Simões MG, Kotzian CB (2007) Taphonomic role of periostracum on the preservational potential of the freshwater bivalve mollusk shells. Geological Society of America Abstracts pp 95

Newcomb LA, Milazzo M, Hall-Spencer JM, Carrington E (2015) Ocean acidification bends the mermaid's wineglass. Biol Lett 11: 20141075 doi 10.1098/rsbl.2014.1075

Orr JC, Fabry VJ, Aumont O, Bopp L, Doney SC, Feely RA, Gnanadesikan A, Gruber N, Ishida A, Joos F (2005) Anthropogenic ocean acidification over the twenty-first century and its impact on calcifying organisms. Nature 437: 681-686 doi 10.1038/nature04095

Palmer AR (1992) Calcification in marine molluscs: how costly is it? Proc Nat Acad Sci 89: 1379-1382

Parker LM, Ross PM, O'Connor WA, Pörtner HO, Scanes E, Wright JM (2013) Predicting the response of molluscs to the impact of ocean acidification. Biology 2: 651-692 doi 10.3390/biology2020651

Peharda M, Morton B (2006) Experimental prey species preferences of *Hexaplex trunculus* (Gastropoda: Muricidae) and predator–prey interactions with the Black mussel *Mytilus galloprovincialis* (Bivalvia: Mytilidae). Mar Biol 148: 1011-1019 doi 10.1007/s00227-005-0148-5

Pérez-Huerta A, Cusack M (2009) Optimizing electron backscatter diffraction of carbonate biominerals—resin type and carbon coating. Microsc Microanal 15: 197-203 doi 10.1017/S1431927609090370

Pérez-Huerta A, Cusack M, Zhu W (2008) Assessment of crystallographic influence on material properties of calcite brachiopods. Mineral Mag 72: 563-568 doi 10.1180/minmag.2008.072.2.563

Pérez-Huerta A, Dauphin Y, Cuif JP, Cusack M (2011) High resolution electron backscatter diffraction (EBSD) data from calcite biominerals in recent gastropod shells. Micron 42: 246-251 doi 10.1016/j.micron.2010.11.003

Porzio L, Buia MC, Hall-Spencer JM (2011) Effects of ocean acidification on macroalgal communities. J Exp Mar Biol Ecol 400: 278-287 doi 10.1016/j.jembe.2011.02.011

Prusina I, Peharda M, Ezgeta-Balic D, Puljas S, Glamuzina B, Golubic S (2015) Life-history trait of the Mediterranean keystone species *Patella rustica*: growth and microbial bioerosion. Mediterr Mar Sci 16: 393-401 doi 10.12681/mms.1121

R Development Core Team (2010) R: A language and environment for statistical computing. R Foundation for Statistical Computing, Vienna, Austria

Ransome E (2007) Determining the effects of ocean acidification on intertidal organisms. MRes Thesis, University of Plymouth, Plymouth, UK

Ries JB (2011) Skeletal mineralogy in a high-CO_2 world. J Exp Mar Biol Ecol 403: 54-64 doi 10.1016/j.jembe.2011.04.006

Ries JB, Cohen AL, McCorkle DC (2009) Marine calcifiers exhibit mixed responses to CO_2-induced ocean acidification. Geology 37: 1131-1134 doi 10.1130/G30210A.1

Rilov G, Benayahu Y, Gasith A (2004) Life on the edge: do biomechanical and behavioral adaptations to wave-exposure correlate with habitat partitioning in predatory whelks? Mar Ecol Prog Ser 282: 193-204

Rodolfo-Metalpa R, Houlbrèque F, Tambutté É, Boisson F, Baggini C, Patti FP, Jeffree R, Fine M, Foggo A, Gattuso J (2011) Coral and mollusc resistance to ocean acidification adversely affected by warming. Nat Clim Change 1: 308-312 doi 10.1038/nclimate1200

Roleda MY, Boyd PW, Hurd CL (2012) Before ocean acidification: calcifier chemistry lessons. J Phycol 48: 840-843 doi 10.1111/j.1529-8817.2012.01195.x

Sawyer JA, Zuschin M, Riedel B, Stachowitsch M (2009) Predator–prey interactions from in situ time-lapse observations of a sublittoral mussel bed in the Gulf of Trieste (Northern Adriatic). J Exp Mar Biol Ecol 371: 10-19 doi 10.1016/j.jembe.2008.12.010

Suzuki M, Kameda J, Sasaki T, Saruwatari K, Nagasawa H, Kogure T (2010) Characterization of the multilayered shell of a limpet, *Lottia kogamogai* (Mollusca: Patellogastropoda), using SEM–EBSD and FIB–TEM techniques. J Struct Biol 171: 223-230 doi 10.1016/j.jsb.2010.04.008

Swiney KM, Long WC, Foy RJ (2016) Effects of high pCO_2 on Taner crab reproduction and early life history - Part I: long-term exposure reduces hatching success and female calcification, and alters embryonic development. ICES J Mar Sci 73: 825-835 doi 10.1093/icesjms/fsv201

Weiner S (2008) Biomineralization: a structural perspective. J Struct Biol 163: 229-234 doi 10.1016/j.jsb.2008.02.001

Weiner S, Addadi L (1997) Design strategies in mineralized biological materials. J Mater Chem 7: 689-702 doi 10.1039/A604512J

Welladsen HM, Southgate PC, Heimann K (2010) The effects of exposure to near-future levels of ocean acidification on shell characteristics of *Pinctada fucata* (Bivalvia: Pteriidae). Molluscan Res 30: 125

Yang W, Zhang G, Liu H, Li X (2011) Microstructural characterization and hardness behavior of a biological *Saxidomus purpuratus* shell. J Mater Sci Tech 27: 139-146 doi 10.1016/S1005-0302(11)60039-X

Table 1. Total sample sizes of shells and their mean length (±SE) for each of four gastropod species collected at ambient, moderate, and low pH seep sites. Also shown are the sample sizes of shells examined from each pH site for x-ray diffraction (XRD) and strength analyses

Species	pH	Total Sample Size	XRD Sample Size	Strength Sample Size
Whelk *H. trunculus*	8.15±0.01 (n=95)	24	13	9
	8.03±0.01 (n=95)	34	13	0
	7.73±0.02 (n=95)	25	14	9
Top-shell *O. turbinatus*	8.15±0.01 (n=95)	50	15	12
	8.03±0.01 (n=95)	31	15	0
	7.73±0.02 (n=95)	28	16	9
Limpet *P. caerulea*	8.15±0.01 (n=95)	20	11	7
	8.03±0.01 (n=95)	31	21	0
	7.73±0.02 (n=95)	47	25	17
Limpet *P. rustica*	8.15±0.01 (n=95)	81	23	23
	8.03±0.01 (n=95)	32	22	0
	7.73±0.02 (n=95)	35	16	15

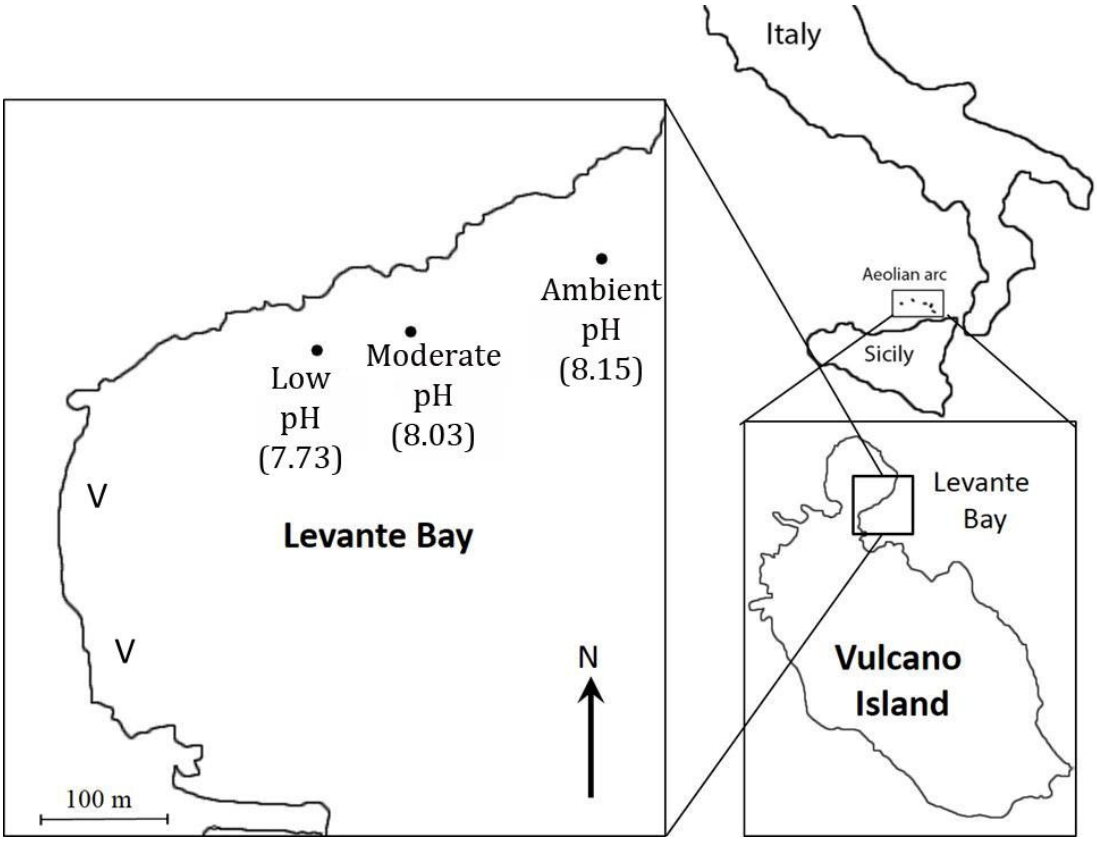

Figure 1. Location of sampling sites along the northeastern shore of Levante Bay, Vulcano Island, Italy. The "V" represents locations of CO_2 seeps

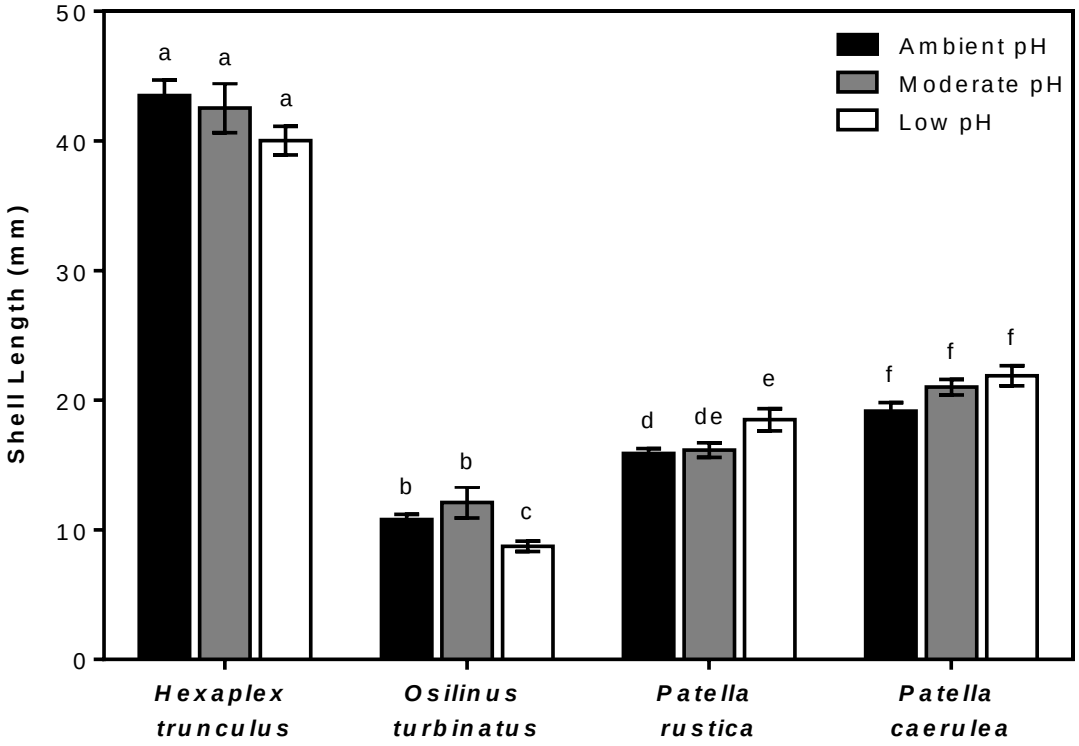

Figure 2. Mean shell length for four species of gastropods collected from ambient, moderate, and low pH sites in shallow water off Vulcano. Error bars are mean ± SE mm. Lowercase letters represent significant differences in mean shell lengths for each species for each of the three seep sites

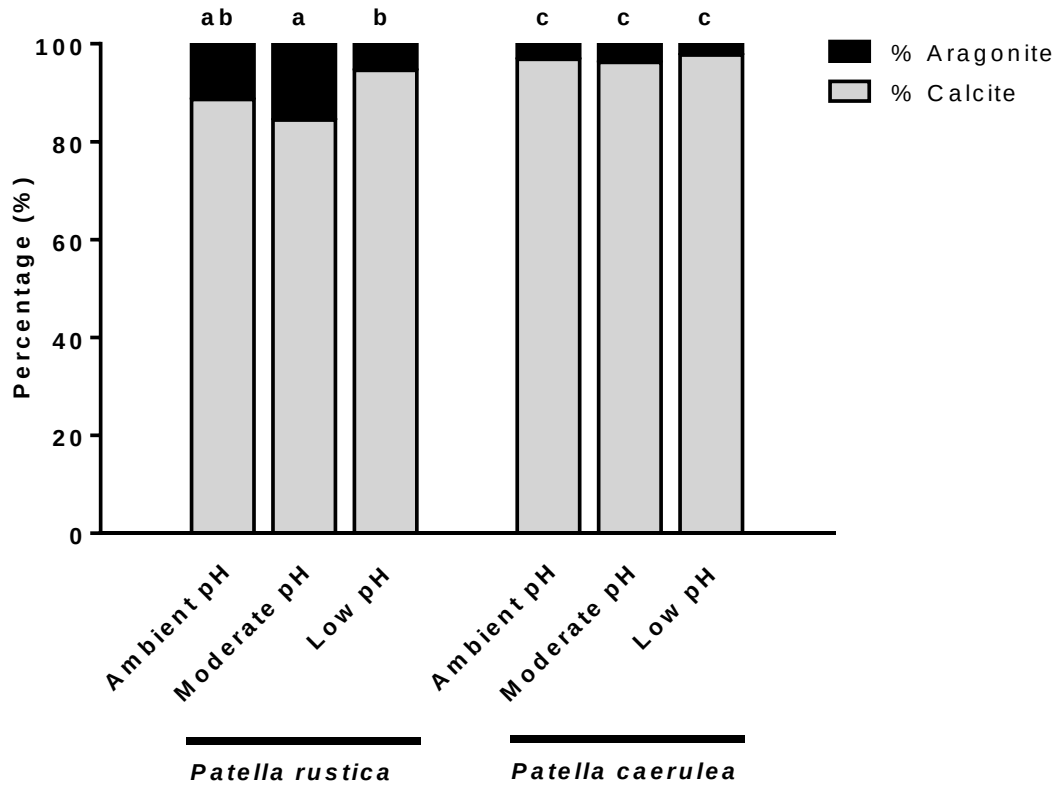

Figure 3. Percentages of aragonite and calcite in the shells of the limpets *P. rustica* and *P. caerulea* collected from ambient, moderate, and low pH sites off Vulcano. Lowercase letters indicate significant differences in the ratio of aragonite to calcite in shells within a given species. Comparisons were made only within, not between, species

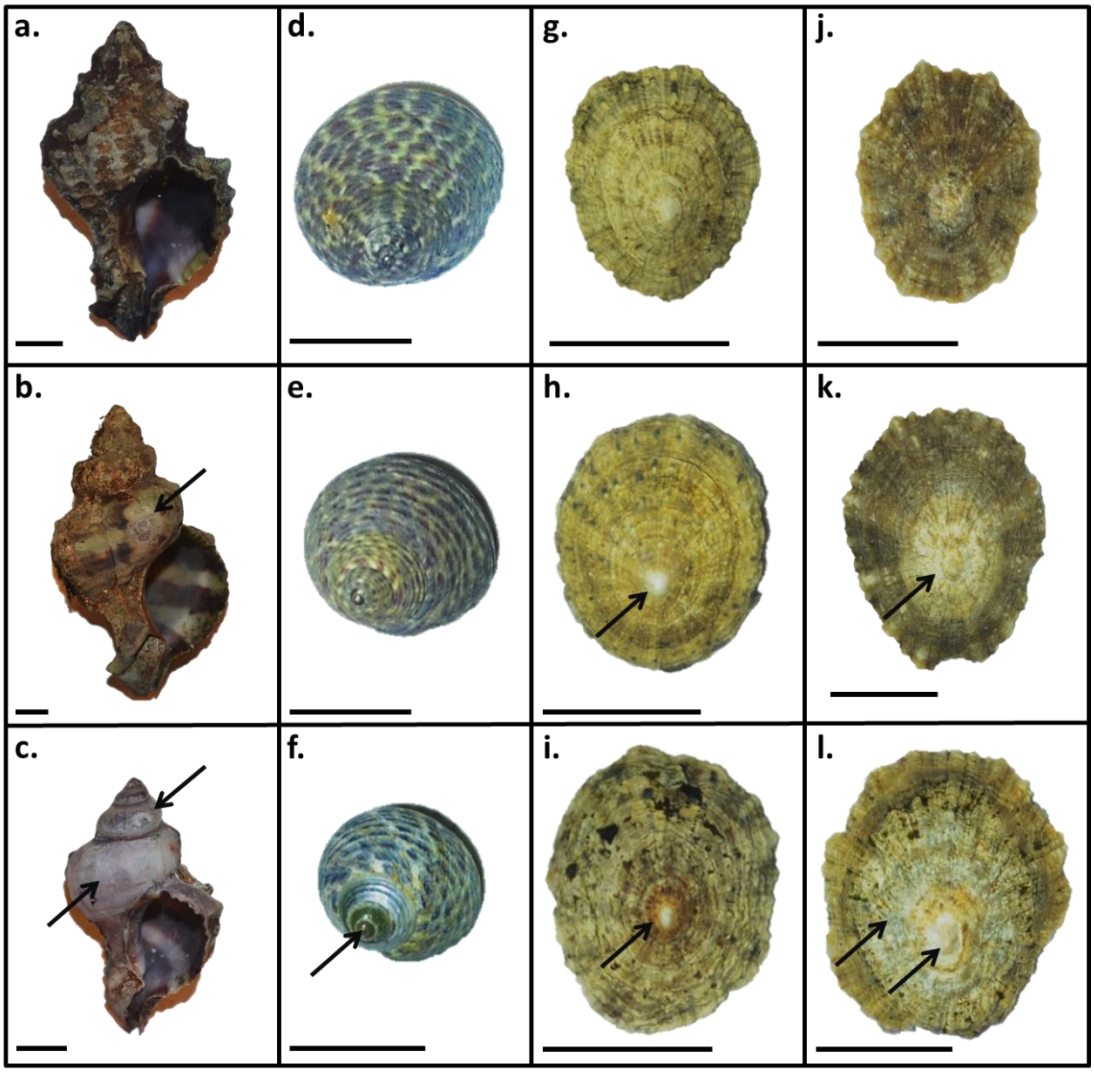

Figure 4. Representative digital photographs of shells collected from ambient (row 1), moderate (row 2), and low (row 3) pH sites off Vulcano for the gastropods *Hexaplex trunculus* (a-c), *Osilinus turbinatus* (d-f), *Patella rustica* (g-i), and *Patella caerulea* (j-l). Scale bars for each picture represent 1 cm. Arrows indicate areas of visible dissolution

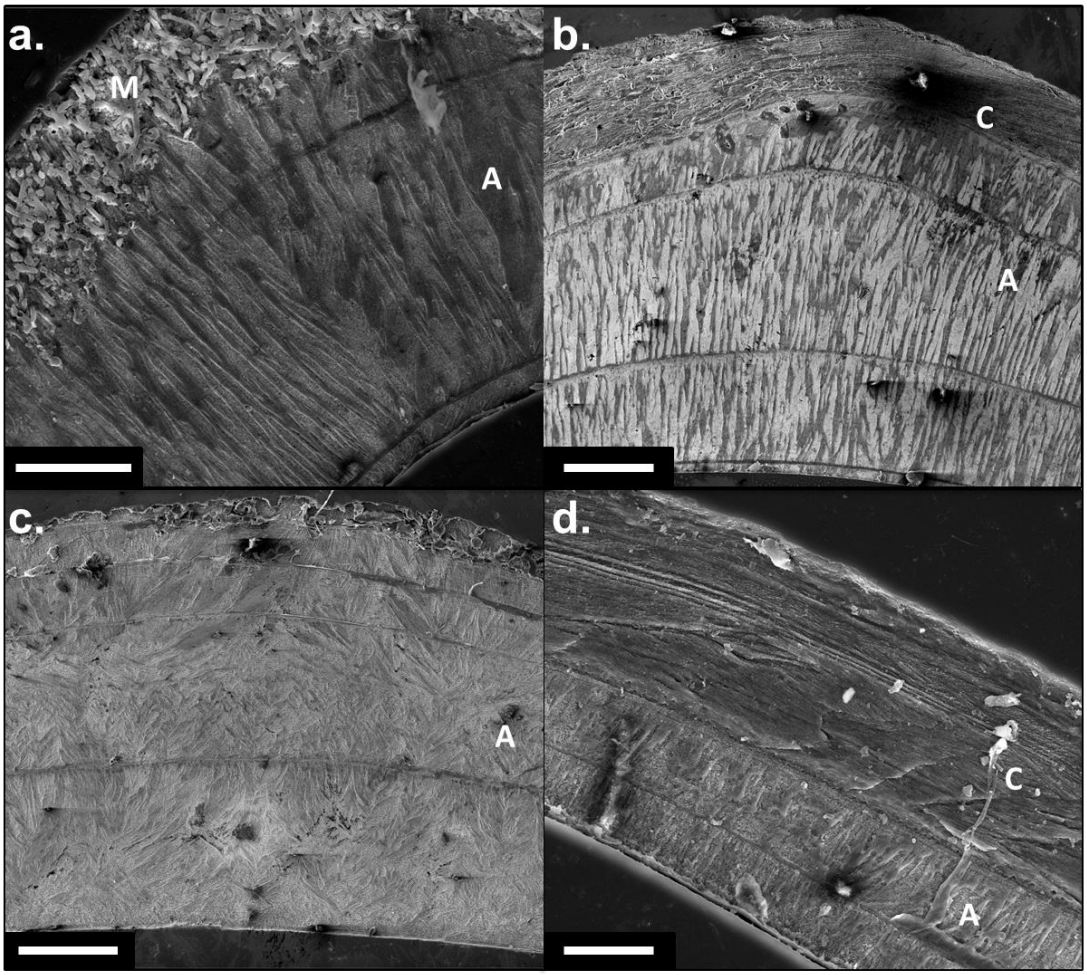

Figure 5 Scanning electron microscopy of shells from both limpet species collected at three CO_2 seep sites off Vulcano Island, Italy. *Patella caerulea* at (a) ambient pH and (b) low pH. *Patella rustica* at (c) ambient pH and (d) low pH. The presence of microbes on the shell is represented by an "M", aragonite layers are marked with an "A", and calcite layers are marked with a "C." Scale bars represent 100 μm

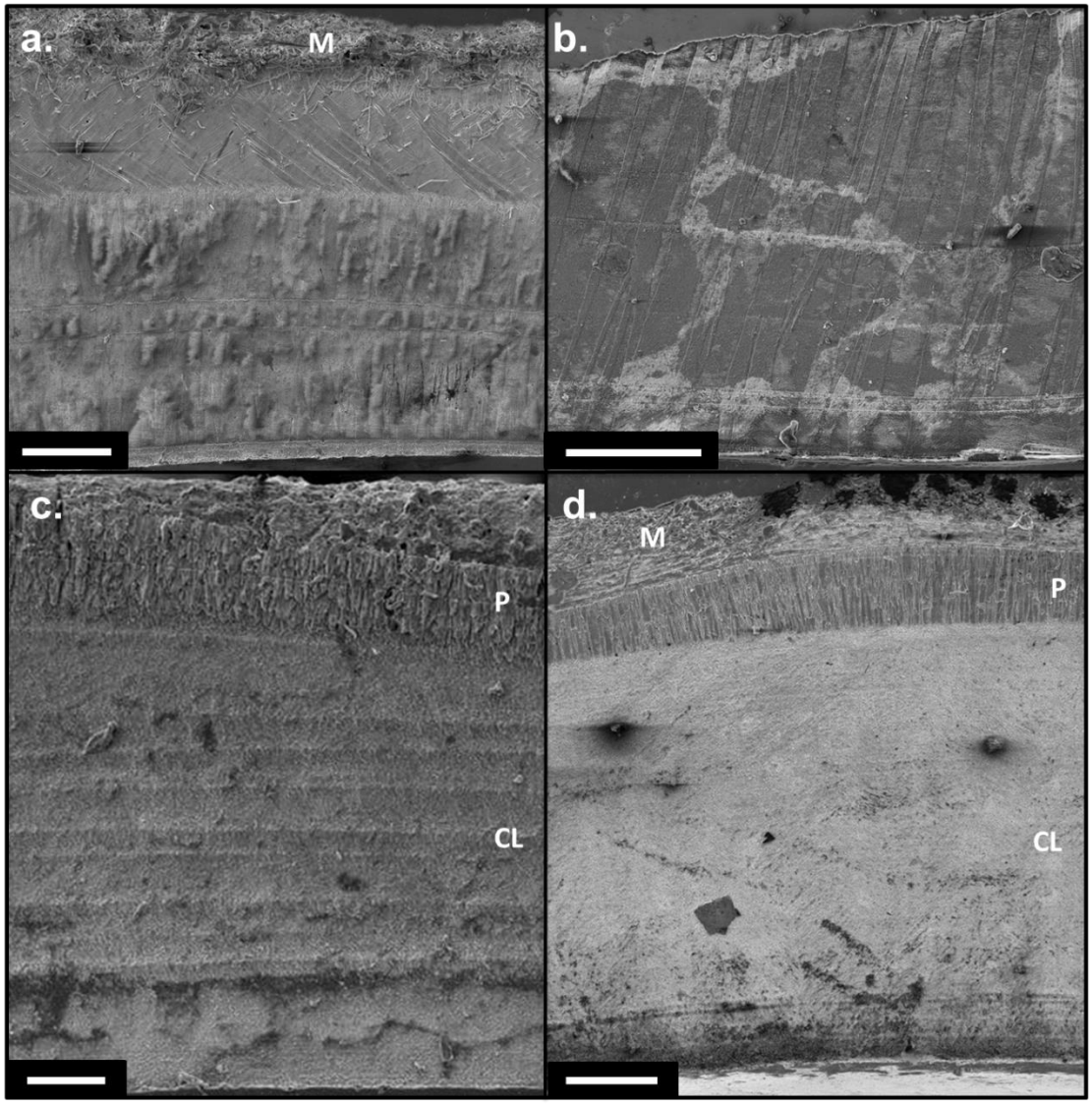

Figure 6 Scanning electron microscopy of shells from two gastropod species collected at three pH vent sites off Vulcano Island, Italy. *Hexaplex trunculus* at (a) ambient pH and (b) low pH. *Osilinus turbinatus* at (c) ambient pH and (d) low pH. The presence of microbes on the shell is represented by an "M"; prismatic layers are marked with a "P"; Crossed-lamellar layers are marked with a "CL." Scale bars represent 100 μm

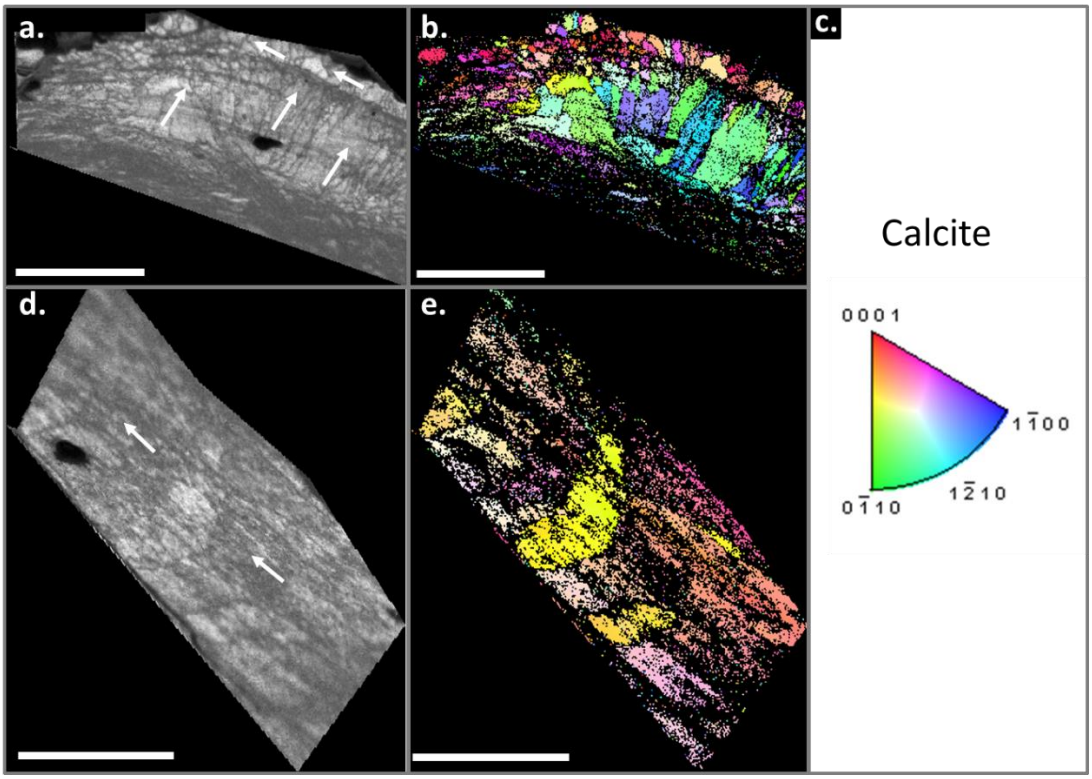

Figure 7 Electron backscatter diffraction data for sections across the thickness of shells of *Patella caerulea* collected from ambient (a-b) and low (d-e) pH seep sites. (a, d) Diffraction intensity maps of shell section with white arrows indicating the preferred orientation of crystals. (b, e) Corresponding crystallographic maps demonstrating the orientation of calcite crystals. (c) Color-key for calcite crystallographic planes. (a, b) Scale bars represent 100 μm. (d-e) Scale bars represent 70 μm

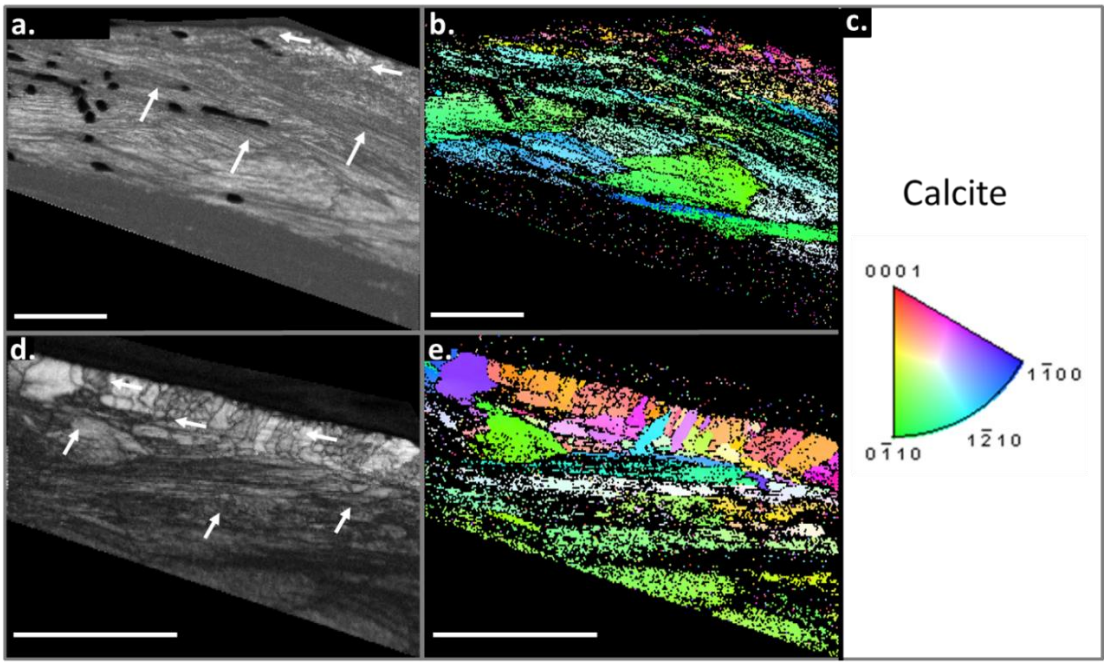

Figure 8 Electron backscatter diffraction data for sections across the thickness of shells of *Patella rustica* collected from ambient (a-b) and low (d-e) pH sites. (a, d) Diffraction intensity maps of shell section with white arrows indicating the preferred orientation of crystals. (b, e) Corresponding crystallographic maps demonstrating the orientation of calcite crystals. (c) Color-key for calcite crystallographic planes. (a-b) Scale bars represent 100 μm. (d-e) Scale bars represent 90 μm

INTER- AND INTRA-SPECIFIC COMPARISONS OF THE MG/CA RATIO OF SKELETAL COMPONENTS IN A SUITE OF ANTARCTIC ECHINODERMS LARGELY SOUTH OF 70 DEGREES LATITUDE

by

ASHLEY DUQUETTE, KENNETH M. HALANYCH, JAMES B. MCCLINTOCK

In preparation for *Antarctic Science*

Format adapted for dissertation

Abstract

Marine invertebrates in the Southern Ocean are considered to be at particularly high risk to ocean acidification (OA). Echinoderms are especially vulnerable because they employ what has historically been referred to as 'high magnesium calcite' (>4% $MgCO_3$) to construct their skeletal components. Calcite comprised of high levels of magnesium is more soluble than either calcite or aragonite alone. Given that the Southern Ocean is predicted by the IPCC to become undersaturated with respect to aragonite and calcite by approximately 2050 and 2100, respectively, undersaturation with respect to high magnesium calcite can be expected to occur even earlier. As the saturation levels of calcite and aragonite in the Southern Ocean reach sub-saturation levels under ocean acidification, echinoderms will confront both increased skeletal dissolution and the potential for an increased energetic cost in producing and maintaining skeletal material. Body component skeletal elements of representatives of the Echinodermata in the classes Echinoidea (test, Aristotle's lantern, spines), Ophiuroidea (whole body or arms and central disk), and Asteroidea (whole body), were collected for analysis of their mineralogy (Mg/Ca ratio) from a variety of biogeographic regions of Antarctica largely south of 70 degrees latitude. Mg/Ca ratios varied among body components in the Echinoidea, but not between those examined in the Ophiuroidea. The inclusion of smaller numbers of species collected north of 70 degrees facilitated the determination that levels of echinoderm skeletal magnesium decreased with increasing latitude between 62 and 76 degrees latitude. However, when restricted only to those individuals collected south of 70 degrees, a correlation between magnesium content and latitude was observed only in asteroids. The basis of the inverse correlation between latitude and skeletal Mg^{2+} in echinoderms remains unknown, but the loss of a correlation in all but the asteroid

samples above 70 degrees south where environmental stasis is pervasive suggests that seawater temperature is a likely causative agent

Introduction

Global oceanic pCO_2 is increasing in response to an ongoing increase in atmospheric carbon dioxide (CO_2) (Gattuso *et al.* 2015). Since the pre-industrial age, atmospheric CO_2 has increased from 278 to 400 ppm (IPCC 2014). As pCO_2 in the ocean increases, it causes a reduction not only in seawater pH but also in the saturation state (Ω) of calcium carbonate ($CaCO_3$) (Gattuso *et al.* 2015). Together, these alterations in seawater chemistry are termed ocean acidification (OA; Caldeira & Wickett 2003). To date, the average pH of ocean surface waters has fallen 0.1 pH units since pre-industrial times and is predicted to fall another 0.3-0.4 pH units by the end of the century (Orr *et al.* 2005). Remarkably, this predicted decline in pH coincides with a 150% increase in H^+ concentration and a 50% decrease in carbonate (CO_3^{2-}) concentration (Orr *et al.* 2005). This will accordingly lead to an increase in bicarbonate ions as free hydrogen ions bind with carbonate. While these estimates are based on a global average of the world's oceans, the Southern Ocean is uniquely susceptible to ocean acidification (Orr *et al.* 2005,Fabry *et al.* 2009,McClintock *et al.* 2009). The Southern Ocean (defined as the oceanic region south of 40°S latitude) represents a vast surface area responsible for approximately 40% of overall global CO_2 uptake (Fabry *et al.* 2009) and is predicted to experience winter aragonite undersaturation as early as 2030 (McNeil & Matear 2008), and year-round aragonite and calcite undersaturation by 2050 and 2100, respectively (Orr *et al.* 2005).

Marine calcifying invertebrates inhabiting the Southern Ocean will be among the first globally to exhibit negative impacts of OA. The characteristics of the Southern Ocean that make it more susceptible to OA include the increased solubility of atmospheric CO_2 at low temperature, a naturally low saturation state (Ω) for $CaCO_3$, and unique patterns of ocean mixing (Fabry *et al.* 2009). When $\Omega > 1$, formation of calcium carbonate is thermodynamically favored, but when $\Omega < 1$, seawater become corrosive to calcium carbonate and dissolution of its two predominant polymorphs, aragonite and calcite, is favored. The saturation horizon ($\Omega = 1$) for aragonite occurs, on average, at approximately 730 meters depth south of 60°S latitude (Collard *et al.* 2015). Under a 'business as usual' greenhouse gas model, the seasonal winter saturation horizon for aragonite is expected to become shallower and reach the surface as early as 2030 between a latitude of 65 to70 degrees south (McNeil & Matear 2008). Since aragonite is twice as soluble as calcite (Mucci 1983), the saturation horizon for calcite in the Southern Ocean will be deeper than that for aragonite. Nonetheless, the incorporation of magnesium in place of calcium can significantly increase the solubility of calcite. 'High magnesium calcite'(≥ 4% MgCO3; Bøggild 1930) is even more soluble than aragonite, and will therefore exhibit a shallower saturation horizon than either aragonite or calcite (Morse *et al.* 2006).

Members of the Echinodermata, a significant carbonate producing phylum in the Southern Ocean, construct high magnesium calcite skeletal elements (Weber 1973,Dickson 2002,Lebrato *et al.* 2010). All five taxonomic classes are, therefore, at increased risk of dissolution in reduced seawater pH and prone to impaired calcification under the reduced saturation states predicted under near-future OA. Echinoids (sea

urchins), ophiuroids (brittle stars), and asteroids (sea stars) occur in notably high abundance on the benthos in Antarctica, and some species play key roles in structuring benthic communities (e.g., Dayton *et al.* 1974). Despite their ecological significance and their largely overlooked but important contribution to the global carbon cycle (Chave 1954,Lebrato *et al.* 2010), there is a paucity of information about the comparative mineralogy of the skeletons of Antarctic echinoderms, and essentially a complete lack of information on any species occurring at 70 degrees south latitude or greater.

It has long been known that the high magnesium content in calcite of the skeletal components of echinoderms is generally linked to the group's taxonomic history (Chave 1954). However, despite the role of taxonomy, for over a half a century there has existed an enigmatic hypothesis that an inverse relationship exists between levels of magnesium content and latitude in the skeletal elements of echinoderms (Chave 1954,Andersson *et al.* 2008,McClintock *et al.* 2011). Despite the recent inclusion of new mineralogical data for a select group of echinoderms collected from the Southern Ocean in the near proximity of 67 degrees latitude (McClintock *et al.* 2011), the global latitudinal hypothesis remains largely based on data from tropical and temperate species. Before further speculating about the various environmental factors (e.g., temperature, salinity, water chemistry, etc.) that may drive this intriguing distributional pattern in mineralogy, it is important to extend the analysis of echinoderm mineralogy to unexplored latitudes above 70 degrees south.

The purpose of the present study was twofold: first, to evaluate intra-class as well as intra-specific differences in Mg/Ca ratios of the skeletal components of three classes of Antarctic echinoderms to evaluate their differential susceptibility to near-future OA.

Moreover, in approximately half of the taxa examined, we also compared Mg/Ca ratios in identical skeletal elements or whole body across different spatial scales. Second, as our study provides the first data on the Mg/Ca ratios of skeletal elements of echinoderms collected south of 70 degrees latitude, we were able to conduct a more comprehensive analysis of the global inverse correlation for skeletal magnesium content and latitude. While the present study does not attempt to evaluate the basis for the latitudinal relationship, our study is relevant to this question because the majority of the echinoderms examined are from the extreme of their southern polar biogeographic range (> 70 degrees south) where environmental factors such as seawater temperature are effectively static.

Methods

The large majority of the echinoderms analyzed in the present study were collected over National Science Foundation (NSF) research cruise NBP12-10 aboard the U.S. R/V *Nathanial B. Palmer* that took place from Jan 1 - Feb 9, 2013. Collections were initiated at 70˚ south latitude at sites along the western Antarctic Peninsula in the Bellingshausen Sea and extending to the Ross Sea to latitude of 76 degrees south. Samples for the present project were collected using a Blake Trawl (1.5 m width) deployed to sample the benthos at 23 different collecting sites (see Table 1). The mean ± 1SE depth at the sampling sites was 534 ± 20.5 m, and ranged from 341 to 764 m (Table1). Echinoderms collected in each of the trawls were separated initially into morphospecies aboard ship. For each sampling site, echinoderm vouchers for each morphotype were photographed, labeled, and then fixed in ethanol or frozen aboard ship

for shipment and subsequent identification to the lowest taxon possible. The benthic collections from the 23 different geographic stations encompassed 20 taxa representative of three of the five classes of Echinodermata, the Echinoidea, Ophiuroidea, and Asteroidea.

Additional samples of Antarctic echinoderms were included in the present study. These were collected on a subsequent NSF research cruise (LMG13-12) aboard the U.S. R/V *Laurence M. Gould* that took place from Nov 22 to Dec 20, 2013. Collection methods on this second cruise were identical to those described above for the first cruise. This cruise sampled echinoderms from 10 additional geographic sites but did so at lower Antarctic latitudes (62° to 65°S) in the region surrounding the northern tip of the Western Antarctic Peninsula (Table 2). Echinoderms collected on this second cruise were photographed, frozen on board ship, and then shipped frozen to Auburn University, USA. Body components or intact individuals from this second cruise that were incorporated into the present study included several sea stars, large brittle star arms, cidaroid sea urchin spines, and intact individuals of the regular sea urchin *Sterechinus* spp..

During the initial cruise in Jan 2013, the echinoderms examined in the present study were processed aboard ship. All brittle stars that had disk diameters > 1.5 cm were dissected with a scalpel into two discrete body components, the central disk and the arms. Smaller brittle stars were analyzed intact. All regular sea urchins were separated into three basic body components: the spines, test, and Aristotle's lantern. The gut and gonad tissues were discarded. For all sea stars and irregular heart urchins, individuals were analyzed intact.

To prepare skeletal material, body components or intact individuals were placed in a drying oven for 24 hr at 35 °C and then digested in a 10% NaClO solution to remove all tissue (McClintock *et al.* 2011). The NaClO solution was exchanged as needed to facilitate complete digestion of organic material. The cleaned skeletal elements were rinsed generously with distilled water, vacuum dried, and then placed in a drying oven for 24 hrs. Each resultant skeletal sample was folded within a sheet of aluminum-foil, placed into a labelled zip-lock bag and hand carried to the University of Alabama at Birmingham, USA. The skeletal material from intact individuals or body components was then ground into a fine powder using an agate mortar and pestle with the addition of several mL of 95% ethanol to reduce heating. The resulting slurry was air dried for 12 hrs and the subsequent powder used in mineralogical analysis. Skeletal preparation was carried out in an identical manner for the echinoderm samples collected during the second cruise (Nov-Dec 2013).

Molar Mg/Ca ratios were determined by X-ray diffraction (XRD) using a Philips X'Pert Analytical X-ray diffraction system (PANalytical B.V., Almelo, Netherlands). The system was set to run at 45kV and 40mV with a 2Θ scan range of 27˚ to 32˚. The scan speed was 2 s/step with a step size of 0.02 to obtain accurate measurements of the calcite peak occurring at 2Θ = 29.5 ˚-30.2 ˚. The resulting diffraction pattern was used to determine the molar Mg/Ca ratio following the equation given in Ries (2011):

$$Mg/Ca=0.17881(2\theta)^2- 10.20926(2\theta)+145.59368$$

The data generated facilitated two intra-taxon statistical comparisons of Mg/Ca ratios. First, comparisons were made for those taxa whose discrete body component skeletal analysis was available. These included large body-sized (> 1.5 cm disk diameter)

brittle stars that were separated into a central disk and arms, as well as the regular sea urchins that had been divided into test, spines, and Aristotle's lantern (feeding apparatus). For each taxon of large brittle star occurring at only one location, mean Mg/Ca ratio of the skeletal material of arms was compared to mean Mg/Ca ratio of the skeletal material of the central disk using a Student's t-test. For those collected at two or more locations, mean Mg/Ca ratio of the skeletal material of the arms was compared to that of the central disk using a two-way ANOVA. The two way ANOVA tested the effect of both body component and station on Mg/Ca ratios. For each taxon of regular sea urchin, the mean Mg/Ca ratios of skeletal material that comprised the test, spines, and lantern apparatus were compared with one another using a one-way ANOVA. A Tukey HSD post-hoc test was carried out to detect which components were significantly different from one another. Prior to carrying out all statistical analyses, Mg/Ca ratios were log (x+1) transformed to fit a normal distribution.

In the second intra-taxon comparison, the ratios of Mg/Ca were compared for each taxon of echinoderm that was collected at multiple geographic sites and that had more than 3 individuals collected per site. This allowed an assessment of whether mineralogical composition of skeletons varied across sites within a given taxon or species. Mg/Ca ratios of body components for large brittle stars and regular sea urchins, as well as intact sea stars, brittle stars, and heart urchins were analyzed accordingly. As above, species of large brittle stars were analyzed using a two-way ANOVA, looking at components and site in the same test. If three or more sites were included in a given intra-taxon geographic comparison, a one-way ANOVA was employed. A Tukey HSD test

was used to specify differences between specific sites. If samples from only two geographic sites were compared for a given taxon, a Student's t-test was employed.

Finally, Mg/Ca ratios were used to evaluate whether or not a correlation existed between skeletal magnesium content (Mg/Ca ratio) and latitude for the echinoderms collected over the two 2013 cruises. This analysis was divided into two separate examinations of this potential relationship across two different sets of latitudes. First, a Pearson's correlation analysis was conducted only for those echinoderms collected from 70 to 76 degrees latitude which included all taxa collected: large brittle star arms and disk, regular sea urchin (cidaroid urchins and *Sterechinus* spp.) test, lantern, and spines, intact sea stars, intact small brittle stars, and intact heart urchins (Table 3). This focused analysis was carried out because these data are essentially the first for echinoderms in this range of latitudes and because environmental variables such as seawater temperature are essentially static above 70°S latitude. A second Pearson's correlation analysis was conducted using echinoderm taxa that were collected on both cruises (from 62 to 76 degrees south). These included large brittle star arms, *Sterechinus* spp. (test, lantern, and spines), cidaroid spines, and intact sea stars (Table 3).

Results

Mg/Ca ratios of skeletal material from body components or intact individuals of the three classes of echinoderms examined ranged from 0 to 0.1894 mol/mol. For brittle star body components, the mean (± SE) Mg/Ca ratios of skeletal material were 0.1109 ± 0.0020 (disks; n = 137) and 0.11 ± 0.0023 (arms; n = 146). For regular sea urchin body components the mean (± SE) Mg/Ca ratios of skeletal material were 0.053 ± 0.0023

(tests; n = 123), 0.0571 ± 0.0024 (lanterns n = 92), and 0.0164 ± 0.0021 (spines; n = 94). Skeletal material of intact sea stars, brittle stars, and heart urchins had mean (± SE) Mg/Ca ratios of 0.0825 ± 0.0026 (n = 60), 0.1019 ± 0.0024 (n = 142), and 0.0535 ± 0.0023 (n = 112), respectively.

The mean Mg/Ca ratio of the central disk of large brittle stars did not differ significantly from the mean Mg/Ca ratio of arms for any of the nine taxa examined (Figure 1): *Ophiocamax* spp. (ANOVA, $F_{(1,30)} = 0.268$, $p = 0.608$), *Ophiocantha pentactus* (ANOVA, $F_{(1,18)} = 1.537$, $p = 0.230$), *Ophionotus* spp. (ANOVA, $F_{(1,16)} = 0.142$, $p = 0.712$), *Ophiopearla koehleri* (ANOVA, $F_{(1,26)} = 1.793$, $p = 0.190$), *Ophioplinthus gelida* (ANOVA, $F_{(1,55)} = 0.056$, $p = 0.810$), *Ophioplinthus* spp. (ANOVA, $F_{(1,22)} = 0.179$, $p = 0.676$), *Ophiura carinifera* (ANOVA, $F_{(1,24)} = 0.779$, $p = 0.386$), *Astrohamma tuburculata* (Student's T-test, $t_{(11)} = 1.288$, $p=0.224$), and an unidentified species (Student's T-test, $t_{(4)} = 1.801$, $p=0.146$). In contrast, the mean Mg/Ca ratios in skeletal mineralogy in several of the body components of the two taxa of regular sea urchins examined, cidaroid urchins and *Sterechinus* spp., differed from one another (Figure 2). Intra-taxon differences in mean Mg/Ca ratios among body components of cidaroids (ANOVA; $F_{(2, 41)} = 102.7$, $p < 0.001$) were attributable to spines having a significantly lower mean Mg/Ca ratio when compared to that of the lantern and test (Tukey HSD test; $p \ll 0.001$). Mean Mg/Ca ratios for the cidaroid lantern and test did not differ significantly (Tukey HSD test; $p = 0.894$) from one another. Similar significant differences in mean Mg/Ca ratios were detected among the body components of *Sterechinus* spp. (ANOVA: $F_{(2,188)} = 30.57$, $p \ll 0.001$), with spines having a lower mean

Mg/Ca ratio than the test and lantern (Tukey HSD test, $p \ll 0.001$), while the mean Mg/Ca ratio did not differ between test and lantern (Tukey HSD test, $p = 0.476$).

When compared across all 33 sampling sites (both cruise collections combined), seven of the nine taxa of large brittle stars fit the criteria for geographic site-specific comparisons of Mg/Ca ratios: *Ophiocamax* spp., *Ophiocantha pentactus*, *Ophionotus* spp., *Ophiopearla koehleri*, *Ophioplinthus gelida*, *Ophioplinthus* spp., and *Ophiura carinifera*. Since no significant differences were found between the Mg/Ca ratios of the arms and disk for each of these taxa, these data were combined for site specific comparisons. Among the seven taxa, *Ophionotus* spp. was the only taxon to demonstrate a significant site-specific difference in mean Mg/Ca ratios (ANOVA; $F_{(1,16)} = 14.26$, $p = 0.002$). The two collecting sites compared for this taxon were located at 71.7˚S and 76.9˚S latitude, and the level of magnesium in the skeletal materials was higher at the lower latitude site (Mg/Ca = 0.049) than at the higher latitude site (Mg/Ca = 0.038). Cidaroid urchins demonstrated no site-specific differences in mean Mg/Ca ratios for the test or the lantern (ANOVA; $F_{(9,29)} = 0.699$, $p=0.705$; and $F_{(6,19)} = 2.515$, $p=0.058$, respectively), but had significant differences in the mean Mg/Ca ratio for spines (ANOVA, $F_{(9,27)} = 3.361$, $p = 0.007$). One site was found to be significantly different from the other collections sites. This collection site was located at 65°S and was the deeper of the ten site collections. Similarly, *Sterechinus* spp. demonstrated significant differences in mean Mg/Ca ratios for spines (ANOVA, $F_{(10,33)} = 3.770$, $p=0.002$) but not for tests (ANOVA, $F_{(14,66)} = 1.378$, $p=0.189$) or lanterns (ANOVA, $F_{(12,41)} = 1.792$, $p = 0.082$). Here again, a single collection site (64.3°S, Weddell Sea) was driving the significant differences among spines.

Three taxa of sea stars were analyzed for intraspecific geographic differences in skeletal Mg content: *Porania antarctica, Cheiraster* spp., and *Bathybiaster* spp. None of the three taxa demonstrated significant site-specific differences in mean Mg/Ca ratio (ANOVA; $F_{(2,6)} = 1.19$, $p = 0.365$; $F_{(3,9)} = 1.87$, $p=0.205$; $F_{(2,7)} = 0.15$, $p = 0.861$, respectively). The three taxa of intact brittle stars examined, *Ophiocantha antarctica*, *Ophiolimna antarctica*, and *Ophioplinthu*s spp., similarly showed no site-specific differences in mean Mg/Ca ratio (ANOVA: $F_{(9,40)} = 0.557$, $p = 0.824$; $F_{(4,30)} = 0.905$, $p = 0.473$; T-test, $t_{(27)} = 0.306$, $p = 0.762$, respectively). Heart urchins (analyzed as a single taxon) also demonstrated no site-specific differences in Mg/Ca ratios (ANOVA; $F_{(12,99)} = 1.018$, $p = 0.439$).

Since no brittle star disks were collected north of 70˚ south, only those collected from 70.8˚-76.9˚ south were included in the correlation analysis between latitude and magnesium content. We found no significant statistical correlation between skeletal Mg/Ca ratios and latitude for brittle star disks (Pearson correlation coefficient, $r = -0.144$, $N = 137$, $p = 0.092$, Figure 3). A significant correlation between skeletal Mg/Ca ratios and latitude was observed neither for brittle star arms collected between 62.8° - 76.9˚S (Pearson correlation coefficient, $r = -0.008$, $N = 146$, $p = 0.924$; Figure 3), nor when brittle star arms from individuals collected north of 70˚S were removed from the correlation analysis (Pearson correlation coefficient, $r = -0.015$, $N = 137$, $p = 0.860$; Figure 3).

Mg/Ca ratios of skeletal material from intact sea stars collected from 62.4° - 76.9°S revealed a significant inverse correlation with latitude (Pearson correlation coefficient; $r = -0.539$, $N = 60$, $p << 0.001$; Figure 3). This inverse relationship remained

significant even when restricted to individuals collected below 70°S (Pearson correlation coefficient; r = -0.349, N = 48, p = 0.015; Figure 3). In contrast, no significant correlation between latitude and Mg/Ca ratios was found for intact brittle stars (Pearson correlation coefficient; r = 0.118, N = 142 p = 0.163; Figure 3) or heart urchins (Pearson correlation coefficient, r = 0.105, N = 112, p = 0.271; Figure 3). No correlation analysis was carried out for latitudes north of 70°S as these two groups were not sampled in this region.

No significant correlation was observed across latitude and Mg/Ca ratios of cidaroid urchin tests or lanterns collected between 70.8° - 76.3°S (Pearson correlation coefficient, r = -0.234, N = 41, p = 0.14; r = -0.099, N = 34, p = 0.576, respectively; Figure 4). Correlation analysis for data north of 70°S was not carried out as no cidaroid urchin tests or lanterns were collected in that region. Correlation analyses revealed a significant negative association between latitude and Mg/Ca ratios for the spines of cidaroid urchins collected from 62.9° - 76.3°S (Pearson correlation coefficient, r = -0.655, N = 43, p < 0.001; Figure 4). This negative association was no longer significant when samples were restricted to those collected south of 70°S (Pearson correlation coefficient, r = -0.272. N=37, p = 0.104; Figure 4). No significant correlation was observed between latitude and Mg/Ca ratios of *Sterechinus* spp. lanterns collected either 62.4°-76.4°S (Pearson correlation coefficient, r = -0.173, N = 58, p = 0.195, respectively) or collected only above 70°S (Pearson correlation coefficient, r = 0.139, N=54, p = 0.315; Figure 4). However, correlation analyses revealed a significant negative association between latitude and Mg/Ca ratios for both the test and spines of *Sterechinus* spp. collected from 62.4°-76.4°S (Pearson correlation coefficient, r = -0.272, N = 82, p = 0.010; and r = -0.474, N=51, p < 0.001, respectively; Figure 4). When tests and spines

only from individuals collected below 70˚S were analyzed, the correlation between latitude and Mg/Ca ratios was no longer significant (Pearson correlation coefficient, r=-0.0003, N=78, p = 0.998; and r = -0.158, N = 47, p = 0.289; respectively).

Discussion

The present study adds significantly to the limited knowledge of mineralogy of the skeletons of Antarctic echinoderms. Prior to our analysis, with the exception of one comparative study of 26 echinoderm species (McClintock *et al.* 2011) collected largely from a single region of the Antarctic Peninsula (64˚S), little information was available for taxa collected for latitudes between 60 and 66˚S. Moreover, other than one echinoid species (Sewell & Hofmann 2011) and two crinoid species (Chave 1954) collected at 71 and 78˚S latitude, respectively, virtually nothing was known about the mineralogy of echinoderms at latitudes greater than 70˚ south. The present study begins to fill this important gap in knowledge for a group of marine invertebrates known to possess mineralogy particularly susceptible to dissolution in a region of the world's oceans known to be uniquely susceptible to early impacts of anthropogenic ocean acidification. While it is largely recognized that the skeletal components of echinoderms are comprised of 'high magnesium calcite,' a much more soluble form of calcium carbonate than either aragonite or low magnesium calcite (Morse *et al.* 2006), it is less appreciated that Mg/Ca ratios of echinoderms, and other calcifying marine invertebrates in general, are highly reliant on seawater saturation state, the Mg/Ca content of seawater, and seawater temperature (Mackenzie *et al.* 1983,Magdans & Hermann 2004,Ries 2004,Andersson *et al.* 2008). Because the Southern Ocean is the coldest sea in the world, there is greater solubility of

carbonate and, when compared to temperate and tropical oceans, naturally low saturation states for carbonate minerals. Accordingly, the Southern Ocean is experiencing some of the first effects of OA. For example, the aragonite shells of pteropods in some regions of the Southern Ocean are already displaying dissolution due to periodic undersaturation (Bednaršek *et al.* 2012). The Southern Ocean will continue to be at the forefront of OA impacts (Andersson *et al.* 2008,Fabry *et al.* 2009).

Given their high magnesium skeletal composition and that seawater in the Southern Ocean is expected to become undersaturated with respect to polymorphs of calcium carbonate within the next twenty-five to fifty years (Orr *et al.* 2005), Antarctic echinoderms are particularly at risk. Understanding whether Antarctic echinoderms will be able to compensate for dissolution by redirecting sufficient energy and resources into skeletal maintenance without reducing fitness or suffering significant mortality is important (Wood *et al.* 2008). Moreover, as Antarctic echinoderms dominate the biomass of many benthic communities throughout the Southern Ocean, they contribute substantially to global carbonate cycles (Arntz *et al.* 1994,David *et al.* 2005,Lebrato *et al.* 2010,Grange & Smith 2013). In addition to their high abundance, many echinoderms in Antarctica play key roles in structuring benthic communities (Dayton *et al.* 1974,Arntz *et al.* 1994). Should ocean warming and ocean acidification lead to the loss of echinoderm species the ecological impacts could be profound. Additionally, the loss of echinoderms would result in a significant depletion of a carbon source released directly to the benthos (Lebrato *et al.* 2010).

To date, previous studies have measured mol% $MgCO_3$ or wt% $MgCO_3$ when evaluating the magnesium content of echinoderm skeletal components. In the present

study we chose another approach, measuring Mg/Ca ratios. Our rationale for using this approach was that our chosen analytical technique, X-ray Diffraction Analysis (XRD, used to determine Mg/Ca ratio), specifically detects only the magnesium that has been incorporated into the calcite crystal lattice structure of skeletal components. Former methodologies employed (e.g., Secondary Ion Mass Spectrometry, Inductively Coupled Plasma Mass Spectrometry, and EDS) detect magnesium that is also present outside of the calcite crystalline structure, for example, organic molecules rich in magnesium (Milliman 1974). The resultant measurements lead to an overestimation of the magnesium content. While our approach of measuring Mg/Ca ratios was more accurate in this context, it also limited our ability to directly compare our findings to past studies. Nonetheless, we were still able to identify patterns in magnesium content and make comparisons to those patterns reported previously using different techniques (Chave 1954,McClintock *et al.* 2011).

McClintock *et al.* (2011) examined the wt% MgCO3 for a suite of Antarctic echinoderms and found that the skeletal components of sea stars contained the highest levels of magnesium when compared to the other classes of echinoderms. In the present study we found that skeletal components of brittle stars had slightly higher magnesium contents (Mg/Ca ratio) than did skeletons of sea stars, heart urchins, and individual body components of regular urchins. However, in both the present study and that of McClintock *et al.* (2011), brittle stars and sea stars were the two classes of echinoderms with the highest magnesium content. The elevation of brittle stars to the class of Antarctic echinoderms with the highest magnesium content in the present study is likely related to our methodology to ascertain a more accurate measure of skeletal magnesium content.

This emphasizes the need to use XRD in future studies to ensure that evaluations of skeletal magnesium content and, therefore, the prospective susceptibility of taxa to ocean acidification, are best interpreted.

Following brittle stars and sea stars, the Mg/Ca ratios were highest to lowest in regular urchin lanterns, heart urchin tests, regular urchin tests and regular urchin spines. While these data suggest that skeletal structures of brittle stars and sea stars may be at greater risk of dissolution under conditions of OA, this must be interpreted in the context of skeletal vulnerability. Sea stars and brittle stars lack the extensive calcified structures that occur in sea urchins, and their ossicles are often embedded within tissues that form the body wall. It is possible that brittle stars and sea stars have evolved skeletal components with high ratios of Mg/Ca because the skeletal elements are more protected from environmental exposure. On the other hand, at least one study to date has found that despite a thicker body wall, sea star skeletons can remain vulnerable to ocean acidification. Gooding *et al.* (2009) reported that the sea star *Pisaster ochraceus* chronically exposed to end-of-the-century [CO_2] (780ppm) over a 70 day period had increased rates of growth but suffered from a reduced calcified mass.

While irregular and regular sea urchins also are classified as possessing endoskeletons, the dermis separating the test from the environment is very thin and highly permeable, offering little protection against exposure to ocean acidification (Binyon 1976,Miles *et al.* 2007,Sewell & Hofmann 2011). Skeletal exposure is taken to the extreme in the heavily calcified species of cidaroid urchins, where the thick pencil-like spines lack any epithelial covering. Interestingly, cidaroids are still able to efficiently calcify in seawater undersaturated with respect to calcium carbonate (David *et al.* 2005).

Clearly, predicting which classes or lower taxa are most vulnerable to ocean acidification is not straightforward, and is further complicated beyond simple issues of solubility given that there are biological controls over skeletal production.

Similar to differences detected in Mg/Ca ratios among classes of echinoderms (McClintock *et al.* 2011; present study), variation may also occur between species within a class and within the skeletal material associated with different body components of individuals. In the present study, brittle stars demonstrated no difference between the mean Mg/Ca ratios of the central disk and arms, but among regular sea urchins we detected significantly different mean Mg/Ca ratios based on body component. This variation is in agreement with past studies of the mineralogy of skeletons of regular sea urchins (Chave 1954,Weber 1969,Byrne *et al.* 2014). We found the highest mean ratios of Mg/Ca in the tests and Aristotle lanterns (with no significant difference between the two), but two- and four-fold lower mean ratios in the spines of *Sterechinus* spp. and cidaroid urchins, respectively, when compared with the other two body components. In contrast, Byrne *et al.* (2014) found that the Aristotle lantern (6.5 % $MgCO_3$) in the sea urchin *Tripneustes gratilla* had the lowest magnesium content (measured as % $MgCO_3$) and tests the highest (8.6 %) magnesium content. Interestingly, the spines of *T. gratilla* had an intermediate content of 7% $MgCO_3$. Such intraspecific differences could be based on functional morphology, but more research is necessary to determine the source or sources of this variation. Byrne *et al.* (2014) attributed the increased magnesium content of tests and lanterns to their function, indicating higher magnesium content strengthens the calcite of the test against crushing or drilling predators, and a stronger lantern may increase resistance to wear and tear, or breakage. Another potential explanation for the

observed variation in magnesium content between body components is that regular sea urchins possess separate calcification processes or pathways for various body components that may result in variation in their mineralogy (Ebert 2007,LaVigne *et al.* 2013).

One of the most unique aspects of the present study was the feasibility of making intraspecific comparisons of Mg/Ca ratios in skeletal body components and intact individuals from geographically separated sub-populations for representatives of species across three classes of echinoderms. Among the three species of sea stars examined, there were no significant differences in mean Mg/Ca ratios of intact skeletons across their respective sites of collection. For *Bathybiaster* spp. (Ross Sea) and *Porania antarctica* (western Antarctic Peninsula), the three sites sampled for each were relatively close to one another (approximately within 74 and 140 km, respectively). In contrast, *Cheiraster* spp. (western Antarctic Peninsula to Ross Sea) was collected from four different sites that ranged across an entire 13.5 degrees of latitude (approximately 1500 km). We are unaware of any comparative studies in other sea stars that take an intraspecific comparative approach other than that of McClintock et al. (2011) who sampled subpopulations of the Antarctic sea star *Labidiaster annulatus* at three sites, one site at 61˚S and the other two sites close to one another near 65˚S. A small but significant difference was found in the wt% $MgCO_3$ between one of the 65˚ sites and the other two geographic sites.

Among the three taxa of intact brittle stars we compared across biogeographic sites, despite sites being separated by as much as 5.3˚ of latitude, there were no significant differences in mean Mg/Ca ratios of skeletons, similar to the pattern seen in

sea stars. Similarly, Mg/Ca ratios in body components of six of the seven species of large brittle stars showed no differences across geographic sites. In the one taxa of large brittle star that differed with collection site (*Ophionotus* spp.), both the skeletal materials in the arms and in the disks differed in Mg/Ca ratios across the two geographically separated sampling sites (71.9˚ and 76.9˚S).

Among the single taxonomic group of irregular sea urchins, no differences in mean Mg/Ca ratios for intact individuals were detected for 13 collecting sites sampled across 7 degrees of latitude. Similarly, with the exception of spines, no differences were detected among sampling sites for cidaroid urchins. However, both the test and the spines of the regular urchin *Sterechinus* spp. varied with collection site. Mean Mg/Ca ratios of the test and spines sampled across 15 and 11 geographic sites, respectively, and spanning latitudes from 64 to 76˚S, had magnesium contents that varied from 0.011 - 0.109 (tests) and 0.001 - 0.078 (spines). When the relationship between latitude and magnesium content of regular sea urchins was examined, we found a significant inverse negative correlation between magnesium content and latitude for spines in both cidaroid urchins and *Sterechinus* spp. when data from all latitudes (not just those above 70°S) were included.

The basis for the variance in the magnesium content of spines in cidaroids and regular urchins is unknown. However, unlike the test and the lantern that are constantly exposed internally to reduced pH and sub-saturation states (e.g., Collard *et al.* 2014), the spines of cidaroid urchins lack an epithelium and are completely exposed to seawater. Moreover, the epithelium of the spines of *Sterechinus* spp. is thin and permeable. It is possible, therefore, that the spines provide a more sensitive, direct measure of

environmental saturation state than do the other body components. Therefore, at higher latitudes where saturation state is reduced, despite the capacity for sea urchins to calcify below the aragonite saturation horizon (David *et al.* 2005), the magnesium content of spines is somewhat reduced.

The present study provides insights into the long-held theory that there is a significant inverse correlation between latitude and skeletal magnesium content in the Echinodermata (Chave 1954,Andersson *et al.* 2008,McClintock *et al.* 2011). Past studies have exclusively used techniques that measure magnesium as wt% $MgCO_3$. The present study exploits measures of the Mg/Ca ratio, a more accurate measure of skeletal magnesium content, which is not directly comparable to former studies but can be used to evaluate basic patterns. In this context, data for Mg/Ca ratios in echinoderms in the present study generally support the global latitudinal hypothesis as previously proposed. As an extension of this analysis we chose to run correlation analyses with data from individuals collected exclusively above 70˚S in addition to those collected from 62 – 76˚S. We did this because we hypothesized that at latitudes above 70˚S the environment is relatively static in terms of seawater temperature. Shallow water temperature can range as much as 3˚C with maximum temperatures near 2˚C in the course of a year for the Western Antarctic Peninsula (Barnes *et al.* 2006). However, shallow water temperature in areas above 70˚ S, such as McMurdo Sound, typically stay below 0˚ C and range by approximately 1.5˚ C or less (Hunt *et al.* 2003). In fact, Hunt *et al*. (2003) reported that temperatures between August and early December varied by less than 0.01˚ C from the surface to 400m. Later season temperatures remained relatively stable below -1.8˚C (Hunt *et al.* 2003). By focusing on the mineralogy of echinoderm species above

70˚S, we essentially removed temperature as a variable. If changes in Mg/Ca ratios continued with increasing latitude above 70˚S, it would imply that a factor other than seawater temperature might be driving the inverse relationship between latitude and skeletal magnesium content in echinoderms. However, because we generally observed no changes in Mg/Ca ratios for body component or intact echinoderms collected above 70˚S, we believe this supports the hypothesis that temperature is likely a factor driving this relationship. Interestingly, sea stars were the only taxon to maintain a correlation between latitude and magnesium content between 70-76˚S. As sea stars generally have more tissue and less continuous calcified mass than sea urchins, it is possible that these characteristics alter how calcification will be impacted by latitude. With the continued correlation in a relatively thermally static environment, it is likely that more than just temperature plays a role in the determination of skeletal magnesium content. The present study thus provides not only the first analysis of a suite of echinoderms above 70° south, but evidence that the correlation between skeletal magnesium content in echinoderms and latitude is driven, at least in part, by changes in seawater temperature.

Acknowledgements

The authors thank Gopi Samudrala and Yogesh Vohra for their assistance with X-ray diffraction measurements performed in the UAB Department of Physics. We thank Pamela Brannock for her assistance with sample collection and preparation aboard the research vessels. We extend our gratitude for logistical and personnel support to Antarctic Support Contract. We thank Margaret Amsler for assistance with sample preparations. The present study was supported in part by National Science Foundation grants ANT-1043745 awarded to KMH and ANT-1041022 awarded to JBM, Charles D.

Amsler, and Robert A. Angus. JBM acknowledges UAB support provided by the Endowed Professorship in Polar and Marine Biology.

References

ANDERSSON, A.J., MACKENZIE, F.T. & BATES, N.R. 2008. Life on the margin: implications of ocean acidification on Mg-calcite, high latitude and cold-water marine calcifiers. *Marine Ecology Progress Series,* **373**, 265–273,

ARNTZ, W., BREY, T. & GALLARDO, V. 1994. Antarctic zoobenthos. *In* Ansell, A., Gibson, R. & Barnes, M., *eds. Oceanography and Marine Biology, An Annual Review*. **32**, London: UCL Press, 241-304.

BARNES, D.K.A., FUENTES, V., CLARKE, A., SCHLOSS, I.R., & WALLACE, M.I. 2006. Spatial and temporal variation in shallow seawater temperatures around Antarctica. *Deep-Sea Research II,* **53**, 853-865.

BEDNARŠEK, N., TARLING, G., BAKKER, D., FIELDING, S., JONES, E., VENABLES, H., WARD, P., KUZIRIAN, A., LÉZÉ, B. & FEELY, R. 2012. Extensive dissolution of live pteropods in the Southern Ocean. *Nature Geoscience*, **5**, 881-885.

BINYON, J. 1976. The permeability of the asteroid podial wall to water and potassium ions. *Journal of the Marine Biological Association of the United Kingdom,* **56**, 639-647.

BØGGILD, O.B. 1930. The shell structure of the mollusks. *Det Kongelige Danske Videnskabernes Selskabs Skrifter, Natruvidenskabelig og Mathematisk, Afdeling, Ser. 9,* **2**, 231-326.

BYRNE, M., SMITH, A.M., WEST, S., COLLARD, M., DUBOIS, P., GRABA-LANDRY, A. & DWORJANYN, S.A. 2014. Warming influences Mg^{2+} content, while warming and acidification influence calcification and test strength of a sea urchin. *Environmental science & technology,* **48**, 12620-12627.

CALDEIRA, K. & WICKETT, M.E. 2003. Oceanography: anthropogenic carbon and ocean pH. *Nature,* **425**, 365-365.

CHAVE, K.E. 1954. Aspects of the biogeochemistry of magnesium 1. Calcareous marine organisms. *The Journal of Geology*, **62**, 266-283.

COLLARD, M., EECKHAUT, I., DEHAIRS, F. & DUBOIS, P. 2014. Acid–base physiology response to ocean acidification of two ecologically and economically important holothuroids from contrasting habitats, *Holothuria scabra* and *Holothuria parva*. *Environmental Science and Pollution Research,* **21**, 13602-13614.

COLLARD, M., DE RIDDER, C., DAVID, B., DEHAIRS, F. & DUBOIS, P. 2015. Could the acid–base status of Antarctic sea urchins indicate a better-than-expected resilience to near-future ocean acidification? *Global Change Biology,* **21**, 605-617.

DAVID, B., CHONÉ, T., MOOI, R. & DE RIDDER, C. 2005. *Antarctic Echinoidea*. ARG Gantner Verlag KG, Lichtenstein, 275 pp.

DAYTON, P.K., ROBILLIARD, G.A., PAINE, R.T. & DAYTON, L.B. 1974. Biological accommodation in the benthic community at McMurdo Sound, Antarctica. *Ecological Monographs*, **44**, 105-128.

DICKSON, J. 2002. Fossil echinoderms as monitor of the Mg/Ca ratio of Phanerozoic oceans. *Science*, **298**, 1222-1224.

EBERT, T.A. 2007. Growth and Survival of Postsettlement Sea Urchins. *In* Lawrence, J.M., *ed. Edible Sea Urchins: Biology and Ecology*. Developments in Aquaculture and Fisheries Science, **37**, Amsterdam: Elsevier, 529.

FABRY, V.J., MCCLINTOCK, J.B., MATHIS, J.T. & GREBMEIER, J.M. 2009. Ocean acidification at high latitudes: the bellweather. *Oceanography*, **22**, 160.

GATTUSO, J.-P., MAGNAN, A., BILLE, R., CHEUNG, W., HOWES, E., JOOS, F., ALLEMAND, D., BOPP, L., COOLEY, S. & EAKIN, C. 2015. Contrasting futures for ocean and society from different anthropogenic CO_2 emissions scenarios. *Science*, **349**, aac4722.

GOODING, R.A., HARLEY, C.D. & TANG, E. 2009. Elevated water temperature and carbon dioxide concentration increase the growth of a keystone echinoderm. *Proceedings of the National Academy of Sciences*, **106**, 9316-9321.

GRANGE, L.J. & SMITH, C.R. 2013. Megafaunal communities in rapidly warming fjords along the West Antarctic Peninsula: hotspots of abundance and beta diversity. *PloS ONE*, **8**, e77917.

HUNT, B.M., HOEFLING, K., & CHENG, C.C. 2003. Annual warming episodes in seawater temperatures in McMurdo Sound in relationship to endogenous ice in notothenioid fish. *Antarctic Science*, **15**, 333-338.

IPCC 2014. Climate Change 2014: Synthesis Report. Contribution of Working Groups, I, II, and III to the Fifth Assessment Report of the Intergovernmental Panel on Climate Change. Geneva, Switzerland: IPCC, 151 pp.

LAVIGNE, M., HILL, T., SANFORD, E., GAYLORD, B., RUSSELL, A., LENZ, E., HOSFELT, J. & YOUNG, M. 2013. The elemental composition of purple sea urchin (*Strongylocentrotus purpuratus*) calcite and potential effects of pCO_2 during early life stages. *Biogeosciences*, **10**, 3465-3477.

LEBRATO, M., IGLESIAS-RODRÍGUEZ, D., FEELY, R.A., GREELEY, D., JONES, D.O., SUAREZ-BOSCHE, N., LAMPITT, R.S., CARTES, J.E., GREEN, D.R. & ALKER, B. 2010. Global contribution of echinoderms to the marine carbon cycle: $CaCO_3$

budget and benthic compartments. *Ecological Monographs,* **80**, 441-467.

MACKENZIE, F.T., BISCHOFF, W.D., BISHOP, F.C., LOIJENS, M., SCHOONMAKER, J. & WOLLAST, R. 1983. Magnesian calcites; low-temperature occurrence, solubility and solid-solution behavior. *Reviews in Mineralogy and Geochemistry,* **11**, 97-144.

MAGDANS, U. & HERMANN, G. 2004. Single crystal structure analysis of sea urchin spine calcites Systematic investigations of the Ca/Mg distribution as a function of habitat of the sea urchin and the sample location in the spine. *European Journal of Mineralogy,* **16**, 261-268.

MCCLINTOCK, J.B., ANGUS, R.A., MCDONALD, M.R., AMSLER, C.D., CATLEDGE, S.A. & VOHRA, Y.K. 2009. Rapid dissolution of shells of weakly calcified Antarctic benthic macroorganisms indicates high vulnerability to ocean acidification. *Antarctic Science,* **21**, 449-456.

MCCLINTOCK, J.B., AMSLER, M.O., ANGUS, R.A., CHALLENER, R.C., SCHRAM, J.B., AMSLER, C.D., MAH, C.L., CUCE, J. & BAKER, B.J. 2011. The Mg-calcite composition of Antarctic echinoderms: important implications for predicting the impacts of ocean acidification. *The Journal of Geology,* **119**, 457-466.

MCNEIL, B.I. & MATEAR, R.J. 2008. Southern Ocean acidification: A tipping point at 450-ppm atmospheric CO_2. *Proceedings of the National Academy of Sciences,* **105**, 18860-18864.

MILES, H., WIDDICOMBE, S., SPICER, J.I. & HALL-SPENCER, J. 2007. Effects of anthropogenic seawater acidification on acid–base balance in the sea urchin *Psammechinus miliaris*. *Marine Pollution Bulletin,* **54**, 89-96.

MILLIMAN, J. 1974. *Marine Carbonates, Part I*. New York: Springer-Verlag,

MORSE, J.W., ANDERSSON, A.J. & MACKENZIE, F.T. 2006. Initial responses of carbonate-rich shelf sediments to rising atmospheric pCO_2 and "ocean acidification": role of high Mg-calcites. *Geochimica et Cosmochimica Acta,* **70**, 5814-5830.

MUCCI, A. 1983. The solubility of calcite and aragonite in seawater at various salinities, temperatures, and one atmosphere total pressure. *American Journal of Science,* **283**, 780-799.

ORR, J.C., FABRY, V.J., AUMONT, O., BOPP, L., DONEY, S.C., FEELY, R.A., GNANADESIKAN, A., GRUBER, N., ISHIDA, A. & JOOS, F. 2005. Anthropogenic ocean acidification over the twenty-first century and its impact on calcifying organisms. *Nature,* **437**, 681-686.

PECK, L.S., WEBB, K.E. & BAILEY, D.M. 2004. Extreme sensitivity of biological function to temperature in Antarctic marine species. *Functional Ecology,* **18**, 625-630.

RIES, J.B. 2004. Effect of ambient Mg/Ca ratio on Mg fractionation in calcareous marine invertebrates: A record of the oceanic Mg/Ca ratio over the Phanerozoic. *Geology,* **32**, 981-984.

RIES, J.B. 2011. Skeletal mineralogy in a high-CO_2 world. *Journal of Experimental Marine Biology and Ecology*, **403**, 54-64.

SEWELL, M.A. & HOFMANN, G.E. 2011. Antarctic echinoids and climate change: a major impact on the brooding forms. *Global Change Biology,* **17**, 734-744.

WEBER, J.N. 1969. The incorporation of magnesium into the skeletal calcites of echinoderms. *American Journal of Science,* **267**, 537-566.

WEBER, J.N. 1973. Temperature dependence of magnesium in echinoid and asteroid skeletal calcite: a reinterpretation of its significance. *Journal of Geology,* **81**, 543-556.

WOOD, H.L., SPICER, J.I. & WIDDICOMBE, S. 2008. Ocean acidification may increase calcification rates, but at a cost. *Proceedings of the Royal Society of London B: Biological Sciences,* **275**, 1767-1773.

Table 1. Latitude, longitude, and depth (m) of the 23 collection sites above 70° south from the January 2013 research cruise.

Latitude	Longitude	Depth (m)
-70° 48.71'	-92 31.30'	430
-71° 42.14'	-91 30.22'	430
-71° 41.94'	-93 41.62'	670
-70° 50.52'	-95 24.67'	472
-71° 45.14'	-102 14.09'	459
-72° 28.95'	-104 33.77'	591
-72° 47.14'	-104 32.24'	496
-73° 43.29'	-103 37.01'	699
-72° 10.64'	-103 30.84'	341
-72° 12.25'	-103 35.78'	612
-71° 08.83'	-107 59.07'	627
-73° 09.53'	-129 53.69'	440
-73° 17.79'	-129 11.54'	506
-73° 29.91'	-129 55.12'	516
-73° 14.81'	-129 30.15'	478
-75° 19.05'	-176 54.12'	570
-76° 21.18'	-170 49.49'	546
-76° 28.76'	-165 44.26'	457
-76° 59.89'	-175 05.59'	541
-76° 14.71'	174 30.24'	604
-76° 54.22'	169 57.91'	764
-75° 50.00'	166 30.32'	552
-74° 42.46'	168 24.76'	489

Table 2. Latitude, longitude, and depth (m) of the 10 collection sites along the Western Antarctic Peninsula from the November 2013 research cruise.

Latitude	Longitude	Depth (m)
-62° 59.75'	-58 35.91'	320
-63° 42.03'	-56 04.71'	293
-64° 18.13'	-56 08.18'	290
-64° 02.11'	-56 43.69'	220
-63° 41.14'	-56 51.54'	NA
-63° 45.22'	-55 41.03'	334
-63° 34.57'	-54 37.76'	227
-62° 26.53'	-55 27.53'	245
-62° 53.63'	-59 10.06'	827
-65° 01.25'	-64 25.50'	312

Table 3. The number of sites at which each taxon was collected either below 70° south or above 70° south latitudes.

Taxa	Body parts analyzed	# Sites < 70˚S	# Sites > 70˚S
Sea Stars	Intact	4	10
Large Brittle Stars	Arms	4	17
	Disk	N/A	17
Small Brittle Stars	Intact	N/A	17
Sterechinus spp.	Spines	2	14
	Test	2	14
	Lantern	2	14
Cidaroid Urchins	Spines	2	11
	Test	N/A	11
	Lantern	N/A	11
Heart urchins	Intact	N/A	13

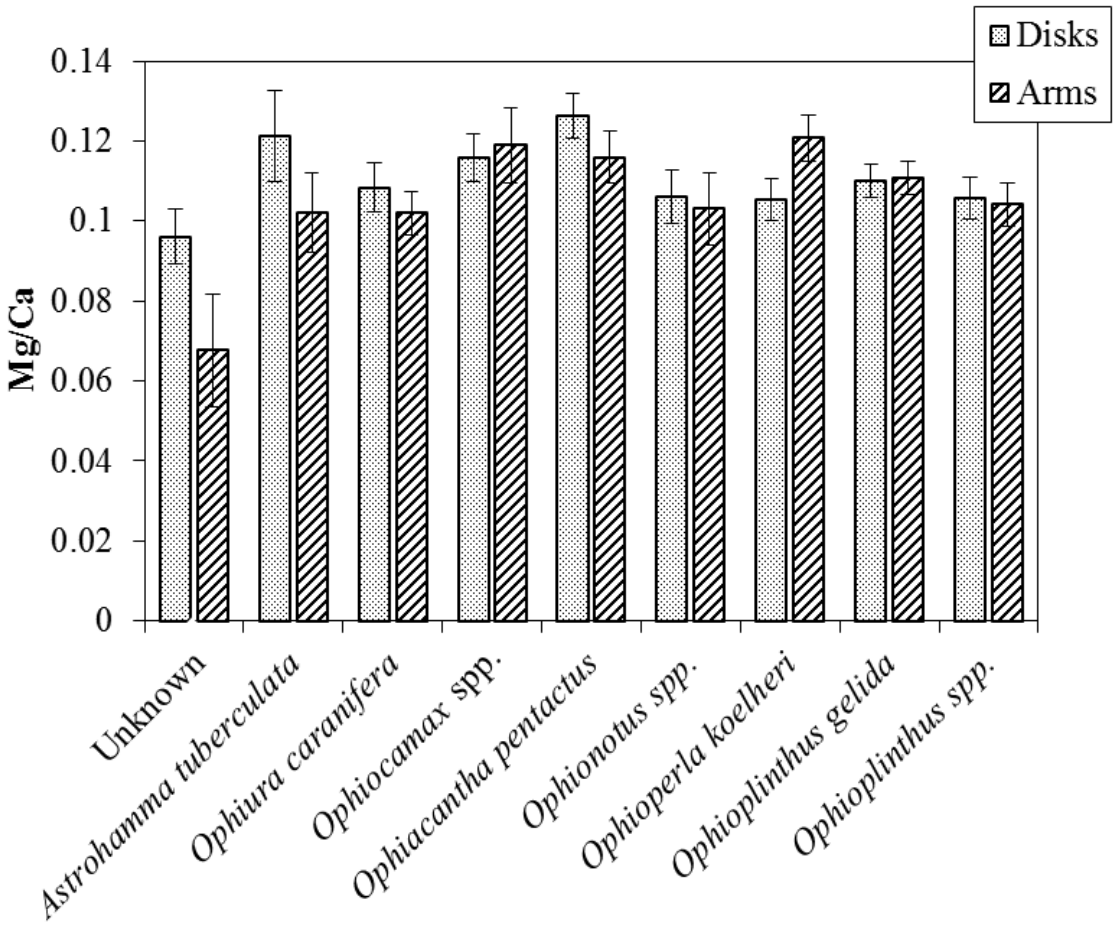

Fig. 1. Mean molar Mg/Ca ratio for distinct body components (disks and arms) within nine species of brittle stars collected along the western coast of Antarctica. Error bars are mean ± 1 SE

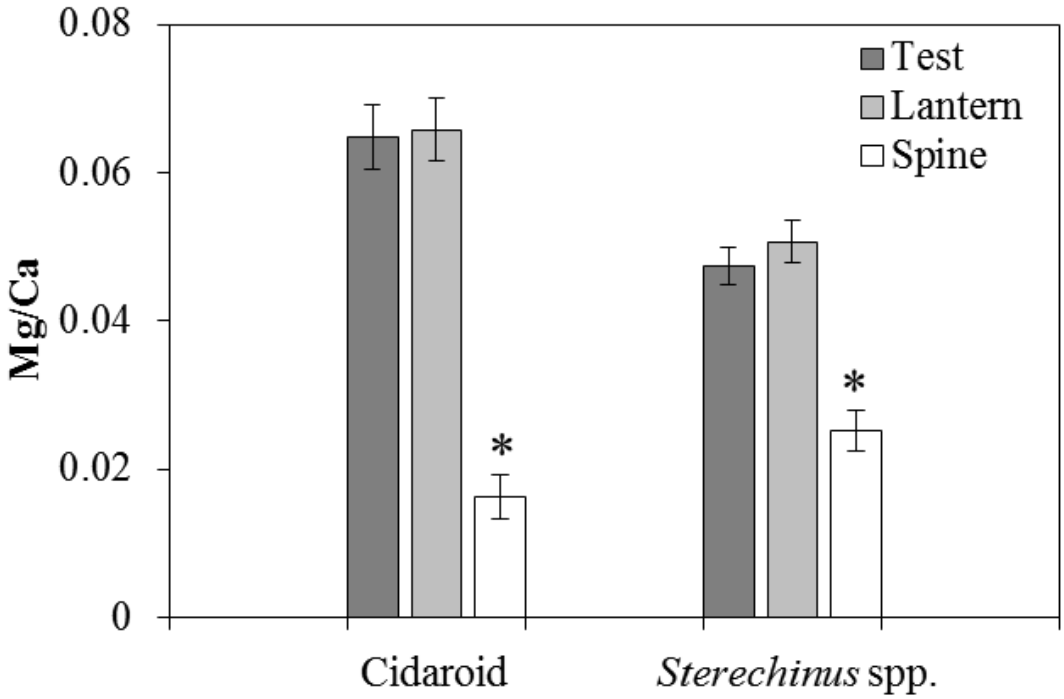

Fig. 2. Mean molar Mg/Ca ratio for distinct body components (tests, spines, and Aristotle's lanterns) within cidaroid sea urchins and the sea urchin genus *Sterechinus* collected along the western coast of Antarctica. Error bars represent mean ± 1 SE. Asterix represents significantly different means.

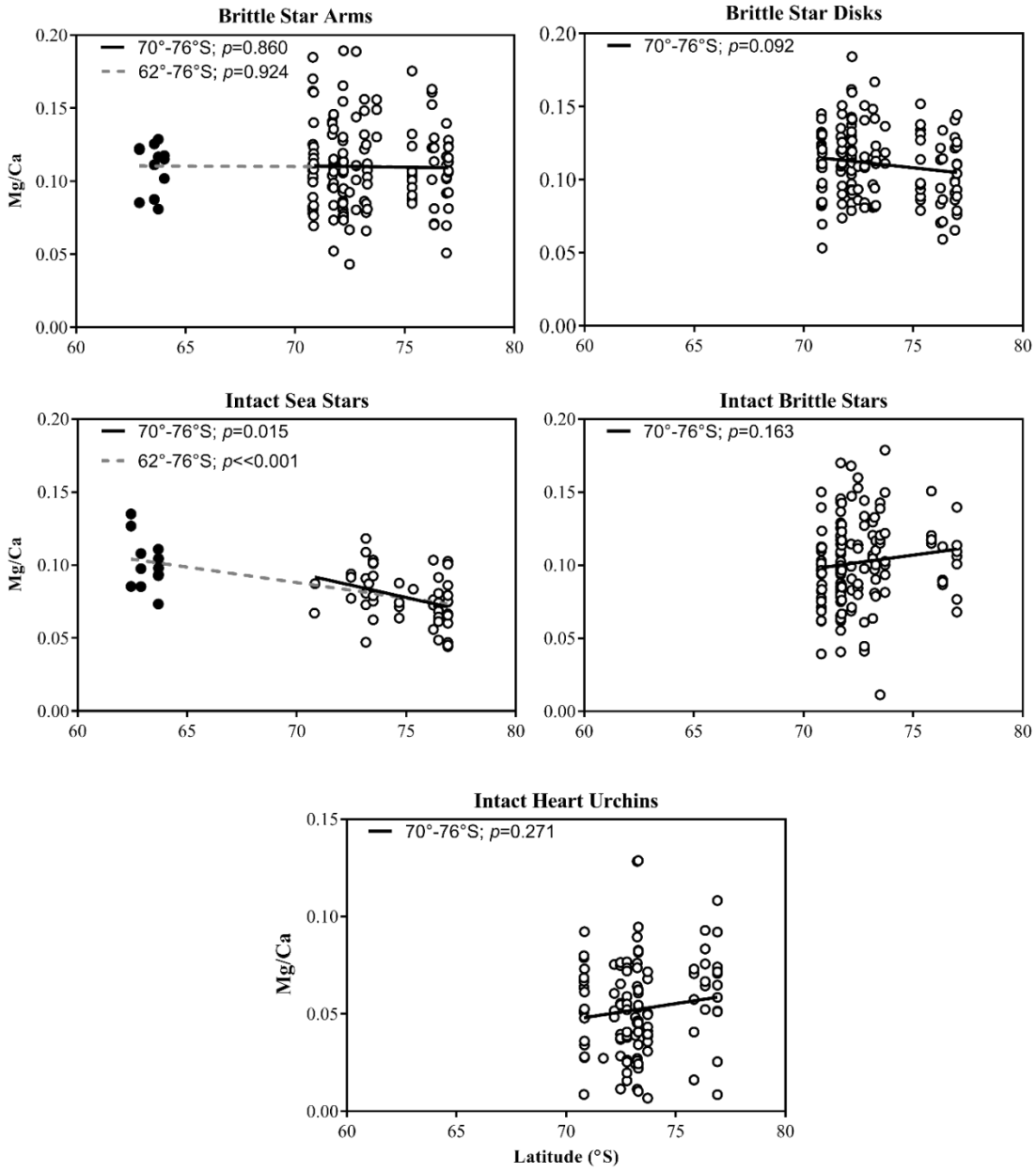

Fig. 3. Correlation between latitude south and molar Mg/Ca ratio of skeletal components of large brittle stars split into arms and central disks, intact sea stars, intact brittle stars, and intact heart urchins. Closed circles represent the molar Mg/Ca ratios for samples collected north of 70°S and open circles represent those collected south of 70°S The solid lines represent the correlation between latitude and molar Mg/Ca ratios above 70°S latitude. The hashed lines represent the correlation between latitude and molar Mg/Ca ratios between 62°-76°S latitude. The p-values below 0.05 represent significant correlations between latitude and molar Mg/Ca ratios of skeletal material.

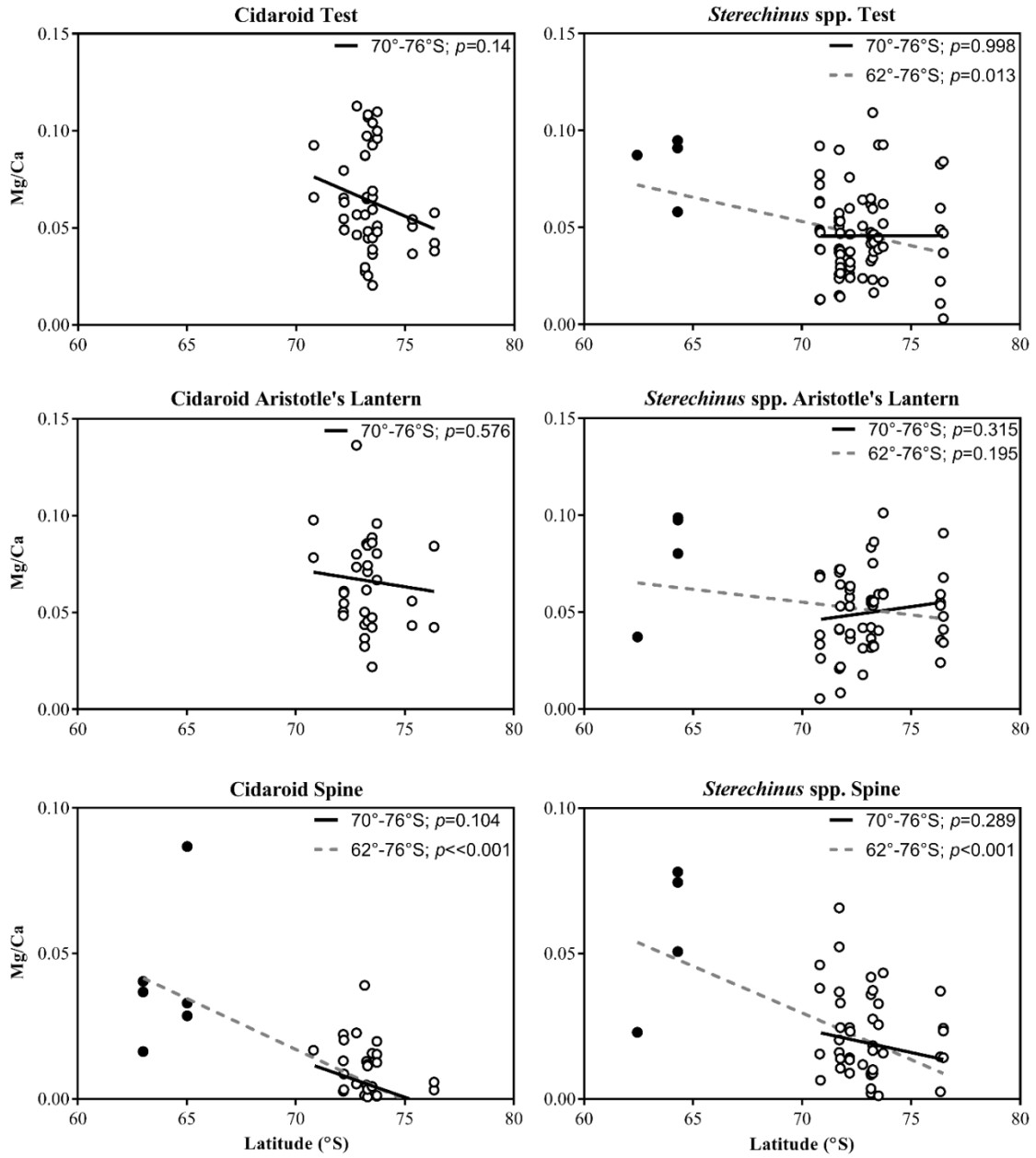

Fig. 4. Correlation between latitude south and molar Mg/Ca ratio of skeletal components of Cidaroid sea urchins and regular sea urchins belonging to the genus *Sterechinus.* Both groups of regular sea urchins were separated into 3 body components for analysis: tests, Aristotle's lanterns, and spines. Closed circles represent the molar Mg/Ca ratios for samples collected north of 70°S and open circles represent those collected south of 70°S. The solid lines represent the correlation between latitude and molar Mg/Ca ratios above 70°S latitude. The hashed lines represent the correlation between latitude and molar Mg/Ca ratios between 62°-76°S latitude. The p-values below 0.05 represent significant correlations between latitude and Mg/Ca ratios of skeletal material.

NEAR-FUTURE ELEVATED TEMPERATURE IMPACTS ON THE Mg/Ca RATIOS IN THE TEST, SPINES, AND ARISTOTLE'S LANTERN OF THE SUB-TROPICAL SEA URCHIN *LYTECHINUS VARIEGATUS*

by

ASHLEY DUQUETTE, JAMES B. MCCLINTOCK, YOGESH K. VOHRA

In preparation for *Journal of Experimental Marine Biology and Ecology*

Format adapted for dissertation

Abstract

Marine invertebrates currently living at the upper reach of their temperature tolerance and that cannot migrate to more physiologically tolerable temperatures are particularly susceptible the impacts of rising seawater temperatures associated with global climate warming. Populations of the common seagrass-associated sea urchin *Lytechinus variegatus* that occur in the northern Gulf of Mexico lack the ability to extend their distribution northward in response to rising seawater temperatures. Previous studies indicate that aspects of the behavior, physiology, and immunology of this sea urchin will soon be temperature stressed, however, nothing is known about potential temperature impacts on its mineralogy. Sea urchins construct their skeletons out of high magnesium calcite, and the magnesium content of calcite can be influenced by a variety of abiotic factors including temperature. In several instances, elevated seawater temperature has been shown to increase levels of magnesium in echinoderm calcite, a result that may render the skeleton more susceptible to the negative impacts of ocean acidification. Understanding how elevated temperature impacts the mineralogy of the skeleton of the ecologically important sea urchin *L. variegatus* will assist in making predictions about susceptibility to ocean acidification. Juvenile sea urchins were collected in Eagle Harbor, FL and chronically exposed for 90 days to either 26°C (control) or to a predicted near-future temperature of 30°C. Individuals were sub-sampled every 30 days and the Mg/Ca ratios of their test, spines, and Aristotle's lantern were determined using X-ray diffraction techniques. Contrary to expectation, Mg/Ca levels in body components were lower in individuals held in the 26°C than the 30°C treatment. The only exception was the test at day 90 and the spines on days 60 and 90, where there was no significant difference in

magnesium levels between the two temperature treatments. There was also no effect of age (growth) on Mg/Ca levels of individual body components at either temperature. Our results suggest that either this sea urchin does not increase its allocation of magnesium to calcite with elevated temperature, or that individuals held at 30°C were stressed and may have been investing their resources elsewhere. For *L. variegatus*, elevated temperature may not increase skeletal solubility under conditions of ocean acidification.

Introduction

As a result of increasing levels of anthropogenic carbon dioxide (CO_2) emissions, marine invertebrates are experiencing environmental changes at an unprecedented rate. Remarkably, the current rate of increase of global atmospheric CO_2 is approximately an order of magnitude greater than that estimated to have occurred over the past several thousands of years (Doney and Schimel, 2007). This increase in such a potent greenhouse gas has resulted in a rise of 0.6°C globally over the past century (Smith et al., 2009). Given that the world's oceans act as sinks for atmospheric heat and CO_2, sea-surface temperature (SST) has risen by approximately 0.4°C (Levitus et al., 2009), and ocean pH has dropped by an average of 0.1 pH units (Rhein et al., 2013a). This increase in SST is expected to continue and result in another 2-3°C of warming by the end of the century (2100) (Collins et al., 2013). Tropical and subtropical in the Northern Hemisphere are expected to experience some of the strongest ocean warming (Collins et al., 2013).

Assuming a business as usual model, the acidification of the world's oceans is also expected to continue, with a further decline of 0.3-0.4 pH units by 2100 (Hoegh-Guldberg et al., 2014). Because these two environmental stressors will occur

concurrently, it is important to understand how impacts on marine invertebrates from one stressor (elevated temperature) may affect their susceptibility to a second stressor (acidification).

Environmental factors such as temperature are known to affect multiple aspects of marine invertebrate physiology and ecology. In some instances, increased temperature within some optimal range can be beneficial by promoting or increasing rates of development, for example (Delorme and Sewell, 2013; Hardy et al., 2014; Li et al., 2011). Moreover, temperature increases within an optimal range can lessen the negative impacts of other environmental factors including stress associated with salinity or pH (Brennand et al., 2010; Byrne et al., 2011; Delorme and Sewell, 2014; McCulloch et al., 2012). Nevertheless, for marine invertebrates currently living at or near their upper thermal tolerance level, temperature increases may result in sub-lethal negative impacts by increasing respiratory demand and ultimately limit resources and energy available for growth and reproduction (Pörtner, 2008; Pörtner and Knust, 2007). Some marine invertebrate species are able to escape warming by extending their geographic range to more physiologically tolerable environments (Jones et al., 2009, 2010; Spencer, 2008). However, not all marine invertebrates are able to do so as some are bound by geological constraints.

Echinoderms are generally impacted by changing temperature (Moore, 1966). These impacts can occur at all life history stages, affecting both development and survival (e.g., Byrne et al., 2013; Delorme and Sewell, 2013; Hardy et al., 2014; Sewell and Young, 1999). There has also been interest in the impacts of temperature on the magnesium content of the skeletal components of echinoderms. Echinoderms construct

their skeletal components out of 'high magnesium calcite,' the most soluble polymorph of calcium carbonate (Vinogradov and Odum, 1953; Weber, 1973). The amount of magnesium present in the calcite determines solubility and also affects the hardness of the mineral (Byrne et al., 2014; Kunitake et al., 2012). As solubility increases, so does the susceptibility to dissolution with increasing ocean acidification (Morse et al., 2006). While magnesium content is generally linked to taxonomic history (Chave, 1954), there is a long standing hypothesis that magnesium content in echinoderm skeletons increases with decreasing latitude (Andersson et al., 2008; Chave, 1954; McClintock et al., 2011). However, the driving cause(s) of this trend remains unclear. Several studies have shown that magnesium content varies with multiple abiotic and biotic factors such as temperature, salinity, Mg/Ca ratio of seawater, diet and carbonate saturation states (Andersson et al., 2008; Asnaghi et al., 2014; Hermans et al., 2010; Marubini et al., 2003; Ries, 2004). It has been further suggested that temperature, as it affects overall growth rates, may be the most important factor for echinoderms, particularly those inhabiting intertidal and shallow subtidal environments (Wolfe et al., 2013).

Lytechinus variegatus is a common intertidal/subtidal sea urchin whose biogeographic distribution ranges from Brazil to North Carolina, including the Gulf of Mexico and Caribbean (Mortensen, 1943; Watts et al., 2001). The species typically inhabits sea grass beds where it is a primary grazer, impacting both energy transfer and density of seagrass beds (Heck and Valentine, 1995; Watts et al., 2013). Some populations occur in shallow, semi-enclosed bays in the Gulf of Mexico where they exist at the extreme northern extension of their biogeographic range in the Gulf of Mexico. While *L. variegatus* is exposed to significant daily and annual variations in temperature

(Beddingfield and McClintock, 2000; Challener et al., 2015), individuals exposed chronically to temperatures of 30°C or more experience stress. For example, Brothers and McClintock (2015) recently reported righting and covering behaviors in *L. variegatus* were negatively affected after a ten day exposure to 32°C.The present study expands on our understanding of the capacity of the common subtropical sea urchin *L. variegatus* to withstand rising seawater temperatures in the extreme northern distribution of its biogeographic range. By exposing individuals to a chronic near-future temperature deemed stressful but not lethal, we examine whether chronic stress-inducing temperature exposure impacts the allocation of magnesium to skeletal calcite. We are accordingly able to address the question of whether *L. variegatus* exposed to near-future elevated temperature will necessarily produce higher magnesium calcite and thus render its skeletal components more susceptible to dissolution with intensifying ocean acidification.

Methods

Juvenile *Lytechinus variegatus* (20-25 mm diameter, n = 85) were hand collected from seagrass beds in Eagle Harbor in Port Saint Joseph Bay, FL (29°45'N, 85°24'W) in June 2014 and transported to the University of Alabama at Birmingham, Birmingham, AL. Upon return to the laboratory, 25 individuals were randomly selected, measured, weighed, and sacrificed for mineralogical analysis to establish baseline mean (± SE) Mg/Ca ratios in discrete skeletal components (spines, test, and Aristotle's lantern). The remaining individuals (n = 60) were randomly distributed into twenty 38-L aquaria containing artificial seawater (Instant Ocean® prepared with reverse-osmosis filtered water) at a salinity of 32 ppt, a temperature of 23°C, and a pH of 8.2. Each of the 20

aquariums held 3 sea urchins in individual plastic, cylindrical cages (25.4 cm x 10.2 cm, HxD). Aquariums were aerated continuously using airstones plumbed to a CORALIFE® Super LuftSL-65 high pressure aquarium pump and water in each aquarium was circulated using a recirculating filter pump (Aqueon Power Filter 10). Water temperatures were controlled with EHEIM Jager 50 W heaters and daily temperature measurements were taken using an YSI 85 temperature meter. Sea urchin feces and uneaten artificial food (see below) were siphoned out of the aquaria every day before feeding, and a 30-50% water change was carried out every other day to maintain good water quality. Measures of water quality (salinity, ammonia, nitrate, nitrite, and pH) were measured every other day for each aquarium using a Fisher Scientific handheld refractometer, Aquarium Pharmaceuticals, Inc. liquid test kits, and a Fisher Scientific Accumet basic model AB 15 pH meter with an ACCUTU pH electrode, respectively.

Before beginning the temperature treatments, sea urchins were kept at a constant temperature for one week (23.09 ± 0.1°C) to allow them to acclimate to laboratory conditions following collection and transport. After this one week acclimation period, each of the twenty aquaria was randomly assigned to one of the two temperature treatments (ambient - 26°C; near- future elevated - 30°C). Each sea urchin was fed an *ad libitum* diet of formulated feed (Hammer et al., 2012). The temperature in each aquarium was gradually increased over one week from 23 C to either 26°C or 30°C. Aquaria were held at their respective temperature for a 3 month period under a photoperiod of 12 h light: 12 hr dark. Every four weeks, each aquarium was cleaned to remove bacterial growth and algal biofilms (Challener and McClintock, 2013).

Every four weeks, a single sea urchin was removed from each of twenty aquaria and its test diameter measured and whole body wet determined after a 30 sec draining period on an absorbent paper towel. Individuals (n = 10 for each of the two temperature treatments) were then sacrificed and the tissue dissected away from the skeletal components: test, spines, and Aristotle's lantern. Skeletal material was then placed into a 10% NaClO solution to dissolve away remaining organic tissue. The NaClO solution was exchanged as necessary to promote complete digestion. The clean skeletal material was rinsed with distilled water, vacuum dried, and then air dried for 24 hrs. Once dry, skeletal components were ground into a fine powder using an agate mortar and pestle while adding approximately 15 drops of 95% ethanol to facilitate grinding. This slurry was air dried for 24 hrs and the resultant finely ground powder used in X-ray Diffraction Analysis (XRD). The XRD was carried out using a Philips X'Pert Analytical X-ray diffraction system. The x-ray tube had a copper target and the wavelength utilized in the experiment was 1.54056 angstroms (0.154056 nanometers). The resulting XRD pattern was used to determine the Mg/Ca ratio following the equation in Ries (2011):

$$Mg/Ca = 0.17881(2\Theta)^2 - 10.20926(2\Theta) + 145.59368$$

The above equation relates Mg/Ca ratio to the 2Θ value of the main calcite peak taken from the resulting XRD pattern.

Mg/Ca ratios were log(x+1) transformed to fit a normal distribution. Mg/Ca ratios, wet weight, and test diameter were compared over time within treatment as well as between treatments. Statistical comparisons over time did not include the baseline data as

it was collected prior to exposure to experimental temperatures. Mg/Ca ratios were also compared within temperature treatments among body components (test, spines, and lantern). A two way RMANOVA was used to determine if whole body wet weight, test diameter, or skeletal Mg/Ca ratio for body components changed with time or temperature. A Tukey HSD post-hoc test was employed to specify which time points differed from others. At each time point (30, 60, or 90 days), a Student's T-test was used to compare mean Mg/Ca ratios between the two temperature treatments. Lastly, a one-way ANOVA was used to determine if skeletal Mg/Ca ratios in the test, spines, and lantern were significantly different from one another at each time period sampled within each temperature treatment. A Tukey HSD post-hoc test differentiated which body components were significantly different from the others.

Results

The original sample size of sea urchins held in the 30°C treatment was reduced by four sea urchins over the course of the experiment due to their displaying indications of stress (significant spine loss). The balance of sea urchins in this temperature treatment appeared healthy and allowed for a statistically robust analysis. All sea urchins held in the ambient 26°C temperature treatment remained viable throughout the experiment.

Time (day 30, 60, and 90) did have a significant effect on wet weight and test diameter of the sea urchins (RMANOVA; $F_{(2,32)} = 61.82$, $p < 0.001$; $F_{(2,32)} = 57.73$, $p < 0.001$, respectively). Both mean wet weight and test diameter increased with time (Figure 1a, b). A Tukey HSD test indicated that, within the 26°C treatment, wet weight changed significantly at each time point (Tukey HSD test; $p < 0.001$). Similarly, within the 30°C

treatment, mean wet weight of sea urchins was significantly different at every time point (Tukey HSD test; 30 vs. 60 $p = 0.005$; 30 vs. 90 $p < 0.001$; 60 vs 90 $p = 0.013$, respectively), but the increase between days 30 and 60 (5.6 g wet wt) was greater than the difference between days 60 and 90 (5.0 g wet wt). Sea urchins held in the 26°C seawater demonstrated significant test diameter increase at each time point (Tukey HSD test; $p < 0.05$). However, sea urchins held in the 30°C seawater demonstrated significant test diameter differences between the 30 and 60 day measurement and the 30 and 90 day measurement (Tukey HSD test; $p < 0.001$). In contrast, mean test diameters from day 60 to 90 were not significantly different from one another, but showed a trend of an increase (Tukey HSD test; $p = 0.327$). In contrast to the growth parameters, Mg/Ca ratios did not vary over time for *L. variegatus* in either temperature treatment for the test (RMANOVA; $F_{(2,32)} = 0.273$, $p = 0.763$; Figure 2a), spines (RMANOVA; $F_{(2,32)} = 2.25$, $p = 0.122$; Figure 2b), or lantern (RMANOVA; $F_{(2,32)} = 0.565$, $p = 0.574$; Figure 2c).

Increased seawater temperature (30°C) did not have a significant effect on either total body wet weight or test diameter in sea urchins (RMANOVA; $F_{(1.16)} = 3.88$, $p = 0.066$; $F_{(1, 16)} = 3.92$, $p = 0.065$, respectively). It is noteworthy that the individuals held in the 26°C treatment were consistently, but not significantly, heavier and larger than those in the 30°C treatment (Table 1). There was a significant effect of temperature on mean Mg/Ca ratios of sea urchin test, spines, and lantern such that the 26°C sea urchins had consistently higher ratios than those raised at 30°C (RMANOVA; $F_{(1.16)} = 18.73$, $p = 0.0005$; $F_{(1, 16)} = 6.61$, $p = 0.021$, $F_{(1, 16)} = 20.55$, $p < 0.001$, respectively; Table 2). The Mg/Ca ratios differed for each body component. For the test, the significant difference in Mg/Ca ratios between the two temperature treatments occurred at both day 30 and 60

(Student T-test; $t_{(16)} = 2.129$, $p = 0.049$; $t_{(16)} = 3.61$, $p = 0.002$, respectively; Figure 2a). For the spines, Mg/Ca ratios differed after day 30 (Student T-test; $t_{(16)} = 2.56$, $p = 0.021$; Figure 2b) but were not significantly different on days 60 and 90. In contrast to the test and spines, the Aristotle's lantern demonstrated significant differences in Mg/Ca ratios between temperature treatments on days 30, 60, and 90 (Student T-test; $t_{(16)} = 3.284$, $p = 0.005$; $t_{(16)} = 2.553$, $p = 0.021$; $t_{(16)} = 2.337$, $p = 0.033$, respectively; Figure 2c).

Mg/Ca ratios were also compared among the body components within each temperature treatment (26°C and 30°C) and at each time point (30, 60, and 90 days; Table 2). At 26°C, the spines had significantly lower ratios than did the test or lantern on days 30, 60, and 90 (ANOVA: $F_{(2,27)} = 15.68$, $p < 0.001$; $F_{(2,27)} = 9.19$, $p = 0.001$; $F_{(2,27)} = 14.02$, $p < 0.001$, respectively; Figure 3a). At 30°C, the spines had significantly lower ratios than the test and lantern, but not at every time point (Figure 3b). The skeletal material in the three body components of individuals held at 30°C did not have significantly different Mg/Ca ratios at day 60 (ANOVA: $F_{(2,21)} = 1.02$, $p = 0.378$), but did at days 30 and 90 (ANOVA: $F_{(2,21)} = 15.59$, $p < 0.001$; $F_{(2,21)} = 7.79$, $p = 0.003$, respectively).

Discussion

While the inverse relationship between latitude and skeletal magnesium content has been reasonably well documented for temperate and tropical echinoderms, the factors driving this relationship remain largely speculative, ranging from seawater temperature to diet (e.g., Asnaghi et al., 2014; Hermans et al., 2010). In the present study, we chose to investigate the effects of temperature since it seems a likely factor involved in regulating

magnesium content (Chave, 1954) and since current global climate change is driving both seawater warming and ocean acidification simultaneously. The expected impact of rising temperature on Mg/Ca ratios of echinoderm skeletons (increased Mg/Ca ratio) will, in turn, render echinoderm skeletons more soluble and potentially more susceptible to dissolution in acidifying seawater. Echinoderms experiencing skeletal dissolution are likely to have to invest their limited resources in skeletal maintenance and, by doing so, compromise fitness (Wood et al., 2010).

Individuals of the sea urchin *Lytechinus variegatus* examined in the present study were collected from a common environment and maintained in laboratory conditions that were identical in every respect except for seawater temperature. Accordingly, any changes observed in sea urchin skeletal Mg/Ca ratios in body components can be confidently attributed to temperature. Whole body wet weight and test diameter increases of individuals of *L. variegatus* observed in both temperature treatments indicate that the sea urchins were in generally good condition and actively growing. Interestingly, changes in growth between observation days 60 and 90 stood out for individuals held in the 30°C treatment. While an increase in whole body wet weight remained significant, the rate of growth was reduced (+4.98g from 30 to 60 days vs +5.58g from 60 to 90 days) in this time period. Moreover, there was a small but non-significant increase in test diameter (+1.49 mm over 30 days). As both total wet weight and test diameter increase slowed in the last thirty days of the 30°C treatment, but did not do so in individuals held in the 26°C treatment, it is possible that chronic exposure to 30°C had become sufficiently stressful to hinder growth. Temperature has a well-known direct impact on echinoderm physiology, including increased growth within the optimal thermal range (Fujisawa and Shigei, 1990;

Hardy et al., 2014). However, if the increase in temperature exceeds an individual's thermal tolerance range, the benefits of increasing temperature (e.g. increased metabolic rate) are lost. Elevated temperature, then, begins to hamper energy availability for physiological processes beyond maintenance, including growth and reproduction (Pörtner, 2008). While not quite statistically significant, the differences in wet weight and test diameter observed between individuals in the temperature treatments at 90 days may indicate physiological stress. As individuals in the 30°C treatment did not gain body size over the last 30 days of the 90 day trial, this temperature is likely to have exceeded the thermal tolerance for chronic exposure, channeling materials and energy away from growth.

Unlike the growth parameters examined in the present study, there were no significant changes in Mg/Ca ratios of skeletal material in the three primary body components over the 90 day course of the experiment in either temperature treatment. We had hypothesized that skeletal Mg/Ca ratios might change as the individuals in our experiment grew from juvenile (pre-gonadal size) to adult body size. Previous studies have demonstrated differential effect of temperature on echinoderms according to life history stage. However, these studies have not examined skeletal mineralogy, per se, emphasizing fertilization success, embryonic development, or larval growth (including larval skeletal morphometrics) (e.g., Byrne, 2011; Byrne et al., 2009; Delorme and Sewell, 2013; Díaz-Pérez and Carpizo-Ituarte, 2011; Sewell and Young, 1999). Other studies have had outcomes suggesting skeletal mineralogy in echinoids might be susceptible to environmental variables. For example, juveniles of the sea urchin *Paracentrotus lividus* that were held over a one month period at a predicted end-of-

century pH (7.7) had tests that were significantly more vulnerable to crushing than those held at ambient pH (Asnaghi et al., 2014). As the test in this study showed a differential response to acidification, it suggests that test responses to temperature may be plastic and might involve changes in mineralogy that would be manifest in altered test biomechanics. Nonetheless, Byrne et al. (2014 and references within) suggests that ocean acidification would seem to more often affect biomechanics of echinoderm skeletons, while temperature is more likely to impact mineralogy of the skeletons

Because temperature is a key predicted factor behind the inverse correlation between latitude and skeletal magnesium (Hermans et al., 2010), we were surprised to find that the mean Mg/Ca ratios for the skeletal material of each of the three body components of *L. variegatus* were consistently higher in sea urchins held at 26°C than in those sustained at 30°C. This pattern is relevant because elevating magnesium with near-future temperature increases may strengthen skeletal components (increased magnesium increases calcite hardness) that are generally facing increased susceptibility to dissolution from ocean acidification. In the absence of elevated magnesium, a weaker test or spines may render individuals more structurally susceptible to crushing, biting, or drilling predators. As for the lantern, a weaker lantern can impair feeding efficiency as the teeth are constantly being ground down (Ma et al., 2009). Clearly, there are trade-offs. Becoming somewhat more susceptible to dissolution may be a good trade off when weighted against loss of structural integrity.

One possible explanation for the surprisingly higher Mg/Ca ratios observed in skeletal components at 26°C than at 30°C is that the individuals chronically exposed to 30°C are experiencing sub-lethal, temperature-induced stress. While *L. variegatus*

periodically experiences 30°C in the northern Gulf of Mexico, to date it is not yet chronically exposed to this temperature (Challener et al., 2015). Previously, Brothers and McClintock (2015) observed that individuals of *L. variegatus* held chronically at 32°C in the laboratory survived for only 14 days despite being held in all respects under culture conditions. Because the individuals of *L. variegatus* in the present study were chronically exposed to 30°C, physiological stress could have a normative allocation of magnesium to calcite with increased temperature under the species' thermal optima.

The present study confirmed that the major skeletal body components of the sea urchin *L. variegatus* (test, spines, and lantern) exhibit significantly different Mg/Ca ratios. In particular, the spines consistently contained less magnesium than did either the test or the lantern. The three components each have a different structure and function, and it has been suggested that biomineralization pathways may differ , leading to altered mineralogy (Goetz et al., 2014; Robach et al., 2009; Veis, 2011). Previous studies have also demonstrated that skeletal magnesium content varies not only between skeletal components but in some instances within components (e.g., Borzęcka-Prokop et al., 2007; Ma et al., 2009). This internal variation allows mineral hardness to vary within a given skeletal component and is likely to have functional consequences (Byrne et al., 2014; Goetz et al., 2014; Ma et al., 2009). While it is evident that increased hardness due to elevated magnesium content in the test and feeding apparatus would have benefits, it is less clear why spines do not require a similar hardness. Spines are a vital defensive structure against predation but remain less vulnerable to dissolution with lower Mg/Ca ratios. Previous studies with echinoids support our findings that spines have a lower magnesium content than other body components. For example, Borzęcka-Prokop et al.

(2007) reported lower levles but also demonstrated that there is a gradient of magnesium with higher levels at tht base of the spine and reduced levels towards the spine tip. Byrne et al. (2014) posited that this gradient facilitates a certain amount of brittleness in the spine tip that may have a functional role in furthering defense or escape.

Acknowledgements

This study was approved by the Institutional Animal Care and Use Committee at the University of Alabama at Birmingham. The authors would like to thank Stephen Watts and Jeff Barry for supplying the urchin feed. Thanks also go out to Gopi Samudrala for assistance with x-ray diffraction. J.B. McClintock acknowledges the support of an Endowed Professorship in Polar and Marine Biology provided by the University of Alabama at Birmingham.

References

Andersson, A.J., Mackenzie, F.T., Bates, N.R., 2008. Life on the margin: implications of ocean acidification on Mg-calcite, high latitude and cold-water marine calcifiers. Mar Ecol Prog Ser 373, 265–273.

Asnaghi, V., Mangialajo, L., Gattuso, J.-P., Francour, P., Privitera, D., Chiantore, M., 2014. Effects of ocean acidification and diet on thickness and carbonate elemental composition of the test of juvenile sea urchins. Mar. Environ. Res. 93, 78-84.

Beddingfield, S.D., McClintock, J.B., 2000. Demographic characteristics of *Lytechinus variegatus* (Echinoidea: Echinodermata) from three habitats in a North Florida Bay, Gulf of Mexico. Mar Ecol 21, 17-40.

Borzęcka-Prokop, B., Wesełucha-Birczyńska, A., Koszowska, E., 2007. MicroRaman, PXRD, EDS and microscopic investigation of magnesium calcite biomineral phases. The case of sea urchin biominerals. J. Mol. Struct 828, 80-90.

Brennand, H.S., Soars, N., Dworjanyn, S.A., Davis, A.R., Byrne, M., 2010. Impact of ocean warming and ocean acidification on larval development and calcification in the sea urchin *Tripneustes gratilla*. PLoS ONE 5, e11372.

Brothers, C., McClintock, J., 2015. The effects of climate-induced elevated seawater temperature on the covering behavior, righting response, and Aristotle's lantern reflex of the sea urchin *Lytechinus variegatus*. J Exp Mar Biol Ecol 467, 33-38.

Byrne, M., 2011. Impact of ocean warming and ocean acidification on marine invertebrates' life history stages: vulnerabilities and potential for persistence in a changing ocean, in: Gibson, R.N., Atkinson, R.J.A., Gordon, J.D.M., Smith, I.P., Hughes, D.J. (Eds.), Oceanography and Marine Biology: An Annual Review. CRC Press New York, pp. 1-42.

Byrne, M., Foo, S., Soars, N.A., Wolfe, K.D., Nguyen, H.D., Hardy, N., Dworjanyn, S.A., 2013. Ocean warming will mitigate the effects of acidification on calcifying sea urchin larvae (*Heliocidaris tuberculata*) from the Australian global warming hot spot. J Exp Mar Biol Ecol 448, 250-257.

Byrne, M., Ho, M., Selvakumaraswamy, P., Nguyen, H.D., Dworjanyn, S.A., Davis, A.R., 2009. Temperature, but not pH, compromises sea urchin fertilization and early development under near-future climate change scenarios. Proc R Soc Lond B 276, 1883-1888.

Byrne, M., Ho, M., Wong, E., Soars, N.A., Selvakumaraswamy, P., Shepard-Brennand, H., Dworjanyn, S.A., Davis, A.R., 2011. Unshelled abalone and corrupted urchins: development of marine calcifiers in a changing ocean. Proc R Soc Lond B 278, 2376-2383.

Byrne, M., Smith, A.M., West, S., Collard, M., Dubois, P., Graba-landry, A., Dworjanyn, S.A., 2014. Warming influences Mg^{2+} content, while warming and acidification influence calcification and test strength of a sea urchin. Environ Sci Tech 48, 12620-12627.

Challener, R.C., McClintock, J.B., 2013. Exposure to extreme hypercapnia under laboratory conditions does not impact righting and covering behavior of juveniles of the common sea urchin *Lytechinus variegatus*. Mar. Freshw. Behav. Physiol. 46, 191-199.

Challener, R.C., Robbins, L.L., McClintock, J.B., 2015. Variability of the carbonate chemistry in a shallow, seagrass-dominated ecosystem: implications for ocean acidification experiments. Mar. Freshw. Res. 67, 163-172.

Chave, K.E., 1954. Aspects of the biogeochemistry of magnesium 1. Calcareous marine organisms. The Journal of Geology 62, 266-283.

Collins, M., Knutti, R., Arblaster, J., Dufresne, J.-L., Fichefet, T., Friedlingstein, P., Gao, X., Gutowski, W.J., Johns, T., Krinner, G., Shongwe, M., Tebaldi, C., Weaver, A.J., Wehner, M., 2013. Long-term Climate Change: Projections, Commitments and Irreversibility, in: T.F.Stocker, Qin, D., Plattner, G.-K., Tignor, M., Allen, S.K., Boschung, J., Nauels, A., Xia, Y., Bex, V., Midgley, P.M. (Eds.), Climate Change 2013: The Physical Science Basis. Contribution of Working Group I to the Fifth Assessment Report of the Intergovernmental Panel on Climate Change. Cambridge University Press, Cambridge, United Kingdom and New York, NY, USA,, pp. 1029–1136.

Delorme, N.J., Sewell, M.A., 2013. Temperature limits to early development of the New Zealand sea urchin *Evechinus chloroticus* (Valenciennes, 1846). J. Therm. Biol. 38, 218-224.

Delorme, N.J., Sewell, M.A., 2014. Temperature and salinity: two climate change stressors affecting early development of the New Zealand sea urchin *Evechinus chloroticus*. Mar Biol 161, 1999-2009.

Díaz-Pérez, L., Carpizo-Ituarte, E., 2011. Effect of thermal stress on survival and delay of metamorphosis in larvae of the purple sea urchin *Strongylocentrotus purpuratus* Cienc. Mar. 37, 403-414.

Doney, S.C., Schimel, D.S., 2007. Carbon and Climate System Coupling on Timescales from the Precambrian to the Anthropocene. Annu. Rev. Envron. Resour. 32, 31 - 66.

Fujisawa, H., Shigei, M., 1990. Correlation of embryonic temperature sensitivity of sea urchins with spawning season. J Exp Mar Biol Ecol 136, 123-139.

Goetz, A.J., Griesshaber, E., Abel, R., Fehr, T., Ruthensteiner, B., Schmahl, W., 2014. Tailored order: The mesocrystalline nature of sea urchin teeth. Acta biomaterialia 10, 3885-3898.

Hardy, N.A., Lamare, M., Uthicke, S., Wolfe, K., Doo, S., Dworjanyn, S., Byrne, M., 2014. Thermal tolerance of early development in tropical and temperate sea urchins: inferences for the tropicalization of eastern Australia. Mar Biol 161, 395-409.

Heck, K.L., Valentine, J.F., 1995. Sea urchin herbivory: evidence for long-lasting effects in subtropical seagrass meadows. J Exp Mar Biol Ecol 189, 205-217.

Hermans, J., Borremans, C., Willenz, P., André, L., Dubois, P., 2010. Temperature, salinity and growth rate dependences of Mg/Ca and Sr/Ca ratios of the skeleton of the sea urchin *Paracentrotus lividus* (Lamarck): an experimental approach. Mar Biol 157, 1293-1300.

Hoegh-Guldberg, O., Cai, R., Poloczanska, E.S., Brewer, P.G., Sundby, S., Hilmi, K., Fabry, V.J., Jung, S., 2014. The Ocean, in: Barros, V.R., Field, C.B., Dokken, D.J., Mastrandrea, M.D., Mach, K.J., Bilir, T.E., Chatterjee, M., Ebi, K.L., Estrada, Y.O., Genova, R.C., Girma, B., Kissel, E.S., Levy, A.N., MacCracken, S., Mastrandrea, P.R., White, L.L. (Eds.), Climate Change 2014: Impacts, Adaptation, and Vulnerability. Part B: Regional Aspects. Contribution of Working Group II to the Fifth Assessment Report of the Intergovernmental Panel on Climate Change, Cambridge, United Kingdom and New York, NY, USA, pp. 1655-1731.

Jones, S.J., Lima, F.P., Wethey, D.S., 2010. Rising environmental temperatures and biogeography: poleward range contraction of the blue mussel, *Mytilus edulis* L., in the western Atlantic. J. Biogeogr. 37, 2243-2259.

Jones, S.J., Mieszkowska, N., Wethey, D.S., 2009. Linking thermal tolerances and biogeography: *Mytilus edulis* (L.) at its southern limit on the east coast of the United States. Biol Bull 217, 73-85.

Kunitake, M.E., Baker, S.P., Estroff, L.A., 2012. The effect of magnesium substitution on the hardness of synthetic and biogenic calcite. MRS Communications 2, 113-116.

Levitus, S., Antonov, J., Boyer, T., Locarnini, R., Garcia, H., Mishonov, A., 2009. Global ocean heat content 1955–2008 in light of recently revealed instrumentation problems. Geophys. Res. Lett 36, L07608.

Li, L., Li, Q., Sun, X., Kong, L., 2011. Effects of temperature and salinity on larval growth, survival, and development of the sea cucumber *Apostichopus japonicus*. N. Am. J. Aquacult. 73, 296-303.

Ma, Y., Aichmayer, B., Paris, O., Fratzl, P., Meibom, A., Metzler, R.A., Politi, Y., Addadi, L., Gilbert, P., Weiner, S., 2009. The grinding tip of the sea urchin tooth

exhibits exquisite control over calcite crystal orientation and Mg distribution. Proc Nat Acad Sci 106, 6048-6053.

Marubini, F., Ferrier–Pages, C., Cuif, J.P., 2003. Suppression of skeletal growth in scleractinian corals by decreasing ambient carbonate-ion concentration: a cross family comparison. Proc R Soc Lond B 270, 179-184.

McClintock, J.B., Amsler, M.O., Angus, R.A., Challener, R.C., Schram, J.B., Amsler, C.D., Mah, C.L., Cuce, J., Baker, B.J., 2011. The Mg-calcite composition of Antarctic echinoderms: important implications for predicting the impacts of ocean acidification. The Journal of Geology 119, 457-466.

McCulloch, M., Falter, J., Trotter, J., Montagna, P., 2012. Coral resilience to ocean acidification and global warming through pH up-regulation. Nat. Clim. Change 2, 623-627.

Moore, H.B., 1966. Ecology of Echinoids, in: R, B. (Ed.), Physiology of Echinodermata. Interscience Publishers, New York.

Morse, J.W., Andersson, A.J., Mackenzie, F.T., 2006. Initial responses of carbonate-rich shelf sediments to rising atmospheric pCO_2 and "ocean acidification": role of high Mg-calcites. Geochim. Cosmochim. Acta 70, 5814-5830.

Mortensen, T., 1943. A Monograph of the Echinoidea. 11.2. Camarodonta.I. CA Reitzel, Copenhagen,.

Pörtner, H.-O., 2008. Ecosystem effects of ocean acidification in times of ocean warming: a physiologist's view. Mar Ecol Prog Ser 373, 203-217.

Pörtner, H.O., Knust, R., 2007. Climate change affects marine fishes through the oxygen limitation of thermal tolerance. Science 315, 95-97.

Rhein, M., Rintoul, S.R., Aoki, S., Campos, E., Chambers, D., Feely, R.A., Gulev, S., Johnson, G.C., Josey, S.A., Kostianoy, A., Mauritzen, C., Roemmich, D., Talley L.D., Wang, F., 2013b. Observations: Ocean, in: Stocker, T.F., Qin, D., Plattner, G.-K., Tignor, M., Allen, S.K., Boschung, J., Nauels, A., Xia, Y., Bex, V., Midgley, P.M. (Eds.), Climate Change 2013: The Physical Science Basis. Contribution of Working Group I to the Fifth Assessment Report of the Intergovernmental Panel on Climate Change. Cambridge University Press, Cambridge, United Kingdom and New York, NY, USA, pp. 255-316.

Ries, J.B., 2004. Effect of ambient Mg/Ca ratio on Mg fractionation in calcareous marine invertebrates: A record of the oceanic Mg/Ca ratio over the Phanerozoic. Geology 32, 981-984.

Ries, J.B., 2011. Skeletal mineralogy in a high-CO_2 world. J Exp Mar Biol Ecol 403, 54-64.

Robach, J., Stock, S., Veis, A., 2009. Structure of first-and second-stage mineralized elements in teeth of the sea urchin *Lytechinus variegatus*. J Struct Biol 168, 452-466.

Sewell, M.A., Young, C.M., 1999. Temperature limits to fertilization and early development in the tropical sea urchin *Echinometra lucunter*. J Exp Mar Biol Ecol 236, 291-305.

Smith, K., Ruhl, H., Bett, B., Billett, D., Lampitt, R., Kaufmann, R., 2009. Climate, carbon cycling, and deep-ocean ecosystems. Proc Nat Acad Sci 106, 19211 19218.

Spencer, P.D., 2008. Density-independent and density-dependent factors affecting temporal changes in spatial distributions of eastern Bering Sea flatfish. Fish. Oceanogr. 17, 396-410.

Veis, A., 2011. Organic matrix-related mineralization of sea urchin spicules, spines, test and teeth. Front. Biosci. 16, 2540-2560.

Vinogradov, A.P., Odum, V., 1953. The elementary chemical composition of marine organisms, Memoir Sears Foundation for Marine Research No. 11., New Haven, p. 677.

Watts, S., McClintock, J., Lawrence, J., 2013. *Lytechinus*, in: Lawrence, J. (Ed.), Sea Urchins: Biology and Ecology, 3rd ed. Academic Press, San Diego, CA, pp. 475 490.

Watts, S.A., McClintock, J.B., Lawrence, J.M., 2001. The ecology of *Lytechinus variegatus*. Developments in Aquaculture and Fisheries Science 32, 375-393.

Weber, J.N., 1973. Temperature dependence of magnesium in echinoid and asteroid skeletal calcite: a reinterpretation of its significance. J Geol 81, 543-556.

Wolfe, K., Dworjanyn, S.A., Byrne, M., 2013. Effects of ocean warming and acidification on survival, growth and skeletal development in the early benthic juvenile sea urchin (*Heliocidaris erythrogramma*). Global Chan Biol 19, 2698 2707.

Wood, H.L., Spicer, J., Lowe, D., Widdicombe, S., 2010. Interaction of ocean acidification and temperature; the high cost of survival in the brittlestar *Ophiura ophiura*. Mar Biol 157, 2001-2013.

Table 1. Mean (±SE) total wet weight and test diameter of *Lytechinus variegatus* kept for 90 days at either 26°C or 30°C and sampled every 30 days. Sample size at the baseline was 25 individuals, 10 individuals in the 26°C treatment, but sample size in the 30°C treatment was 8 individuals at each time point.

Time (days)	Wet Weight (g)		Test Diameter (Rhein et al.)	
	26°C	**30°C**	**26°C**	**30°C**
Baseline	7.02 ± 0.45		24.04 ± 0.56	
30	17.89 ± 0.77	17.58 ± 0.83	32.0 ± 0.8	31.3 ± 0.5
60	24.56 ± 1.26	23.16 ± 0.72	36.9 ± 0.4	36.5 ± 0.3
90	31.87 ± 1.59	28.14 ± 0.78	39.7 ± 0.9	37.9 ± 0.5

Table 2. Mean (± SE) molar Mg/Ca ratios of individuals of *Lytechinus variegatus* sampled every thirty days for a total of ninety days. Sea urchins were kept at either 26°C or 30°C. Sample size was 10 individuals for 26°C and 8 individuals for 30°C at each time point.

Body Component	Day	Mean Molar Mg/Ca (± SE)	
		26°C	30°C
Lantern	30	0.168 ± 0.009	0.130 ± 0.007
	60	0.172 ± 0.013	0.125 ± 0.013
	90	0.181 ± 0.013	0.138 ± 0.012
Spine	30	0.110 ± 0.009	0.075 ± 0.010
	60	0.122 ± 0.010	0.102 ± 0.014
	90	0.110 ± 0.009	0.088 ± 0.010
Test	30	0.179± 0.010	0.147 ± 0.012
	60	0.183 ± 0.009	0.127 ± 0.014
	90	0.171 ± 0.008	0.147 ± 0.012

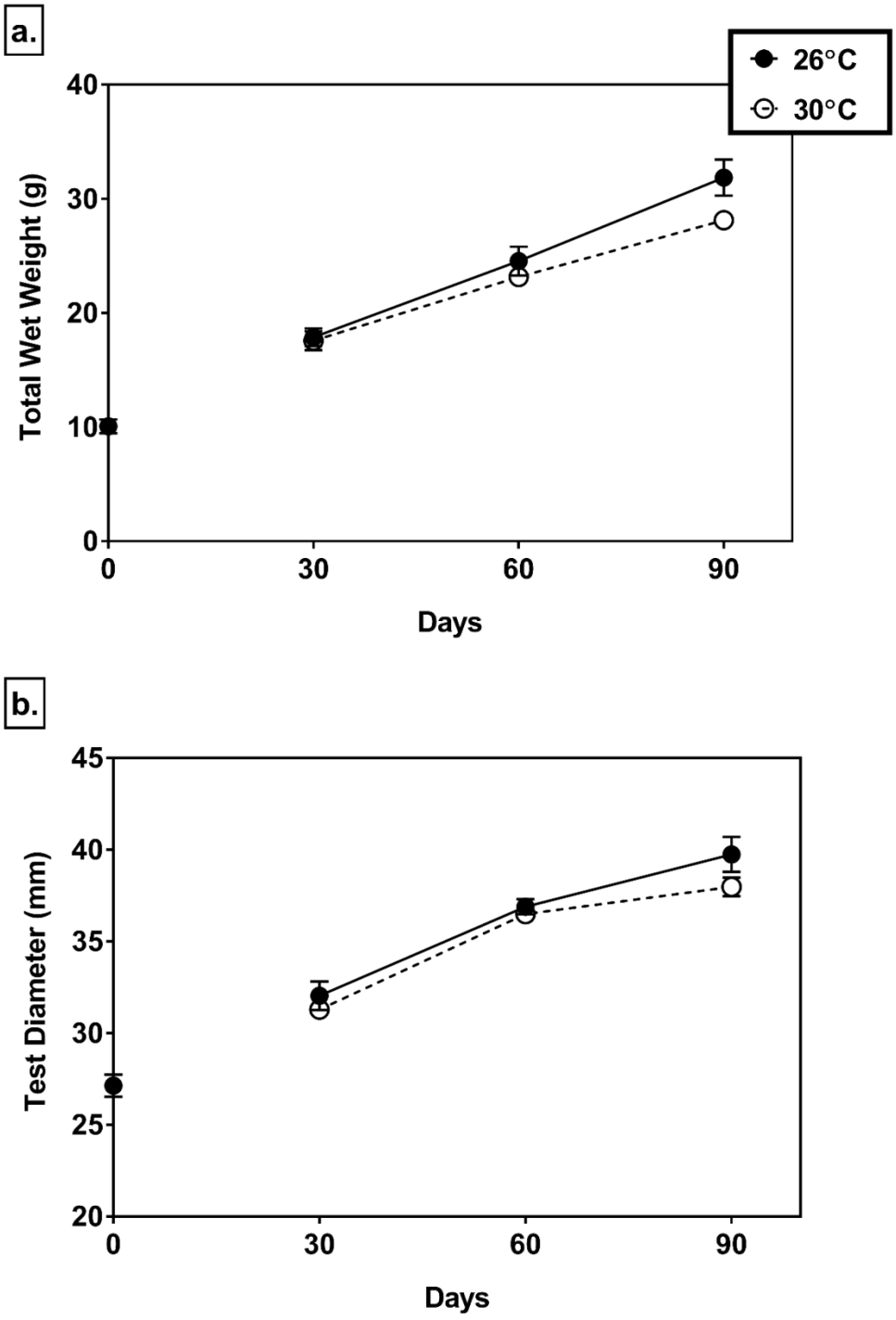

Figure 1. Growth of individuals of the sea urchin *Lytechinus variegatus* kept at either 26°C (filled circles) or 30°C (open circles) for 90 days. Measurements were taken at 30, 60, and 90 days after the beginning of the experiment. a) mean wet weight (g) and b) mean test diameter (mm). Error bars are mean ± SE

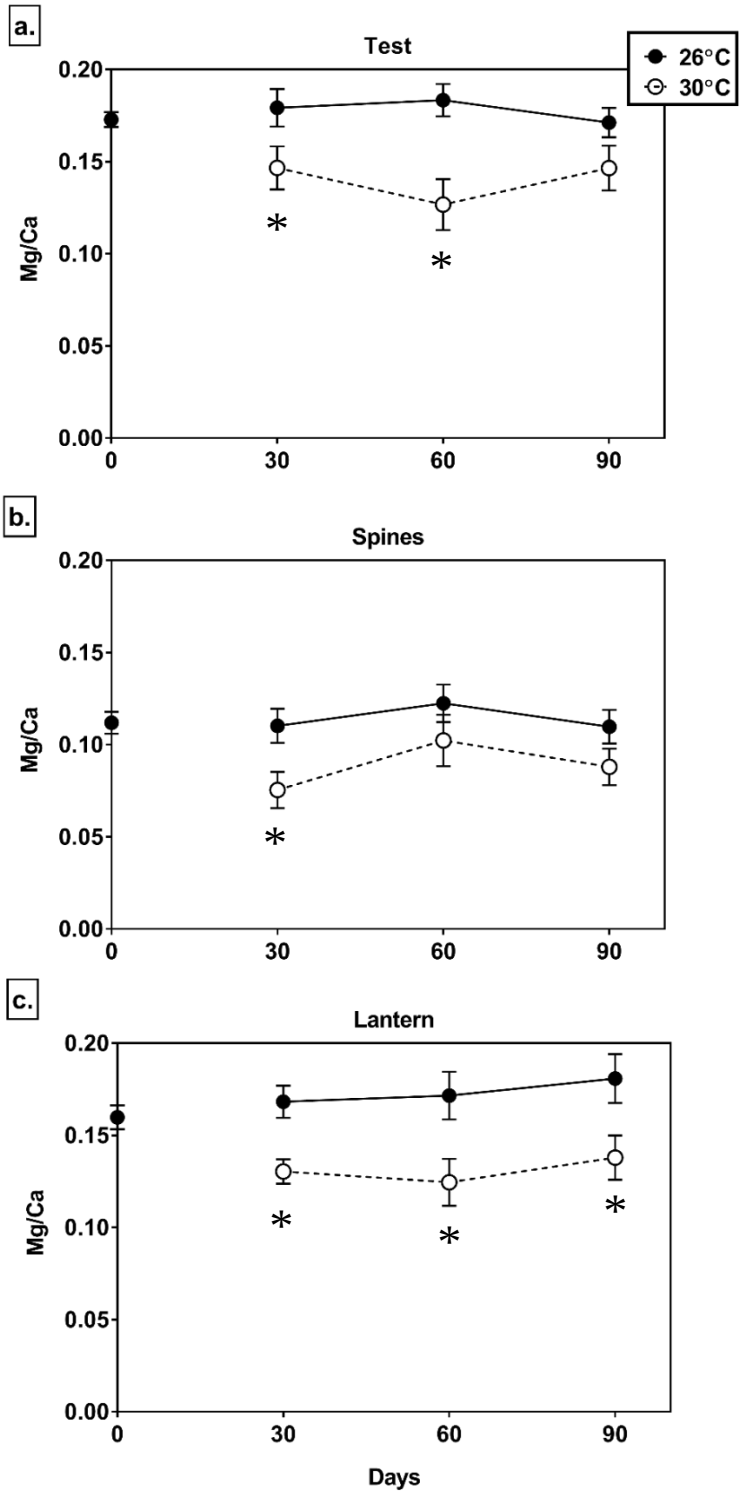

Figure 2. Change in mean molar Mg/Ca ratios for distinct body components (test, spines, and Aristotle's lantern) of individuals of the sea urchin *Lytechinus variegatus* kept at either 26°C (filled circles) or 30°C (open circles) for 90 days. Measurements were taken at 30, 60, and 90 days after the beginning of the experiment. Mean molar Mg/Ca ratios over the course of the experiment for the sea urchin (a) test, (b) spines, and (c) Aristotle's lantern. The error bars are mean ± SE

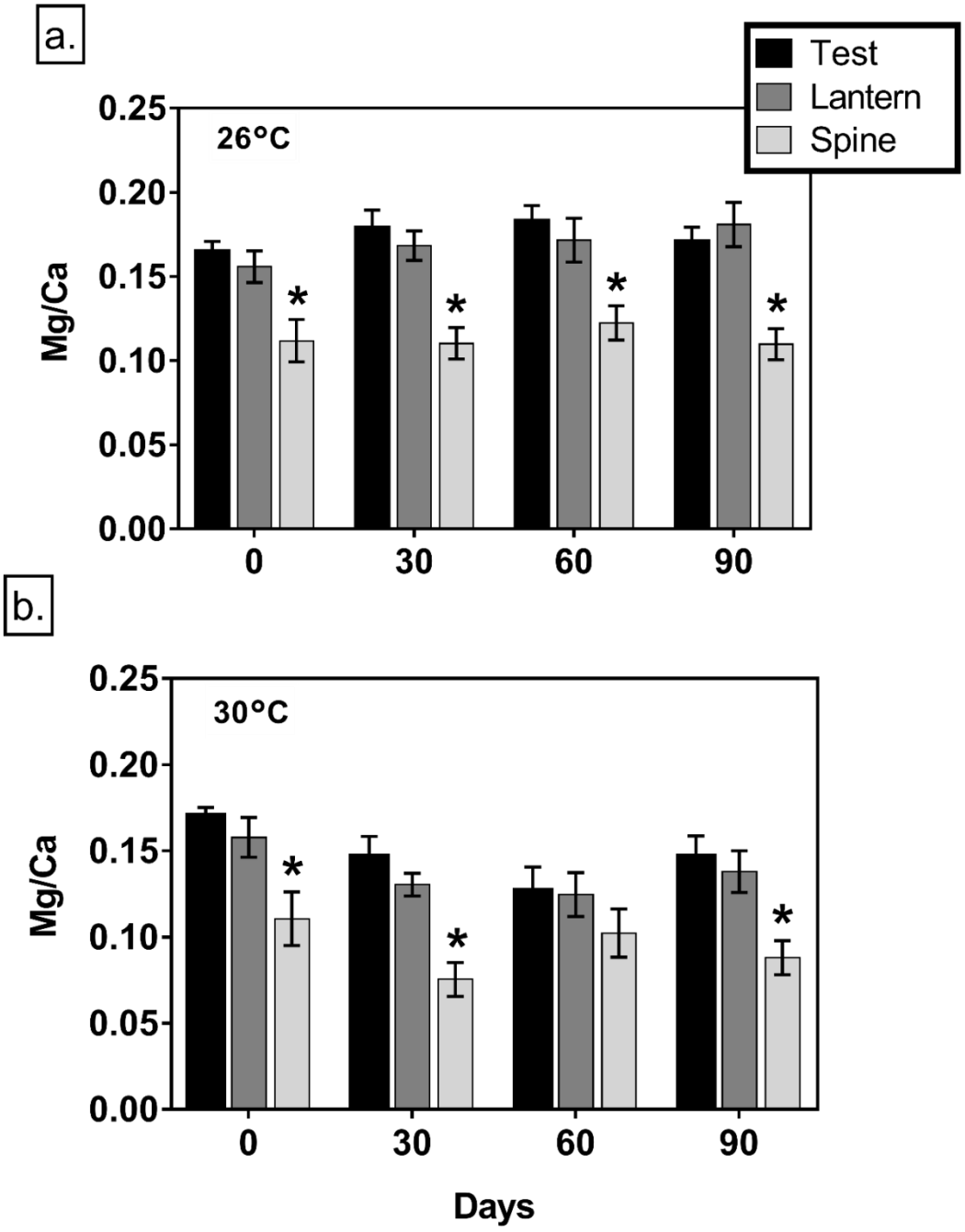

Figure 3. Comparisons of mean molar Mg/Ca ratios among body components (test, spine, and Aristotle's lantern) of the sea urchin *Lytechinus variegatus* within the (a) 26°C or (b) 30°C treatments at days 0, 30, 60, and 90. The lightest bar represents the spines, the light grey bar represents the lantern, and the black bars represent the test of the sea urchin *Lytechinus variegatus.* Error bars represent mean ± SE. The asterix represents the body component that is significantly different from the others.

General References

Albright R, Bland C, Gillette P, Serafy JE, Langdon C, Capo TR (2012) Juvenile growth of the tropical sea urchin *Lytechinus variegatus* exposed to near-future ocean acidification scenarios. J Exp Mar Biol Ecol 426: 12-17

Andersson AJ, Mackenzie FT, Bates NR (2008) Life on the margin: implications of ocean acidification on Mg-calcite, high latitude and cold-water marine calcifiers. Mar Ecol Prog Ser 373: 265–273

Asnaghi V, Chiantore M, Mangialajo L, Gazeau F, Francour P, Alliouane S, Gattuso J-P (2013) Cascading effects of ocean acidification in a rocky subtidal community. PloS ONE 8: e61978

Asnaghi V, Mangialajo L, Gattuso J-P, Francour P, Privitera D, Chiantore M (2014) Effects of ocean acidification and diet on thickness and carbonate elemental composition of the test of juvenile sea urchins. Mar Environ Res 93: 78-84

Baggini C, Issaris Y, Salomidi M, Hall-Spencer J (2015) Herbivore diversity improves benthic community resilience to ocean acidification. J Exp Mar Biol Ecol 469: 98-104

Barry JP, Baxter CH, Sagarin RD, Gilman SE (1995) Climate-related, long-term faunal changes in a California rocky intertidal community. Science 267: 672-675

Barry JP, Tyrell T, Hall-Spencer JM (2010) *In situ* perturbation experiments: natural venting sites, spatial/temporal gradients in ocean pH, manipulative *in situ p*CO_2 perturbations. In: Riebesell U, Fabry VJ, Hansson L, Gattuso J-P (eds) Guide to best practices for ocean acidification research and data reporting. Publications Office of the European Union, Luxembourg, pp 123 - 136

Bednaršek N, Tarling G, Bakker D, Fielding S, Jones E, Venables H, Ward P, Kuzirian A, Lézé B, Feely R (2012) Extensive dissolution of live pteropods in the Southern Ocean. Nat Geosci 5: 881-885

Beniash E, Ivanina A, Lieb NS, Kurochkin I, Sokolova IM (2010) Elevated level of carbon dioxide affects metabolism and shell formation in oysters *Crassostrea virginica*. Mar Ecol Prog Ser 419: 95-108

Binyon J (1976) The permeability of the asteroid podial wall to water and potassium ions. J Mar Biol Ass UK 56: 639-647

Binyon J (1980) Osmotic and hydrostatic permeability of the integument of the starfish *Asterias rubens* L. J Mar Biol Ass UK 60: 627-630

Bøggild OB (1930) The shell structure of the mollusks. Det Kongelige Danske Videnskabernes Selskabs Skrifter, Natruvidenskabelig og Mathematisk, Afdeling, Ser 9 2: 231-326

Bray L, Pancucci-Papadopoulou M, Hall-Spencer J (2014) Sea urchin response to rising pCO_2 shows ocean acidification may fundamentally alter the chemistry of marine skeletons. Mediterr Mar Sci 15: 510-519

Byrne M, Ho M, Wong E, Soars NA, Selvakumaraswamy P, Shepard-Brennand H, Dworjanyn SA, Davis AR (2011) Unshelled abalone and corrupted urchins: development of marine calcifiers in a changing ocean. Proc R Soc Lond B 278: 2376-2383

Cazenave A, Lombard A, Llovel W (2008) Present-day sea level rise: A synthesis. Comptes Rendus Geoscience 340: 761-770

Challener RC, McClintock JB, Makowsky R (2013) Effects of reduced carbonate saturation state on early development in the common edible sea urchin *Lytechinus variegatus*: implications for land-based aquaculture. J Appl Aquacult 25: 154-175

Chan KYK, Grünbaum D, Arnberg M, Dupont S (2015) Impacts of ocean acidification on survival, growth, and swimming behaviours differ between larval urchins and brittlestars. ICES J Mar Sci 73 951-961

Chave KE (1954) Aspects of the biogeochemistry of magnesium 1. Calcareous marine organisms. J Geol 62: 266-283

Christen N, Calosi P, McNeill C, Widdicombe S (2013) Structural and functional vulnerability to elevated pCO_2 in marine benthic communities. Mar Biol 160: 2113-2128

Cigliano M, Gambi M, Rodolfo-Metalpa R, Patti F, Hall-Spencer J (2010) Effects of ocean acidification on invertebrate settlement at volcanic CO_2 vents. Mar Biol 157: 2489-2502

Coleman DW, Byrne M, Davis AR (2014) Molluscs on acid: gastropod shell repair and strength in acidifying oceans. Mar Ecol Prog Ser 509: 203-211

Collard M, Eeckhaut I, Dehairs F, Dubois P (2014) Acid–base physiology response to ocean acidification of two ecologically and economically important holothuroids from contrasting habitats, *Holothuria scabra* and *Holothuria parva*. Environ Sci Pollut R 21: 13602-13614

Collard M, Rastrick SP, Calosi P, Demolder Y, Dille J, Findlay HS, Hall-Spencer JM, Milazzo M, Moulin L, Widdicombe S (2015) The impact of ocean acidification

and warming on the skeletal mechanical properties of the sea urchin *Paracentrotus lividus* from laboratory and field observations. ICES J Mar Sci 73 727-738

Comeau S, Jeffree R, Teyssié J-L, Gattuso J-P (2010) Response of the Arctic pteropod *Limacina helicina* to projected future environmental conditions. PloS ONE 5: e11362

Cyronak T, Schulz KG, Jokiel PL (2015) The Omega myth: what really drives lower calcification rates in an acidifying ocean. ICES J Mar Sci 73: 558-562

Day EG, Branch GM, Viljoen C (2000) How costly is molluscan shell erosion? A comparison of two patellid limpets with contrasting shell structures. J Exp Mar Biol Ecol 243: 185-208

Desrosiers RR, Désilets J, Dubé F (1996) Early developmental events following fertilization in the giant scallop *Placopecten magellanicus*. Can J Fish Aquat Sci 53: 1382-1392

Dickinson GH, Ivanina AV, Matoo OB, Pörtner HO, Lannig G, Bock C, Beniash E, Sokolova IM (2012) Interactive effects of salinity and elevated CO_2 levels on juvenile eastern oysters, *Crassostrea virginica*. J Exp Biol 215: 29-43

Doney SC, Fabry VJ, Feely RA, Kleypas JA (2009) Ocean acidification: the other CO_2 problem. Annu Rev Mar Sci 1: 169-192

Doney SC, Ruckelshaus M, Duffy JE, Barry JP, Chan F, English CA, Galindo HM, Grebmeier JM, Hollowed AB, Knowlton N (2012) Climate change impacts on marine ecosystems. Annu Rev Mar Sci 4: 11-37

Doney SC, Schimel DS (2007) Carbon and Climate System Coupling on Timescales from the Precambrian to the Anthropocene. Annu Rev Envron Resour 32: 31-66

Dubois P (2014) The skeleton of postmetamorphic echinoderms in a changing world. Biol Bull 226: 223-236

Dupont S, Dorey N, Stumpp M, Melzner F, Thorndyke M (2013) Long-term and trans-life-cycle effects of exposure to ocean acidification in the green sea urchin *Strongylocentrotus droebachiensis*. Mar Biol 160: 1835-1843

Dupont S, Dorey N, Thorndyke M (2010) What meta-analysis can tell us about vulnerability of marine biodiversity to ocean acidification? Estuar Coast Shelf Sci 89: 182-185

Dupont S, Havenhand J, Thorndyke W, Peck LS, Thorndyke M (2008) Near-future level of CO_2-driven ocean acidification radically affects larval survival and development in the brittlestar *Ophiothrix fragilis*. Mar Ecol Prog Ser 373: 285-294

Ellis RP, Bersey J, Rundle SD, Hall-Spencer JM, Spicer JI (2009) Subtle but significant effects of CO_2 acidified seawater on embryos of the intertidal snail, *Littorina obtusata*. Aquat Biol 5: 41-48

Eyre BD, Andersson AJ, Cyronak T (2014) Benthic coral reef calcium carbonate dissolution in an acidifying ocean. Nat Clim Change 4: 969-976

Fabricius K, De'ath G, Noonan S, Uthicke S (2014) Ecological effects of ocean acidification and habitat complexity on reef-associated macroinvertebrate communities. Proc R Soc Lond B 281: 20132479

Fabry VJ, McClintock JB, Mathis JT, Grebmeier JM (2009) Ocean acidification at high latitudes: the bellweather. Oceanography 22: 160

Fabry VJ, Seibel BA, Feely RA, Orr JC (2008) Impacts of ocean acidification on marine fauna and ecosystem processes. ICES J Mar Sci 65: 414-432

Feely R, Sabine C, Lee K, Millero F, Lamb M, Greeley D, Bullister J, Key R, Peng TH, Kozyr A (2002) *In situ* calcium carbonate dissolution in the Pacific Ocean. Glob Biogeochem Cycles 16: 1144

Findlay HS, Kendall MA, Spicer JI, Widdicombe S (2009) Future high CO_2 in the intertidal may compromise adult barnacle *Semibalanus balanoides* survival and embryonic development rate. Mar Ecol Prog Ser 389: 193-202

Fitzer SC, Phoenix VR, Cusack M, Kamenos NA (2014) Ocean acidification impacts mussel control on biomineralisation. Sci Rep 4: 6218

Garilli V, Rodolfo-Metalpa R, Scuderi D, Brusca L, Parrinello D, Rastrick SP, Foggo A, Twitchett RJ, Hall-Spencer JM, Milazzo M (2015) Physiological advantages of dwarfing in surviving extinctions in high-CO_2 oceans. Nat Clim Change 5: 678-682

Garrard SL, Hunter R, Frommel A, Lane A, Phillips J, Cooper R, Dineshram R, Cardini U, McCoy S, Arnberg M (2013) Biological impacts of ocean acidification: a postgraduate perspective on research priorities. Mar Biol 160: 1789-1805

Gattuso J-P, Magnan A, Bille R, Cheung W, Howes E, Joos F, Allemand D, Bopp L, Cooley S, Eakin C (2015) Contrasting futures for ocean and society from different anthropogenic CO_2 emissions scenarios. Science 349: aac4722

Gaylord B, Kroeker KJ, Sunday JM, Anderson KM, Barry JP, Brown NE, Connell SD, Dupont S, Fabricius KE, Hall-Spencer JM (2015) Ocean acidification through the lens of ecological theory. Ecology 96: 3-15

Gazeau F, Quiblier C, Jansen JM, Gattuso JP, Middelburg JJ, Heip CH (2007) Impact of elevated CO_2 on shellfish calcification. Geophys Res Lett 34: L07603

Gooding RA, Harley CD, Tang E (2009) Elevated water temperature and carbon dioxide concentration increase the growth of a keystone echinoderm. Proc Nat Acad Sci 106: 9316-9321

Green MA, Jones ME, Boudreau CL, Moore RL, Westman BA (2004) Dissolution mortality of juvenile bivalves in coastal marine deposits. Limnol Oceanogr 49: 727-734

Hall-Spencer JM, Rodolfo-Metalpa R, Martin S, Ransome E, Fine M, Turner SM, Rowley SJ, Tedesco D, Buia M-C (2008) Volcanic carbon dioxide vents show ecosystem effects of ocean acidification. Nature 454: 96-99

Harvey BP, McKeown NJ, Rastrick SP, Bertolini C, Foggo A, Graham H, Hall-Spencer JM, Milazzo M, Shaw PW, Small DP (2016) Individual and population-level responses to ocean acidification. Sci Rep 6: 20194

Hermans J, Borremans C, Willenz P, André L, Dubois P (2010) Temperature, salinity and growth rate dependences of Mg/Ca and Sr/Ca ratios of the skeleton of the sea urchin *Paracentrotus lividus* (Lamarck): an experimental approach. Mar Biol 157: 1293-1300

Hillyer R, Silman MR (2010) Changes in species interactions across a 2.5 km elevation gradient: effects on plant migration in response to climate change. Global Chan Biol 16: 3205-3214

Hoegh-Guldberg O, Cai R, Poloczanska ES, Brewer PG, Sundby S, Hilmi K, Fabry VJ, Jung S (2014) The Ocean, Cambridge, United Kingdom and New York, NY, USA

Hofmann GE, Barry JP, Edmunds PJ, Gates RD, Hutchins DA, Klinger T, Sewell MA (2010) The effect of ocean acidification on calcifying organisms in marine ecosystems: an organism-to-ecosystem perspective. Annu Rev Ecol Evol Syst 41: 127-147

Hyrenbach KD, Veit RR (2003) Ocean warming and seabird communities of the southern California Current System (1987–98): response at multiple temporal scales. Deep-Sea Res Pt II 50: 2537-2565

IPCC (2014) Climate Change 2014: Synthesis Report. Contribution of Working Groups, I, II, and III to the Fifth Assessment Report of the Intergovernmental Panel on Climate Change, Geneva, Switzerland

Johnson MD, Carpenter RC (2012) Ocean acidification and warming decrease calcification in the crustose coralline alga *Hydrolithon onkodes* and increase susceptibility to grazing. J Exp Mar Biol Ecol 434: 94-101

Jones SJ, Lima FP, Wethey DS (2010) Rising environmental temperatures and biogeography: poleward range contraction of the blue mussel, *Mytilus edulis* L., in the western Atlantic. J Biogeogr 37: 2243-2259

Jones SJ, Mieszkowska N, Wethey DS (2009) Linking thermal tolerances and biogeography: *Mytilus edulis* (L.) at its southern limit on the east coast of the United States. Biol Bull 217: 73-85

Keeling RF, Körtzinger A, Gruber N (2010) Ocean deoxygenation in a warming world. Annu Rev Mar Sci 2: 199-229

Kroeker KJ, Kordas RL, Crim R, Hendriks IE, Ramajo L, Singh GS, Duarte CM, Gattuso JP (2013a) Impacts of ocean acidification on marine organisms: quantifying sensitivities and interaction with warming. Global Chan Biol 19: 1884-1896

Kroeker KJ, Micheli F, Gambi MC (2013b) Ocean acidification causes ecosystem shifts via altered competitive interactions. Nat Clim Change 3: 156-159

Kroeker KJ, Micheli F, Gambi MC, Martz TR (2011) Divergent ecosystem responses within a benthic marine community to ocean acidification. Proc Nat Acad Sci 108: 14515-14520

Kurihara H, Kato S, Ishimatsu A (2007) Effects of increased seawater pCO_2 on early development of the oyster *Crassostrea gigas*. Aquat Biol 1: 91-98

Langer G, Nehrke G, Baggini C, Rodolfo-Metalpa R, Hall-Spencer J, Bijma J (2014) Limpets counteract ocean acidification induced shell corrosion by thickening of aragonitic shell layers. Biogeosci 11: 7363-7368

Lardies MA, Arias MB, Poupin MJ, Manríquez PH, Torres R, Vargas CA, Navarro JM, Lagos NA (2014) Differential response to ocean acidification in physiological traits of *Concholepas concholepas* populations. J Sea Res 90: 127-134

LaVigne M, Hill T, Sanford E, Gaylord B, Russell A, Lenz E, Hosfelt J, Young M (2013) The elemental composition of purple sea urchin (*Strongylocentrotus purpuratus*) calcite and potential effects of pCO_2 during early life stages. Biogeosci 10: 3465-3477

Lebrato M, Iglesias-Rodríguez D, Feely RA, Greeley D, Jones DO, Suarez-Bosche N, Lampitt RS, Cartes JE, Green DR, Alker B (2010) Global contribution of echinoderms to the marine carbon cycle: $CaCO_3$ budget and benthic compartments. Ecol Monogr 80: 441-467

Levitus S, Antonov J, Boyer T, Locarnini R, Garcia H, Mishonov A (2009) Global ocean heat content 1955–2008 in light of recently revealed instrumentation problems. Geophys Res Lett 36: L07608

Lischka S, Riebesell U (2012) Synergistic effects of ocean acidification and warming on overwintering pteropods in the Arctic. Global Chan Biol 18: 3517-3528

Martin S, Rodolfo-Metalpa R, Ransome E, Rowley S, Buia M-C, Gattuso J-P, Hall-Spencer J (2008) Effects of naturally acidified seawater on seagrass calcareous epibionts. Biol Lett 4: 689-692

McClintock JB, Amsler MO, Angus RA, Challener RC, Schram JB, Amsler CD, Mah CL, Cuce J, Baker BJ (2011) The Mg-calcite composition of Antarctic echinoderms: important implications for predicting the impacts of ocean acidification. The Journal of Geology 119: 457-466

Melatunan S, Calosi P, Rundle SD, Widdicombe S, Moody AJ (2013) Effects of ocean acidification and elevated temperature on shell plasticity and its energetic basis in an intertidal gastropod. Mar Ecol Prog Ser 472: 155-168

Michaelidis B, Ouzounis C, Paleras A, Pörtner HO (2005) Effects of long-term moderate hypercapnia on acid-base balance and growth rate in marine mussels *Mytilus galloprovincialis*. Mar Ecol Prog Ser 293: 109-118

Milazzo M, Rodolfo-Metalpa R, San Chan VB, Fine M, Alessi C, Thiyagarajan V, Hall-Spencer JM, Chemello R (2014) Ocean acidification impairs vermetid reef recruitment. Sci Rep 4: 4189

Miles H, Widdicombe S, Spicer JI, Hall-Spencer J (2007) Effects of anthropogenic seawater acidification on acid–base balance in the sea urchin *Psammechinus miliaris*. Mar Pollut Bull 54: 89-96

Morse JW, Andersson AJ, Mackenzie FT (2006) Initial responses of carbonate-rich shelf sediments to rising atmospheric pCO_2 and "ocean acidification": role of high Mg-calcites. Geochim Cosmochim Acta 70: 5814-5830

Mucci A (1983) The solubility of calcite and aragonite in seawater at various salinities, temperatures, and one atmosphere total pressure. Am J Sci 283: 780-799

Mueter FJ, Litzow MA (2008) Sea ice retreat alters the biogeography of the Bering Sea continental shelf. Ecol Appl 18: 309-320

Orr JC, Fabry VJ, Aumont O, Bopp L, Doney SC, Feely RA, Gnanadesikan A, Gruber N, Ishida A, Joos F (2005) Anthropogenic ocean acidification over the twenty-first century and its impact on calcifying organisms. Nature 437: 681-686

Parker LM, Ross PM, O'Connor WA, Pörtner HO, Scanes E, Wright JM (2013) Predicting the response of molluscs to the impact of ocean acidification. Biology 2: 651-692

Ries JB (2004) Effect of ambient Mg/Ca ratio on Mg fractionation in calcareous marine invertebrates: A record of the oceanic Mg/Ca ratio over the Phanerozoic. Geology 32: 981-984

Ries JB (2011) Skeletal mineralogy in a high-CO_2 world. J Exp Mar Biol Ecol 403: 54-64

Ries JB, Cohen AL, McCorkle DC (2009) Marine calcifiers exhibit mixed responses to CO_2-induced ocean acidification. Geology 37: 1131-1134

Rodolfo-Metalpa R, Houlbrèque F, Tambutté É, Boisson F, Baggini C, Patti FP, Jeffree R, Fine M, Foggo A, Gattuso J (2011) Coral and mollusc resistance to ocean acidification adversely affected by warming. Nat Clim Change 1: 308-312

Roleda MY, Boyd PW, Hurd CL (2012) Before ocean acidification: calcifier chemistry lessons. J Phycol 48: 840-843

Ross PM, Parker L, O'Connor WA, Bailey EA (2011) The impact of ocean acidification on reproduction, early development and settlement of marine organisms. Water 3: 1005-1030

Sabine CL, Feely RA, Gruber N, Key RM, Lee K, Bullister JL, Wanninkhof R, Wong C, Wallace DW, Tilbrook B (2004) The oceanic sink for anthropogenic CO_2. Science 305: 367-371

Schram JB, Schoenrock KM, McClintock JB, Amsler CD, Angus RA (2015) Multi-frequency observations of seawater carbonate chemistry on the central coast of the western Antarctic Peninsula. Polar Res 34: 25582

Sewell MA, Hofmann GE (2011) Antarctic echinoids and climate change: a major impact on the brooding forms. Global Chan Biol 17: 734-744

Sewell MA, Millar RB, Yu PC, Kapsenberg L, Hofmann GE (2013) Ocean acidification and fertilization in the Antarctic sea urchin *Sterechinus neumayeri:* the importance of polyspermy. Environ Sci Tech 48: 713-722

Shirayama Y, Thornton H (2005) Effect of increased atmospheric CO_2 on shallow water marine benthos. J Geophys Res-Oceans 110: C09S08

Spencer PD (2008) Density-independent and density-dependent factors affecting temporal changes in spatial distributions of eastern Bering Sea flatfish. Fish Oceanogr 17: 396-410

Stumpp M, Hu M, Casties I, Saborowski R, Bleich M, Melzner F, Dupont S (2013) Digestion in sea urchin larvae impaired under ocean acidification. Nat Clim Change 3: 1044-1049

Stumpp M, Hu MY, Melzner F, Gutowska MA, Dorey N, Himmerkus N, Holtmann WC, Dupont ST, Thorndyke MC, Bleich M (2012) Acidified seawater impacts sea urchin larvae pH regulatory systems relevant for calcification. Proc Nat Acad Sci 109: 18192-18197

Talmage SC, Gobler CJ (2009) The effects of elevated carbon dioxide concentrations on the metamorphosis, size, and survival of larval hard clams (*Mercenaria*

mercenaria), bay scallops (*Argopecten irradians*), and Eastern oysters (*Crassostrea virginica*). Limnol Oceanogr 54: 2072-2080

Thomsen J, Gutowska M, Saphörster J, Heinemann A, Trübenbach K, Fietzke J, Hiebenthal C, Eisenhauer A, Körtzinger A, Wahl M (2010) Calcifying invertebrates succeed in a naturally CO_2-rich coastal habitat but are threatened by high levels of future acidification. Biogeosci 7: 3879-3891

Vinogradov AP (1953) The elementary chemical composition of marine organisms. Memoir Sears Foundation for Marine Research No. 11. New Haven: Yale Univ. Press. 677 p

Weber JN (1973) Temperature dependence of magnesium in echinoid and asteroid skeletal calcite: a reinterpretation of its significance. J Geol 81: 543-556

Wolfe K, Dworjanyn SA, Byrne M (2013) Effects of ocean warming and acidification on survival, growth and skeletal development in the early benthic juvenile sea urchin (*Heliocidaris erythrogramma*). Global Chan Biol 19: 2698-2707

Wood HL, Spicer J, Lowe D, Widdicombe S (2010) Interaction of ocean acidification and temperature; the high cost of survival in the brittlestar *Ophiura ophiura*. Mar Biol 157: 2001-2013

Wood HL, Spicer JI, Widdicombe S (2008) Ocean acidification may increase calcification rates, but at a cost. Proc R Soc Lond B 275: 1767-1773

Yamamoto-Kawai M, McLaughlin FA, Carmack EC, Nishino S, Shimada K (2009) Aragonite undersaturation in the Arctic Ocean: effects of ocean acidification and sea ice melt. Science 326: 1098-1100

APPENDIX A

APPROVAL OF INSTITUTIONAL ANIMAL CARE AND USE

THE UNIVERSITY OF ALABAMA AT BIRMINGHAM

Institutional Animal Care and Use Committee (IACUC)

NOTICE OF APPROVAL

DATE: May 12, 2014

TO: JAMES B MCCLINTOCK, Ph.D.
CH -368
(205) 975-2525

FROM:

Robert A. Kesterson, Ph.D., Chair
Institutional Animal Care and Use Committee (IACUC)

SUBJECT: Title: Impact of Temperature on Mg-Calcite Composition of Lytechinus Variegatus Skeletal Body Components (Ashley D. Douglas)
Sponsor: Internal
Animal Project_Number: 140510141

As of May 12, 2014 the animal use proposed in the above referenced application is approved. The University of Alabama at Birmingham Institutional Animal Care and Use Committee (IACUC) approves the use of the following species and number of animals:

Species	Use Category	Number In Category
Invertebrates	A	85

Animal use must be renewed by May 11, 2015. Approval from the IACUC must be obtained before implementing any changes or modifications in the approved animal use.

Please keep this record for your files, and forward the attached letter to the appropriate granting agency.

Refer to Animal Protocol Number (APN) 140510141 when ordering animals or in any correspondence with the IACUC or Animal Resources Program (ARP) offices regarding this study. If you have concerns or questions regarding this notice, please call the IACUC office at (205) 934-7692.

Institutional Animal Care and Use Committee (IACUC)
CH19 Suite 403
933 19th Street South
(205) 934-7692
FAX (205) 934-1188

Mailing Address:
CH19 Suite 403
1530 3rd Ave S
Birmingham, AL 35294-0019

APPENDIX B

X-RAY DIFFRACTION DATA FOR *LYTECHINUS VARIEGATUS*

Lantern	Calcite 2Θ Spine	Test	Treatment (°C)	Time (days)
29.85658	29.63536	29.83328	baseline	0
29.91841	29.72466	29.87014	baseline	0
29.79677	29.67649	29.8933	baseline	0
29.75821	29.73791	29.83297	baseline	0
29.76863	29.68144	29.82918	baseline	0
29.79918	29.70975	29.8649	baseline	0
29.8323	29.70475	29.7729	baseline	0
29.86776	29.6896	29.80092	baseline	0
29.77827	29.70948	29.92389	baseline	0
29.78089	29.61563	29.86936	baseline	0
29.87397	29.66094	29.83581	baseline	0
29.78411	29.6335	29.86928	baseline	0
29.90196	29.73833	29.89312	baseline	0
29.70256	29.61632	29.86567	baseline	0
29.71813	29.74271	29.84993	baseline	0
29.84904	29.82439	29.89805	baseline	0
29.83427	29.72885	29.85992	baseline	0
29.78046	29.93388	29.85694	baseline	0
29.81035	29.70438	29.91102	baseline	0
29.86969	29.68854	29.79714	baseline	0
29.82868	29.77223	29.75663	baseline	0
29.80476	29.67296	29.81371	baseline	0
29.8073	29.77786	29.82591	baseline	0
30.04976	29.74522	29.91289	baseline	0
29.82754	29.73462	29.89396	baseline	0
29.78515	29.75455	29.88188	26	30
29.78938	29.68875	29.81774	26	30
29.8443	29.76813	29.76938	26	30
29.95848	29.77755	29.94402	26	30
29.7729	29.66634	29.85361	26	30
29.90482	29.78378	29.85128	26	30
29.79413	29.76063	29.79912	26	30
29.86936	29.55486	30.00065	26	30
29.84772	29.66437	29.87672	26	30
29.86315	29.68343	29.8647	26	30
29.73593	29.83549	29.94429	26	60
29.81629	29.64322	29.83723	26	60
29.83416	29.70804	29.89674	26	60
29.97295	29.80474	29.9281	26	60
29.75357	29.64307	29.82703	26	60
29.90733	29.81702	29.81797	26	60

Lantern	Calcite 2Θ Spine	Test	Treatment (°C)	Time (days)
29.87889	29.67814	29.93052	26	60
29.98786	29.78946	29.81161	26	60
29.82201	29.67901	29.94315	26	60
29.77788	29.79177	29.81446	26	60
30.00327	29.7598	29.77535	26	90
29.76564	29.78096	29.84835	26	90
29.85287	29.70044	29.81093	26	90
29.87237	29.75953	29.87688	26	90
29.96935	29.60592	29.85493	26	90
29.7576	29.71403	29.90172	26	90
29.90191	29.55428	29.80718	26	90
29.9308	29.74642	29.78145	26	90
29.75011	29.72621	29.91609	26	90
29.87894	29.74166	29.92189	26	90
29.77624	29.60122	29.94079	30	30
29.73511	29.60385	29.89195	30	30
29.77673	29.54466	29.73788	30	30
29.79124	29.68475	29.74737	30	30
29.81752	29.60412	29.78657	30	30
29.76476	29.54863	29.7827	30	30
29.71714	29.73109	29.70827	30	30
29.68034	29.71011	29.75192	30	30
29.7501	29.57632	29.82354	30	30
29.67867	29.6958	29.83066	30	30
29.65719	29.75403	29.91354	30	60
29.75888	29.69469	29.71164	30	60
29.77281	29.84273	29.67149	30	60
29.7411	29.61433	29.80714	30	60
29.68933	29.64612	29.63805	30	60
29.83017	29.58622	29.69168	30	60
29.62705	29.78219	29.74739	30	60
29.87234	29.59674	29.80411	30	60
29.76847	29.74215	29.813	30	90
29.81059	29.59548	29.82625	30	90
29.70457	29.68483	29.84761	30	90
29.8603	29.57161	29.73518	30	90
29.67239	29.59194	29.92984	30	90
29.70152	29.61045	29.75875	30	90
29.794	29.73719	29.68093	30	90
29.88722	29.71075	29.76249	30	90